

PROCESS DESIGN FOR GALLIUM RECOVERY INCLUDING LIXIVIANT
REGENERATION

by
Brandon Ott

A thesis submitted to the Faculty and the Board of Trustees of the Colorado School of Mines in partial fulfillment of the requirements for the degree of Doctorate of Philosophy (Metallurgical and Materials Engineering).

Golden, Colorado

Date _____

Signed: _____

Brandon Ott

Signed: _____

Dr. Patrick Taylor
Thesis Advisor

Golden, Colorado

Date _____

Signed: _____

Dr. Angus Rockett
Professor and Department Head
Department of Metallurgical and Materials Engineering

ABSTRACT

Gallium extraction from a zinc smelter waste stream is designed, discussed, and evaluated. Gallium separation is achieved via precipitation behavior from zinc and via caustic leach behavior from iron. The process developed showed a recovery of 38% of the gallium from the zinc smelter waste product.

The process economics are developed to show the conditions under which the process may be operated economically to recover gallium from this resource. The economic analysis is useful to identify the specific operations and factors that contribute to the process costs.

One of the most significant parameters that affects cost is the acid consumption of the leaching unit operation and the soda ash consumption of the pH adjustment unit operation. In order to address this large cost parameter a novel process for recovering sulfuric acid and soda ash from the leach solution after metals have been precipitated is developed and studied. This novel operation has the potential to significantly impact a range of industries that are consumers of chemicals including any mining project where reagent consumption is a major cost item.

TABLE OF CONTENTS

Abstract.....	ii
TABLE OF FIGURES.....	ix
TABLE OF TABLES.....	xiii
Acknowledgments.....	xv
Chapter 1 INTRODUCTION.....	1
Chapter 2 LITERATURE REVIEW OF GALLIUM EXTRACTION TECHNOLOGIES	4
2.1 Background on Gallium.....	4
2.2 Gallium extraction from Bayer liquors.....	6
2.3 Gallium Extraction from Zinc Processing.....	8
2.4 Gallium Extraction from Coal fly ash.....	8
2.5 E scrap.....	9
2.6 Phosphorus flue dust.....	9
2.7 Gallium solvent extraction.....	10
2.8 Cyanex-923.....	11
2.9 Kelex-100.....	12
2.10 Gallium Precipitation.....	12
2.11 Summary of Separations Literature Review.....	13
Chapter 3 EXPERIMENTAL EQUIPMENT AND PROCEDURES.....	14
3.1 Sampling Details.....	14
3.2 Leaching.....	14
3.3 Filtering.....	15
3.4 pH adjustment.....	16
3.5 Solvent Extraction Procedures.....	17
3.5.1 Cyanex-923 Procedures.....	17
3.5.2 Kelex-100 Procedures.....	18

3.5.3 Novel Extractant Procedures	18
3.6 Precipitation Procedures.....	18
3.7 Acid Regeneration Procedures	19
3.8 Design of Experiments and Statistical Methodology	20
3.9 Wet Chemical Method: Copper Chloride Precipitation	20
3.10 X-Ray Diffractometry	21
3.11 ICP-MS.....	24
3.11.1 ICP-MS Dilution Procedure	24
3.12 ICP-AES, ICP-OES.....	25
3.13 Total Digestion procedure.....	25
Chapter 4 DISCUSSION OF SEPARATIONS RESULTS.....	26
4.1 Proposed flowsheets concepts.....	26
4.1.1 solvent extraction.....	26
4.1.2 Precipitation.....	27
4.1.3 Lixiviant Regeneration	27
4.2 Mineralogy and quantification of feed material.....	28
4.2.1 Summary of samples	28
4.2.2 Sample Preparation.....	28
4.2.3 LA-ICP-MS	29
4.2.4 Digestion of CLP sample.....	30
4.2.5 CLP XRD Results.....	30
4.3 Leaching studies	31
4.3.1 Leaching Conditions Test work.....	32
4.3.2 Temperature dependence of leach behavior	34
4.3.3 Alternative Leach Strategies.....	35

4.3.4 Summary of Leach results	38
4.4 Solvent Extraction Studies	39
4.4.1 Cyanex-923.....	39
4.4.2 Kelex-100	41
4.4.3 Novel Extractants	42
4.4.4 Summary of Solvent Extraction Results/Solvent extraction flowsheet.....	43
4.5 Precipitation studies	44
4.5.1 pH Precipitation.....	45
4.5.2 Precipitation by zinc addition.....	46
4.5.3 Iron Precipitation	47
4.5.4 Combined Precipitation test work	48
4.6 Precipitation flowsheet and summary	48
4.6.1 Initial sequential precipitation test work	48
4.6.2 Preliminary complete flowsheet test work	51
4.6.3 Large sample test work.....	51
4.6.4 Alternative feedstock test work	55
4.7 Discussion of precipitation thermodynamics	55
Chapter 5 ECONOMICS OF GALLIUM SEPARATION.....	59
5.1 Cost model.....	59
5.1.1 Gallium market and value of products produced.....	59
5.1.2 Fraction B	61
5.1.3 Fraction C	61
5.1.4 Fraction D	62
5.1.5 Fraction E	62
5.1.6 Estimation of major costs	62

5.2 Base Case Incremental analysis	66
5.2.1 Increment A	66
.....	69
5.2.2 Increment B	70
5.2.3 Increment C	73
5.2.4 Increment D	75
5.2.5 Summary of Incremental Analysis	78
5.3 Economic Decision Making	78
5.3.1 Sensitivity Analysis	78
5.3.2 Process Alternatives	88
5.3.3 Breakeven Analysis	90
 Chapter 6 STATE OF THE ART OF REAGENT RECOVERY AND MANUFACTURE	
.....	92
6.1 Industrially relevant processes for sulfuric acid manufacture.....	92
6.2 Muriatic acid	93
6.3 Cyanide.....	94
6.4 Soda ash.....	96
6.5 Economic considerations of reagent regeneration	97
6.6 Sulfuric acid regeneration in the petroleum industry	101
6.7 Sulfur Dioxide Sequestration by the Contact Process.....	103
6.8 Chlor-Alkali regeneration at Mountain Pass Operation.....	104
6.9 Cyanide Regeneration from Thiocyanate.....	105
6.10 Carbon Sequestration by the Solvay Process	106
6.11 Limitations of Reagent Regeneration.....	106
6.12 Reduction of sodium sulfate to sodium sulfide.....	107

6.13 Summary of literature review	108
Chapter 7 THERMODYNAMIC CONSIDERATIONS FOR LIXIVIANT	
REGENERATION.....	109
7.1 Sodium sulfate formation in the separations process	109
7.2 Sodium sulfate reduction to sodium sulfide.....	109
7.3 Proposed alternative reaction Na_2SO_4 to Na_2CO_3	111
7.4 Reaction Energetics.....	115
7.5 Process Alternatives	116
7.5.1 Aqueous Reduction of Sodium Sulfate	116
7.5.2 Methane Reduction.....	118
7.6 Summary of Thermodynamics	120
Chapter 8 ACID REGENERATION RESULTS AND DISCUSSION.....	
8.1 Initial Test work	121
8.2 Aqueous Reaction Alternative	122
8.3 Higher temperature test work.....	123
8.3.1 Ashing and the boudouard reaction	123
8.3.2 87-1	125
8.3.3 87-2.....	125
8.3.4 87-3.....	125
8.4 Separation of sodium carbonate from sodium sulfate.....	126
8.5 Experiments near the sodium sulfate-sodium pyrosulfate liquidus	126
8.5.1 113-A	127
8.5.2 113-B	128
8.5.3 113-E	129
8.5.4 115-A	129

8.5.5 115-B	131
8.6 Summary of Acid Regeneration Results	134
Chapter 9 ACID REGENERATION ECONOMICS.....	136
9.1 Engineering mass and energy balance	136
9.1.1 Acid Regeneration Unit Operation.....	137
9.2 Oxidation of Off Gases	138
9.2.1 Scrubbing of Off Gases	140
9.2.2 Sulfate/Carbonate Separation	140
9.3 Estimation of CAPEX.....	140
9.4 Estimation of OPEX.....	141
9.5 Cashflow Model	141
9.6 Combination of acid regeneration and Separations Economics.....	144
9.7 Comparison to sodium sulfide process.....	144
9.8 Summary	146
Chapter 10 CONCLUSIONS.....	147
10.1 Conclusions	147
10.2 Suggestions for future research.....	148
REFERENCES	150
Appendix A.....	154
Appendix B.....	158

TABLE OF FIGURES

Figure 2.1: Porbaix diagram for Gallium in water	6
Figure 3.1: The CLP Sample used for this research was delivered in three pales, each having a different visual appearance, the first two containers had agglomerations covering a large cake like that seen in the third image.....	14
Figure 3.2: Picture of stirred vat leach apparatus.....	15
Figure 3.3: Laboratory pressure filter; the filter body and lid swing into place above the pad in the middle of the image	16
Figure 3.4: Furnace setup for acid regeneration testwork.....	19
Figure 3.5: Copper Chloride wet chem method for determining sodium carbonate amount (left is the copper chloride solution, middle is the solid white precipitate formed by the reaction of sodium carbonate and copper chloride, and right is the filtered precipitate for analysis..	21
Figure 3.6: Example of XRD pattern, this one is for the CLP sample.....	22
Figure 3.7: Overlapping XRD peaks can be seen with the broad peak at 34 degrees	23
Figure 4.1: Proposed flowsheet for gallium recovery by solvent extraction	26
Figure 4.2: Conceptual flowsheet for gallium recovery via precipitation	27
Figure 4.3: Conceptual flowsheet for acid regeneration as part of a gallium recovery process	28
Figure 4.4: Picture of the CLP sample after crushing to break up large agglomerations	29
Figure 4.5: LA-ICP-MS results from the CLP sample	29
Figure 4.6: XRD result for the CLP sample along with major phases.....	31
Figure 4.7: Flowsheet to illustrate leaching test procedure.....	32
Figure 4.8: graphical illustration of gallium recovery (circle diameter) as a function of acid concentration and leaching time	33
Figure 4.9: Effect of temperature on leach recovery. Slurry Density: Time: Acid Con:.....	34
Figure 4.10: Roast leach study flowsheet	37
Figure 4.11: Cyanex loading isotherms based on ore leach samples.....	40
Figure 4.12: Cyanex loading at several temperatures with ore leach samples.....	40
Figure 4.13: Kelex loading for metals of interest	41
Figure 4.14: Gallium grade and recovery for various precipitation tests.....	44
Figure 4.15: Precipitation behavior of major metals upon change in pH.	45
Figure 4.16: Precipitation behavior upon zinc addition.....	46

Figure 4.17: Precipitation behavior upon iron addition	47
Figure 4.18: Precipitation behavior presented as gallium recovery (circle diameter) in relation to pH and amount of zinc addition.....	48
Figure 4.19: Precipitation-Leach flowsheet concept.....	49
Figure 4.20: Flowsheet for larger test with stock CLP leach sample.....	50
Figure 4.21: Flowsheet for first leach-precipitation test	52
Figure 4.22: Flowsheet for 1kg sample.....	53
Figure 4.23: Eh-pH diagram for gallium.....	56
Figure 4.24: Eh-pH diagram for copper	56
Figure 4.25: Eh-pH diagram for Iron	57
Figure 4.26: Eh-pH diagram for zinc	57
Figure 4.27: Eh-pH diagram for gallium and Iron	58
Figure 5.1: Gallium recovery flowsheet used for the economic model	59
Figure 5.2: Five-year spot price for zinc metal [20]	60
Figure 5.3: Incremental flowsheet A.....	67
Figure 5.4: Incremental flowsheet B.....	70
Figure 5.5: Incremental flowsheet C.....	73
Figure 5.6: Incremental flowsheet D.....	75
Figure 5.7: Sensitivity of the 5 increments and total process to changes or uncertainty in CAPEX...	79
Figure 5.8: Sensitivity to Sulfuric acid costs	80
Figure 5.9: Sensitivity to soda ash costs	82
Figure 5.10: Sensitivity to total reagent costs	83
Figure 5.11: Sensitivity to leach recovery	85
Figure 5.12: Sensitivity to Zinc fraction value	85
Figure 5.13: Sensitivity to gallium fraction value.....	87
Figure 5.14: Sensitivity to disposal cost of fraction C.....	87
Figure 5.15: Sensitivity to value of fraction E	88
Figure 6.1: Flowsheet for the contact process for sulfuric acid manufacture	93
Figure 6.2: An original flowsheet from Adrussow's work for the cyanide production process	95
Figure 6.3: Sulfuric acid price index since the 1980s	98

Figure 6.4: Price index for a range of inorganic acids including muriatic acid and sulfuric acid discussed in the paper	99
Figure 6.5: Price index for soda ash.....	100
Figure 6.6: Flow diagram of the sulfuric acid regeneration process used in the petroleum industry	102
Figure 7.1: Enthalpy for sodium sulfide intermediary process	110
Figure 7.2: Enthalpy for sodium sulfide oxidation	111
Figure 7.3: Free energy for several reactions for the conversion of sodium sulfate directly to carbonate.	112
Figure 7.6: Enthalpy for several reactions for reduction of sodium pyrosulfate to sodium sulfate...	113
Figure 7.5: Free energy for several reactions for reduction of sodium pyrosulfate to sodium sulfate	113
Figure 7.7: Entropy and Enthalpy for aqueous reaction with carbon monoxide/hydrogen and methane	117
Figure 7.8: Equilibrium for aqueous reaction with carbon monoxide and hydrogen.	118
Figure 7.9: Equilibrium for aqueous reaction with methane	118
Figure 7.10: Equilibrium for the methane reaction.....	120
Figure 8.1: Reactor for aqueous lixiviant regeneration test work.....	122
Figure 8.2: Graph of the equilibrium condition of the boudouard reaction from 0 to 1600°C [39] ..	124
Figure 8.3: Grade and recovery for sodium carbonate separation with single stage methanol leaching.	126
Figure 8.4: XRD result for the product of test 113-A	128
Figure 8.5: XRD result for the product of test 113-B	128
Figure 8.6: XRD result for the product of test 113-E	129
Figure 8.7: XRD result for the product of test 115-A.....	130
Figure 8.8: estimated relative phase amounts from the XRD for the product of test 115-A	131
Figure 8.9: XRD result for the product of test 115-B	132
Figure 8.10: Estimated relative phase amounts based on the XRD result for 115-B.	133
Figure 8.11: XRD result for the product of test 115-C	133
Figure 9.1: Flowsheet for lixiviant regeneration process.....	137
Figure 9.2: Segment of flowsheet relating to the high temperature salt reaction for acid regeneration	137

TABLE OF TABLES

Table 3.1: Cyanex SX Parameters	18
Table 4.1: Metals composition of the CLP sample via complete digestion	30
Table 4.2: Parameters for sulfuric acid leaching tests	32
Table 4.3: Metal recovery results for caustic leach tests	35
Table 4.4: Sequential leach results	36
Table 4.5: Comparison of recoveries for various metals of interest for the reduced sample from the CLP leach.....	38
Table 4.6: Metals grades of the leach liquors for the reduction-leach test	38
Table 4.7: Kelex strip results	42
Table 4.8: Recoveries and extraction conditions for several novel extractants.....	43
Table 4.9: Conditions for test results in Figure 4.15	45
Table 4.10: Details on the various fractions recovered as according to the flowsheet in Figure 4.19.	49
Table 4.11: Analysis results from various materials sampled from the flowsheet in figure 16.	50
Table 4.12: Recovery for leach-precipitation flowsheet.....	53
Table 5.1: Summary of values of each fraction produced by the sequential leach-precipitation process.....	60
Table 5.2: CAPEX model for plant	63
Table 5.3: OPEX model for the complete processing plant	64
Table 5.4: Cashflow model for the gallium recovery process	65
Table 5.5: Capex for Increment A	67
Table 5.6: OPEX for increment A	68
Table 5.7: Cashflow model for Increment A	69
Table 5.8: Capex for Increment B	70
Table 5.9: OPEX for Increment B	71
Table 5.10: Cashflow model for increment B	72
Table 5.11: CAPEX model for Increment C	73
Table 5.12: OPEX model for increment C	73
Table 5.13: Cashflow model for increment C	74
Table 5.14: CAPEX model for Increment D	75

Table 5.15: OPEX model for increment D	76
Table 5.16: Cashflow model for Increment D	77
Table 5.17: Summary of results from incremental economic analysis.....	78
Table 5.18: Cashflow model for Increment A considering the ferrite feed stock	90
Table 7.1: Temperature for sulfide evolution, and sodium carbonate equilibrium amount for various furnace atmospheres.....	114
Table 7.2: Energy balance for sodium sulfate to sodium carbonate conversion reaction	115
Table 7.3: Energy balance for oxidation of off gases	116
Table 7.4: Thermodynamics for conversion directly to sodium carbonate with methane.....	119
Table 8.1: Results of initial furnace tests.....	121
Table 9.1: Mass and energy balance for acid regeneration unit operation	138
Table 9.2: Mass and energy balance for off gas oxidation unit operation.....	139
Table 9.3: Capex estimate for acid regeneration plant	141
Table 9.4: OPEX model for acid regeneration plant	141
Table 9.5: Cashflow model for acid regeneration process	143
Table 9.6: Cashflow model for acid regeneration process	143
Table 9.7: Cashflow model for acid regeneration process	143
Table 9.8: Cashflow model for acid regeneration process	143
Table 9.9: Summary of separations increments from Chapter 5 and acid regeneration considered as an incremental investment to the separations plant model	144
Table 9.10: Energy balance for sodium sulfate reduction to sodium sulfide.	145
Table 9.11: Energy balance for sodium sulfide oxidation to form sodium carbonate.....	145
Table A.1: Equilibrium chart for feed gas ratio of 3CO:1H ₂	154
Table A.2: Equilibrium chart for feed gas ratio of 1CO:1H ₂	155
Table A.3: Equilibrium chart for feed gas ratio of 1CO:1H ₂ :0.25O ₂	156
Table A.4: Equilibrium chart for feed gas ratio of 1CO:1H ₂ :0.5O ₂	157
Table B.1: Summary chart of parameters effects on zinc recovery.....	158
Table B.2: Summary of leaching parameters effects on gallium recovery.....	158
Table B.3: Summary chart of parameters' effects on iron recovery	159

ACKNOWLEDGMENTS

This research was completed with support from the Critical Materials Institute and I would like to extend my gratitude to them for that support.

I would like to sincerely thank my advisor Dr. Patrick Taylor for his guidance and direction for this research work, as well as my committee members Dr. Corby Anderson, Professor Erik Spiller, and Dr. Roderick Eggert for their ongoing advice and support.

I would also like to thank my colleagues from the Kroll Institute for Extractive Metallurgy past and present for the friendships and personal and technical advice during the completion of this research.

The faculty and Staff of the Colorado School of Mines Metallurgical and Materials Engineering and Mining Engineering departments have been enormously helpful to me during this project. In particular Scott Pawelka and Bruce Yoshioka have been vital to ensuring the safe operating condition of laboratory equipment used for this project.

I wish to acknowledge Marley Smith for her undying support through my work on this project and especially over the unique challenges of 2020 in delaying parts of this research.

I wish to thank my family for their love and support during the time of this research and writing. Namely Allen, Elaine, Brianna, & Joy.

I appreciate the contribution of my friends both in discussing technical ideas for this work and in appropriate distractions from work. Particularly Ryan, Zach, Ryan, Marty, and Cody.

Finally, I would like to thank God for the opportunity and insight granted to complete this work.

Thank You all.

CHAPTER 1 INTRODUCTION

The goal of the Critical Materials Institute is the development of technologies that can contribute to an economic process for the recovery of critical materials from domestic sources. Past research at the Colorado School of Mines focused on the physical and chemical separation of indium and gallium from residues. These included jarosite tailings from hydrometallurgical processing of sphalerite, ferrite residue from pyrometallurgical zinc operations, and zinc mine tailings. Due to their dilute indium content the extraction of indium by hydrometallurgical processing was found to be non-economical in previous work. A primary reason for this is the high level of acid consumption during leaching. Novel separation processes as well as novel technologies for lixiviant regeneration will be evaluated and discussed.

Gallium, Germanium, and Indium are classified by the US department of Energy as critical materials. The principle use of these elements is in the manufacture of transistors, diodes, and rectifiers which are basic components used in a wide range of communications and control systems. The amount used in each individual component is small but the number of these devices manufactured provides a significant market. Gallium is additionally used to modify other semiconductor materials for various applications.

Gallium as an alloying element forms a range of low-melting-temperature alloys. It also has potential uses as a catalyst. Gallium is currently considered to have a medium criticality the United States of America based on its importance to the economy and supply risk. The importance to the economy includes an estimate of whether gallium can be substituted for or replaced. Gallium is relatively irreplaceable in its common applications. Additionally, several market research firms are of the opinion that the adoption of new communications technologies will increase the criticality of gallium in the future. [1]

A recent article from Roskill identifies Gallium as having a medium criticality to both the US and EU, among others. Roskill considers it possible that a higher criticality will be assessed in the future. They suggest that the COVID-19 Pandemic will cause an increase in gallium demand due to shift toward remote work and remote living. This shift will require faster networking to more remote regions of all major industrialized countries. Gallium arsenide is widely used in wireless communication applications including 4G and 5G base stations. Gallium Nitride is a likely contributor to 5G base stations and may replace silicon-based technologies due to its capacity for higher frequency operation. Regardless of the specific architecture of new

communications technologies it is expected that gallium demand will be high. Similar to other metals with relatively small markets the gallium market exhibits significant volatility. For example, from mid-2000 to Q1-2001 gallium prices moved from \$500-600/kg to \$2300/kg based on supply concerns. By the latter half of 2001 the price gains had retraced.

Indium and germanium are considered to have a medium criticality to the United States economy. Currently the market is dominated by potential economically adversarial countries and as such the domestic markets could be stabilized by domestic sources of these materials.

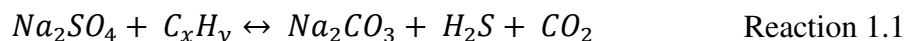
Domestic supplies of these materials would contribute to the metal's markets by firstly, providing expanded supply to satisfy demand, and secondarily de-risking supply by diversifying sources from high-risk foreign sources to lower risk domestic sources. The additional supply would be expected to reduce the cost of gallium, germanium, and indium for domestic consumers of these metals. The de-risking of the supply sources makes investment in this market easier for market participants. De-risking the supply in this market may lead to more stable prices in the long term.

The industry standard for gallium recovery is by ion exchange from Bayer process liquors. Other reagents are discussed in the literature for extraction from acidic leach liquors. Initial study for this thesis, with respect to process development for domestic gallium recovery, included an analysis of the technical applicability of solvent extraction. Further, novel separations technologies were developed and compared to the solvent extraction results. The comparison is accomplished based on economic assessment of the various process alternatives. The extractants of interest included Cyanex-923 produced by Solvay Chemical, Kelex-100 which is well documented in the literature for recovery of gallium mostly from Bayer process liquors, additionally three novel extractants produced by Oak Ridge National Lab (ORNL) were evaluated for efficacy in concentrating gallium. It is envisioned that the novel extractants can improve process economics. Previous studies have also ignored precipitation behavior as a possibility for recovery of gallium. A novel process of leaching and sequential precipitation may be a viable alternative depending on technical and economic considerations.

One of the challenges of any resource extraction project is the social good-will and the permitting of operations. This concern is minimized by the industrial partner of CMI because they currently operate a zinc smelter and the intent of the project is to recover co-products from a waste stream in an economically and socially efficient manner. It is expected that this co-

production at an established smelter will face fewer social and regulatory hurdles than greenfield resource extraction projects.

Industrial lixiviant regeneration is more broadly applicable than to just Ga, Ge, and In, however, it is anticipated that the economics of Ga, Ge and In recovery can significantly benefit by the development of a novel regeneration process. Most present work on lixiviant regeneration has been limited to small scale laboratory experiments using reagent grade feed materials for demonstration. One of the only examples of operating plants using reagent regeneration was the chlor-alkali plant at the Mountain Pass operation. Regeneration of the acid used for the process does not only contribute to process economics in the form of reduced input costs, it also serves to minimize waste through re-use and, for future projects, may contribute significantly to their social license to operate. The consumption of CO as a carbon sink, may contribute social and environmental benefits to the industry in addition to economic benefits. Most projects related to carbon capture are focused on depositing carbon in chemical structures where long residence times are expected. For example, in concretes where the structure will remain intact and continue to hold carbon for many years. Though not in the same stead, the capture of carbon and application as a chemical reagent may be equally viable and possibly more supportive of industry. The lixiviant regeneration process is equally useful in its production of sulfuric acid which is consumed in the leaching of such materials but also in the regeneration of sodium carbonate for other plant processes or resale. The reduction of this salt to sodium carbonate while evolving dihydrogen sulfide according to the generalized reaction below is explored as part of this research.



The economic models included in the study will be used to contribute to conclusions of whether the technology currently exists to economically extract gallium from this domestic source, or help identify the remaining engineering challenges where innovation may contribute to a useful industrial process.

CHAPTER 2 LITERATURE REVIEW OF GALLIUM EXTRACTION TECHNOLOGIES

Lu et al published an excellent review to summarize the various resources and extraction technologies for gallium from a range of primary sources. That survey along with an earlier review by Zhao provide a summary to begin to understand the state of the art of gallium extraction and recent research progress toward gallium recovery.

2.1 Background on Gallium

Gallium is a soft, silvery metal that was first discovered in 1875 by French Chemist Paul-Emile Lecoq de Boisbaudran. Gallium is considered a trace metal with an average abundance of 17ppm in the earth's crust. The metal is known for its extreme liquid temperature range with a melting point at 300.98°K and a boiling point of 2676°K. The metal exhibits low vapor pressures even at relatively high temperatures. Stable solid gallium structure crystallizes in orthorhombic unit cells with conchoidal fracture similar to glass. Gallium interestingly expands upon solidification (by about 3.1%). Gallium has six isotopes of which two are stable (^{69}Ga and ^{71}Ga). Gallium has two primary oxidation states of Ga^+ and Ga^{3+} . Gallium readily forms compounds with bromides, chlorides, hydrides, iodides, nitrides, oxides, selenides, sulfides, and tellurides. The metal is insoluble in water and dissolves in acids with $\text{pH} < 2$ and E_h above 600mV. The thermodynamic aqueous solution behavior of gallium is discussed further in section 4.7. It also dissolves in concentrated basic aqueous media.

The industrial usage of gallium began in the United States in the post WWII era. It saw increased demand in the 1970s when the semiconducting properties of gallium-pnictogen compounds were developed and became viable for the electronics industry. Gallium semiconductors are now important in the manufacture of many electronic devices including cell phones, photovoltaics for power generation, optical devices, computers, networking equipment, etc. Gallium has very unique properties that make its replacement in these applications virtually impossible with current technologies. Gallium arsenide is a superior semiconductor technology to silicon. This is due to faster transmittance speed, better optical properties, and higher radiation hardness.

Gallium bearing minerals are rare. The majority of gallium produced presently is produced as a co-product of aluminum extraction. The balance of gallium production is as a co-product of zinc processing operations. Efficient technologies for the recovery of gallium have

been of interest to the metallurgical industry primarily because gallium demand is expected to increase drastically in the near future.

The three main resources of gallium worldwide are; bauxite ores, zinc ores, and coal resources. Current minable resources of gallium are large and could supply gallium for hundreds of years at the current consumption rate. However, only a small fraction of this gallium is economically recoverable, most gallium in these resources reports to a waste fraction with zinc, aluminum, or coal operations. Several waste streams from the processes for base metals and energy minerals have been identified as potential gallium resources.

Waste produced from Bayer process alumina production called 'red mud' contains significant amounts of trace metals including gallium, nominally 20-80ppm. Gallium in mud occurs generally as oxide hydroxides and gallium hydroxides. About 120 million tons of red mud are generated annually with a global inventory on the order of 3 billion tons. Coal fly ash produced from power plants is a second abundant waste stream which contains gallium. Coal fired power plants produce about 1 part of fly ash for every 4 parts raw coal combusted. The annual production of fly ash in 2015 was nominally 580million tons. Gallium in fly ash is contained at a concentration of 30-100ppm. Gallium occurs in raw coal mainly as part of the inorganic phase replacing aluminum in aluminiferous minerals (boehmite).

Recycling sources for gallium are a growing resource but cannot be used to satisfy the growing demand for gallium in semiconductors. The primary phases that contain high gallium amounts are gallium arsenide, gallium nitride, and indium gallium nitride. The waste from manufacturing with these materials is a significant resource at relatively high grades and low recycling cost but the volume is insufficient to satisfy growth in the gallium market. There is also the constant consideration in recycling of manufacturers reducing cost and reducing waste in their processing. Previous work at Colorado School of Mines [2] showed that hard drive manufacturers were fast to adopt technologies to reduce their consumption of critical materials when the prices spiked in 2011. Similar behavior, not necessarily to replace gallium in its common applications (as this has already been established as being quite difficult), but to reduce gallium consumption, and particularly to minimize waste material may make this an unreliable source as gallium demand increases and gallium price increases in association with this demand.

The aqueous chemistry of gallium is of particular importance to this research. Gallium forms anionic complexes in solutions. The gallium three ion is the dominant species at extremely

low pH values and begins to drop in relative speciation above pH=1. At pH=5 this species is not observed in the solution. The species $\text{Ga}(\text{OH})_2$ and $\text{Ga}(\text{OH})_3$ are present over only a small pH range from about 3 to about 6. The species gallium hydroxide with a net 2 positive charge is dominant at pHs in the range of 3 to 5 which is the operating condition for the Cyanex-923 extractant discussed further in section 4.7. The last common species is $\text{Ga}(\text{OH})_4$ and is dominant

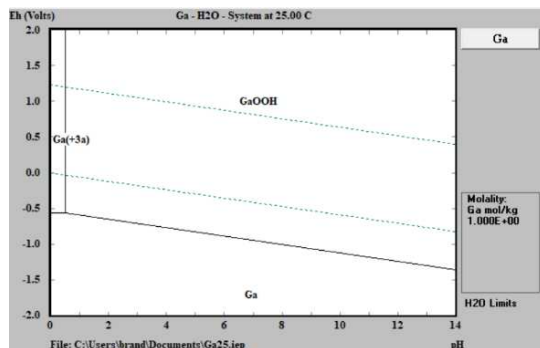


Figure 2.1: Pourbaix diagram for Gallium in water

across the range of higher pHs. Figure 2.1 shows the phase stability diagram for gallium in water.

Gallium also complexes with chloride, sulfate, fluoride, and phosphate in aqueous solution. These are discussed in the work of Wood and Samson. [3] The gallium hydroxide phase present in red mud is leachable in acidic solutions below pH 4.3. The authors mention that solubility is improved significantly at higher temperature. [4]

Gallium commonly takes on either a trivalent or monovalent oxidation state. Gallium is insoluble in water but can be dissolved in acidic solutions according to the pourbaix diagram in figure 2.2. As apparent on the pourbaix diagram it can also be dissolved in alkali aqueous solutions.

Gallium is mostly produced as a by-product of bauxite processing in the Bayer process. The remainder is produced from zinc-processing residues.

The authors Zhao et al. summarize various extraction methods of gallium from gallium resources. A brief summary of their survey is found here. [5]

2.2 Gallium extraction from Bayer liquors

Gallium recovery methods from Bayer liquors that have been well studied include precipitation, electrochemical deposition, solvent extraction, and ion exchange processes. The fractional precipitation approach is achieved via carbon dioxide reaction to form $\text{Al}(\text{OH})_3$ and

$\text{Ga}(\text{OH})_3$ which can be separated by leaching with caustic or lime solutions. After which gallium is recovered from the $\text{NaGa}(\text{OH})_4/\text{NaAl}(\text{OH})_4$ containing solution by a carbonization process. Electrochemically gallium is recovered by either mercury cathode electrolysis or cementation. Mercury cathode electrolysis is uncommon due to legal and environmental considerations. Cementation involves adding a reductant such as sodium amalgam or solid aluminum. The solvent extraction method uses a cation exchange mechanism to partition gallium to the organic phase. The kinetics of this exchange are generally slow and the cost of extractant degradation and dissolution is high. Ion exchange is the most well proven technology for this separation. The first patent for this technology was issued to Kataoka et al in 1984. They discovered that certain chelating resins exhibit excellent selective extraction ability for gallium. The process flowsheet is shown in figure 2.3.

Discussion of gallium extraction from Bayer liquors has been discussed with greater depth by Zhao et al.

In addition to Bayer liquors there are several alumina/aluminum by products that contain potentially useful gallium concentrations. Red mud has been of interest for base metals recovery for years but critical materials recovery has seen little development. One proposed approach is published by Abdulvaliyev et al in 2015 [6] for recovering gallium and vanadium from red muds using the Bayer-hydrogarnet process. This process specifically takes advantage of the reaction between caustic and gallium hydroxide or gallium oxide hydroxide to form a sodium gallium hydroxide complex. Other technologies explored for recovering gallium from red mud include a bioleaching process explored by Qu et al [7].

The other primary gallium containing waste stream from alumina operations is electrostatic precipitator dust formed during aluminum hydroxide calcination. Several studies have focused on recovering base metals from the dust but gallium extraction has only been of interest more recently. Gladyshev et al [8] published a proposed process to recover gallium from dust via sintering with soda ash and then digesting in an alkaline solution of sodium oxide followed by a carbonation process to precipitate aluminum hydroxide that contained most of the gallium. This could be further leached and then electrolyzed to produce a final concentrate.

There are other projects focusing on recovery of gallium from aluminum electrolysis dust. The dust tends to accumulate gallium oxide (Ga_2O_3) during the sublimation process with the primary diluent being alumina. The researchers Carvalho et al proposed a sintering, followed

by hydrochloric leaching at temperature to achieve very high gallium leach recoveries. The leach liquor was extracted using polyurethane foam and was re-extracted with 80% ethanol solution. The recovered gallium could be precipitated via a sodium hydroxide solution and then purified and reprecipitated to produce a high-grade gallium oxide product.

2.3 Gallium Extraction from Zinc Processing

Bayer liquor is the primary source of new gallium for the industry and the previously discussed processes are all of interest to increase gallium supply and increase plant revenue, however, these Bayer liquor processes are not necessarily beneficial for diversifying supply and in turn reducing criticality. The discussion of zinc industry wastes is more aligned to the goals of the US DOE's Critical Materials Institute.

Zinc residues are considered an important resource for gallium. Gallium is primarily part of the zinc ferrite structure ($ZnO \cdot Fe_2O_3$) as a substitution with iron. Combined pyro/hydrometallurgical extraction is employed industrially for extraction of gallium. The zinc plant in Porto Marghera in Italy first extracted gallium from zinc residues in 1969. The process utilized is illustrated in figure 2.7. [4] A similar process was used in china in 1975. These processes suffer from low recovery, high energy consumption, long reaction times, and environmental concerns. More environmentally friendly methods for gallium recovery are of importance to social license and continued extractive success.

Other processes have been proposed including counter-current foam separation (by Kinoshita et al)[9] to extract gallium from a leach refinery residue. And a pressure acid leaching process (by Liu et al). [10] both of these processes showed impressive recoveries but are "limited to laboratory scale studies due to high costs and technical problems." [4]

2.4 Gallium Extraction from Coal fly ash

There has been recent effort devoted to developing processes for recovery of gallium from fly ash produced at coal-fired powerplants. an example in 1996 demonstrated a process using a hydrochloric acid leach. Gutierrez et al studied gallium recovery from fly ash via solvent extraction in a hydrochloric acid medium. The extractant studied was Amberlite LA-2 (5 vol% in Kerosene) which co-extracted gallium and iron and stripped with water, from which iron could be precipitated via caustic addition. The gallium remaining in solution was extracted with LIX 54 (10% in Kerosene) and stripped with hydrochloric acid. Oriol et al studied a caustic leaching

method for extraction of gallium from fly ash and treated the leachate in a two-stage carbonation process to recover gallium.

A pilot scale plant was built in 2012 in west China by the Shenhua Energy Company. The pilot plant was based on laboratory scale process development. Iron is removed by magnetic separation and gallium is recovered via leaching-ion exchange-electrolysis.

Coal represents a large fraction of global gallium resources and therefore gallium recovery from fly ash has and will attract significant attention volume of this waste material. It is of less interest in the United States where the expansion of coal power generation is a fraction of that in China.

2.5 E scrap

Lee and Nam in 1998 investigated leaching of gallium arsenide to recover gallium with nitric acid. More recently gallium has been recovered from industrial scrap resulting from gallium arsenide manufacturing in several countries. These processes are not well documented in the literature. There are two main light-emitting diode (LED) wastes of interest in the context of discussing gallium resources. The first is manufacturing waste, the other is end of life LEDs for recycling. The waste contains significant gallium and indium mostly as gallium nitride. Swain studied a leaching-annealing technology to extract gallium from this waste that is illustrated by figure 2.8.

As end-of-life LEDs are more complex than manufacturing wastes this process is not suitable for recovery of that gallium. Lu et al tested a vacuum distillation technology to recycle LED waste for gallium. The process used pyrolysis and comminution to produce fine metal particles from which gallium could be extracted as an evaporate. [4]

2.6 Phosphorus flue dust

Gallium is also found in the flue dust associated with smelting of phosphate for production of phosphorous. Xu et al used sulfuric acid to leach gallium from the flue dust. They used a 20% sulfuric acid solution at 80°C and a 10% slurry density. Phosphorous smelting is an aging technology being replaced by hydrometallurgical processes due to energy efficiency, and the modern process for phosphorous production does not have gallium enriched waste streams.

2.7 Gallium solvent extraction

There are several papers in the literature discussing gallium solvent extraction. One of particular interest is the study by Fayram & Anderson on development of a hydrometallurgical gallium and germanium recovery technology. The study focused on the Pasmenco US Inc. Gordonsville operation which had been producing zinc concentrates since 1975. They identified that several potential co-products were concentrated as part of the zinc process. The gallium and germanium were present as interstitials in the sphalerite mineral from the Gordonsville operation. This material was refined at the Clarksville zinc refinery. The majority of the impurities are partitioned to a waste stream within the hydrometallurgical processing plant at Clarksville. This residue represented a 5000 ton per year potential resource containing 0.8% gallium and 0.6% germanium along with significant iron, zinc, silica, and lead. This residue was sold for the germanium value and no value was realized for gallium.

These researchers mention three previous studies for recovery of gallium from this material. One covered an acidic leach procedure and the other two explored a nearly identical caustic leach operation. The concept for the acidic leach processes suggests the iron in the leach liquor had to be reduced to the ferrous oxidation state, and then the recovery of gallium was possible via solvent extraction. The final concentrate was generated via electrowinning. The alkaline leaching processes were based on work for Dow and Cominco, They used alkaline leaching to form a jarosite, precipitated major impurities with calcium hydroxide, precipitated

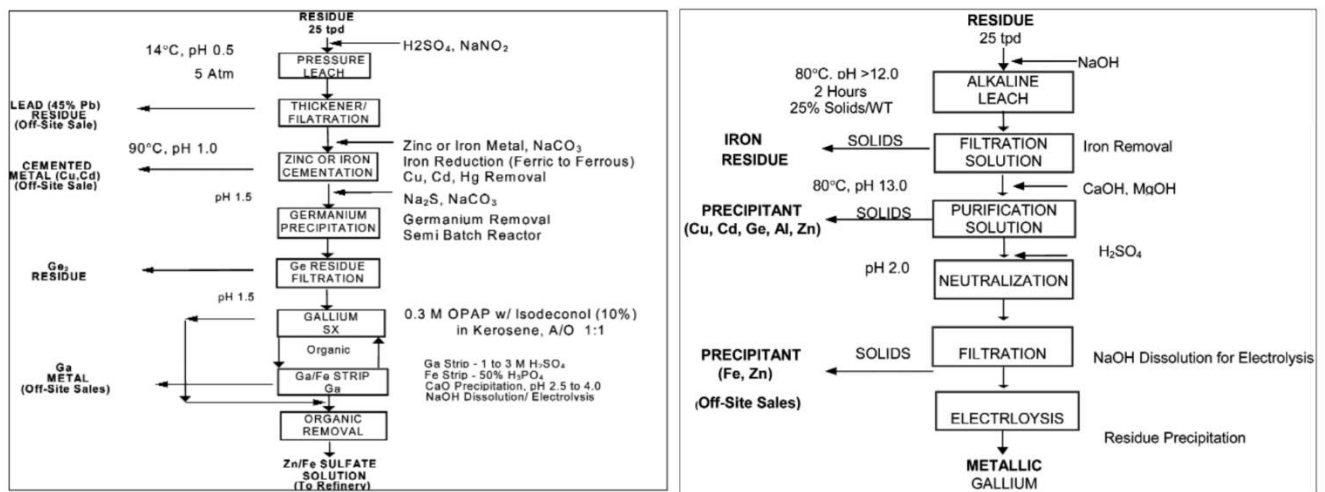


Figure 2.2: Flowsheets from previous solvent extraction and ion exchange work reviewed in the Fayram, Anderson paper

germanium with magnesium hydroxide, and finally recovered gallium by electrowinning. The flowsheets for these two processes are shown in figure 2.2.

The researchers developed an ion exchange and solvent extraction flowsheet. They eliminated alkaline leaching on the basis of lead solubility in the alkaline solution which interfered with gallium recovery to the organic. The ion exchange flowsheet is shown in figure 2.3. They tested three waste products from the clarksville smelter. Their leach results were

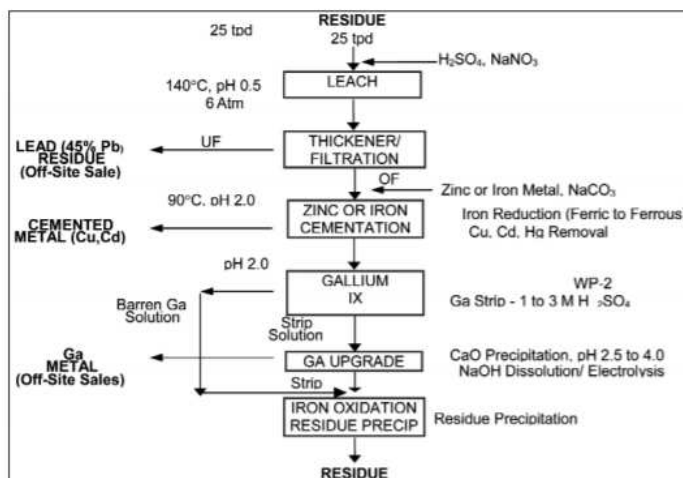


Figure 2.3: Proposed flowsheet tested as part of the Faryam, Anderson experimental work

similar to the results of the research conducted for this thesis. Their cementation step did not produce a gallium concentrate as their extractants/resins were conducted at a pH of 2.1, lower than the pH at which gallium and iron precipitated. At this pH ferric iron can be reduced to ferrous iron without precipitating significant gallium. The extractant used was octylphenyl acid phosphate (OPAP). Ion exchange tests focused on WP-2 a silica based resin. They are among the few researchers who showed economics based on laboratory and pilot scale work. [11]

2.8 Cyanex-923

Several papers discuss laboratory results for extraction of gallium by Cyanex-923 in solvent extraction. The paper by Gupta et al guided the experimental design for the experimental procedures discussed herein significantly. The researchers prepared stock solutions of various metals by dissolution of metals salts (nitrates, chlorides, or sulphates) in mineral acid and standardized by titration. All of the chemicals and solvents were analytical grade materials. They studied the effects of acid concentration on extraction of gallium from various mineral acids.

They also considered the effect of temperature on the extraction of gallium and the effect of Cyanex-923 concentration. The researchers also studied the stripping of gallium from Cyanex-923. The work resulted in conditions at which gallium may be separated from base metals with Cyanex-923. [12]

Mishra et al was also influential in the design of Cyanex test work. The authors tested gallium extraction by Cyanex 921 in toluene in the pH range of 1.0 to 6.0. The range of 4.5-6.0 showed good extraction of gallium. They specifically reported a 99.6% gallium recovery at a pH of 4.5 stripped with 4M nitric acid. [13]

There are previous patents on the extraction of germanium with Cyanex-923 including 4,915,919 and 3,760,060. These patents, particularly the later of the two listed discuss the mechanism by which germanium is extracted by the neutral Cyanex extractant.

2.9 Kelex-100

There are several similar papers that inspired the Kelex-100 experimental design of this thesis. Of particular note are G.V.K Puvvada's work studying various volume fractions of Kelex in kerosene with Versatic 10 used to decrease the time to reach equilibrium. [14,15] Kekesi also published results for gallium selectivity from alumina precipitation liquors at a pH= 14.3 using 10-20% Kelex. The published stripping procedure for Kelex included stripping aluminum with 5-6M HCl and gallium with 2M HCl. This procedure was directly tested and varied in the research herein. [16]

2.10 Gallium Precipitation

There are relatively fewer articles about the precipitation behavior of gallium. One paper that showed very similar results to the results eventually determined as part of the gallium recovery test work showed a domain of pH where gallium could be preferentially precipitated over iron. Figure 2.4 shows the potential for gallium and iron separation via preferential precipitation.

The authors of this paper focused their research on flue dust mostly consisting of apatite, quartz, amorphous silicates, and coke. [17]

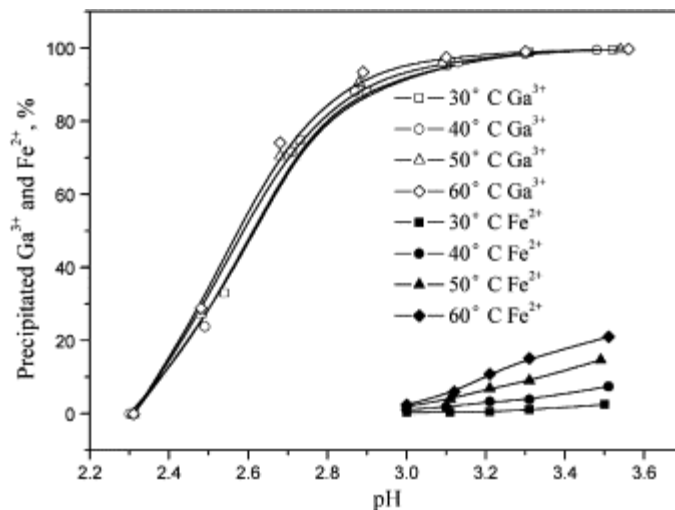


Figure 2.4: Gallium and iron precipitation

2.11 Summary of Separations Literature Review

The significant resources of interest for extraction of gallium are Bayer process liquors, Bayer process wastes, zinc process wastes, and coal fly ash. There is room for a novel separations process particularly if it can be applied on a larger than laboratory scale.

CHAPTER 3 EXPERIMENTAL EQUIPMENT AND PROCEDURES

3.1 Sampling Details

Five samples were provided from industry contacts and used for the separations experimentation presented herein. The Clarksville Leach Product (CLP) sample was selected from the others as it had significant gallium and significant gallium reported to the leach liquor. Pictures of this sample can be seen in figure 3.1. It was delivered in three 4-gallon pales with significant moisture content, much of the material was muddy and had formed agglomerations. The sample was partially dried in a drying oven at $\sim 100^{\circ}\text{C}$ and a jaw crusher was used to break up the agglomerations. The sample was blended and split using a jones splitter to produce nominally 1kg congruent splits for testing. The sample of particular interest for this research was the CLP sample as others did not have significant gallium present.



Figure 3.1: The CLP Sample used for this research was delivered in three pales, each having a different visual appearance, the first two containers had agglomerations covering a large cake like that seen in the third image.

3.2 Leaching

For precipitation and solvent extraction test work, the sample material required leaching to produce a liquor with the various ions of interest in solution. In early test work an overnight leach was used as the leach kinetics were not a concern. Later, Once the process steps were established in some detail, leach studies were conducted to determine the time necessary for the leaching unit operation. The agglomerations that remained from the jaw crusher mentioned above disintegrated to a very fine particle size during leaching by combined reaction with the solution and agitation. The particle size distribution of solids in the slurry was not precisely measured as it represented a run of mill material. Additional grinding of this material was not considered desirable due to economic reasons. The leach procedures took two forms. Either as stirred batch leaches preformed in appropriately sized beakers or flasks with magnetic stir bars. In parallel experiments conditions were held exactly equal including agitation rate, container

size, etc., but these conditions varied as appropriate between experiments. Later testing using larger samples particularly the 1kg sample, used a top stirred agitated 5-gallon tank. A picture of this setup is shown in figure 3.2.

3.3 Filtering

Filtering was necessary after several operations steps including; leaching, pH adjustment, precipitation via zinc addition, and others. The filtering procedure was largely based on the volume of material that needed to be filtered. Small tests could be readily filtered directly using

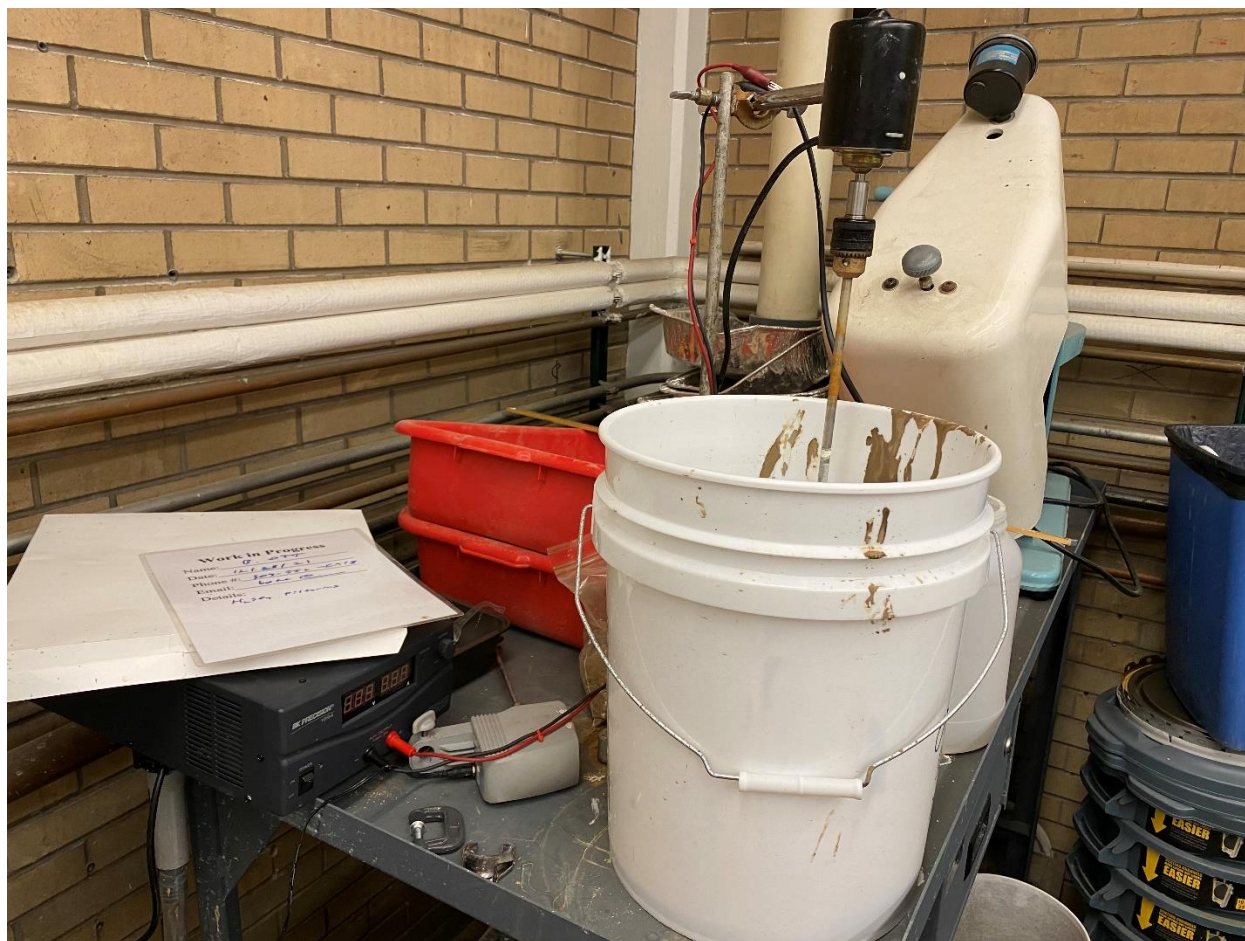


Figure 3.2: Picture of stirred vat leach apparatus

fine filter paper (2.5micron pore size) note that pore size is not a definition of the particles passing through as the filter cake causes most of the filtering action rather than the paper. Larger tests were filtered either A) with larger gravity filters, B) with vacuum filters, or C) in a large pressure filter. Filtering at ambient pressures is slow but was sometimes observed to produce a well filtered product that could not be duplicated using higher pressures. For this reason tests

were often run in parallel with patience during filtering being required. Particularly for SX tests a very clean filtrate was desired and so filtrates were often re-filtered to achieve a sufficiently clean solution. Pressure filtering was desirable for large slurry volumes. Generally, the procedure consisted of filtering a portion of the slurry until the filtrate ran observably clear, at this point the dirty filtrate was recirculated to the filter to filter across the built-up filter cake and produce a clean filtrate. The pressure filter is shown in figure 3.3. This filter was particularly useful for the 10-liter flowsheet test.

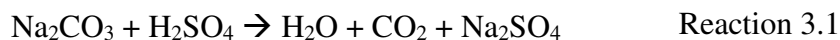
3.4 pH adjustment

The leach liquor pH was adjusted by soda ash addition, for tests conducted over a range of pH values. In these cases, the leaches were carried out with a high acid concentration and that



Figure 3.3: Laboratory pressure filter; the filter body and lid swing into place above the pad in the middle of the image

acid was neutralized partially by soda ash to adjust the pH to the desired range. The loaded pulp was filtered after pH adjustment as gallium, iron, and copper were more stable than in lower pH solutions. After filtering, the leach liquors at various pH's could be used for solvent extraction or precipitation experimentation. Soda ash must be added carefully as CO₂ evolution from the sulfuric acid, soda ash neutralization reaction (as seen in reaction 3.1) can cause excessive froth and overflow the container.



This was normally carried out for small samples using a mixing plate with magnetic agitation similar to the setup used for leach tests. Sodium carbonate was added in solid form to grossly raise the pH from leach conditions to near precipitation or solvent extraction conditions. As the pH approached those used for precipitation or solvent extraction, sodium carbonate was added as a solution using a pipette for precise pH control. The level of care with respect to base addition is mandated by the titration curve behavior sensitivity. Additionally, titration with sodium hydroxide, lead to other problems with metal stability in the aqueous phase and so soda ash was used for this experimentation. The pH changes drastically with relatively little addition of base around the inflection point. This is due to the low equilibrium constant for the second proton in the sulfuric acid structure. Some early work used caustic rather than soda ash for pH adjustments but samples often gelled in these cases which led to difficult filtering and solvent extraction processing.

3.5 Solvent Extraction Procedures

Solvent extraction (SX) requires contact between two liquid phases; pregnant leach liquor and an organic phase. Two extractants were tested in initial tests, these being Kelex-100 and Cyanex-923. Cyanex is produced by Solvay chemical company. Kelex is produced by several Chinese companies and is well studied in the literature.

3.5.1 Cyanex-923 Procedures

Cyanex-923 test procedures were originally based on data published by Gupta [9]. Exploratory tests typically referred to as shakeout tests followed the parameters presented in Table 3.1.

Table 3.1: Cyanex SX Parameters

Parameter	Base Case Value, Range
Mixing time	5 min, 1-10 min
Temperature	Room Temperature, up to 90°C
Cyanex concentration	1.8g/l toluene
Solution pH	4.5, 3.0-5.0
Liquid : Organic ratio	1:1, 2:1 to 1:10

These variables were modified as will be discussed in the results section, Chapter 4. The Cyanex loading unit operation always consisted of shakeout tests in separatory funnels. The stripping operation was similarly designed according to Gupta's results utilizing shakeout tests similar to the loading tests.

3.5.2 Kelex-100 Procedures

Kelex-100 experimental testing design was primarily based on the results published by Kekesi. [10] This consisted of 13 hour mixing periods which required mixing using magnetic stir plates. The stirring speed was adjusted such that the phases maintained proper mixing, in different sized containers.

3.5.3 Novel Extractant Procedures

The novel SX extractants received from ORNL were diluted with Isopar to 0.1 molar concentration. The initial tests were completed at pH 0.5 after a 3M sulfuric acid leach of the CLP sample. The first test employed a 5-minute shakeout procedure in a separatory funnel based on those conducted for Cyanex previously. One of the three extractants showed significant absorption for this test. The other two extractants were retested with 2 hour mixing times using beakers with magnetic stir bars as done for Kelex-100 and then disengagement and separation of phases by separatory funnel.

3.6 Precipitation Procedures

Precipitation was carried out by zinc and/or iron addition with amounts as specified in the discussion section. Several experiments had samples at several pHs, in this case a feed was prepared and filtered. A measured amount of this feed was split into the several samples and pH

was adjusted as necessary. Upon the pH adjustment zinc and/or iron were added, then samples were filtered. The filter residue was analyzed by re-dissolving in sulfuric acid and then analysis by ICP-MS.

3.7 Acid Regeneration Procedures

The acid regeneration work started with thermodynamic modeling of the system using HSC. It was determined that the equilibrium conditions of a mixture of fuel gases and sodium sulfate would yield soda ash and hydrogen sulfide. These results are discussed in more detail in Chapter 7.

An apparatus was designed to test these conditions with a designed maximum temperature of 350°C. After results showed low conversions, the furnace was upgraded to allow tests up to 800°C. The second furnace can be seen in figure 3.5. The furnaces were designed for handling excess reactant gases (carbon monoxide, hydrogen, and methane) as well as dihydrogen sulfide from the reaction. Analytical methods and procedures

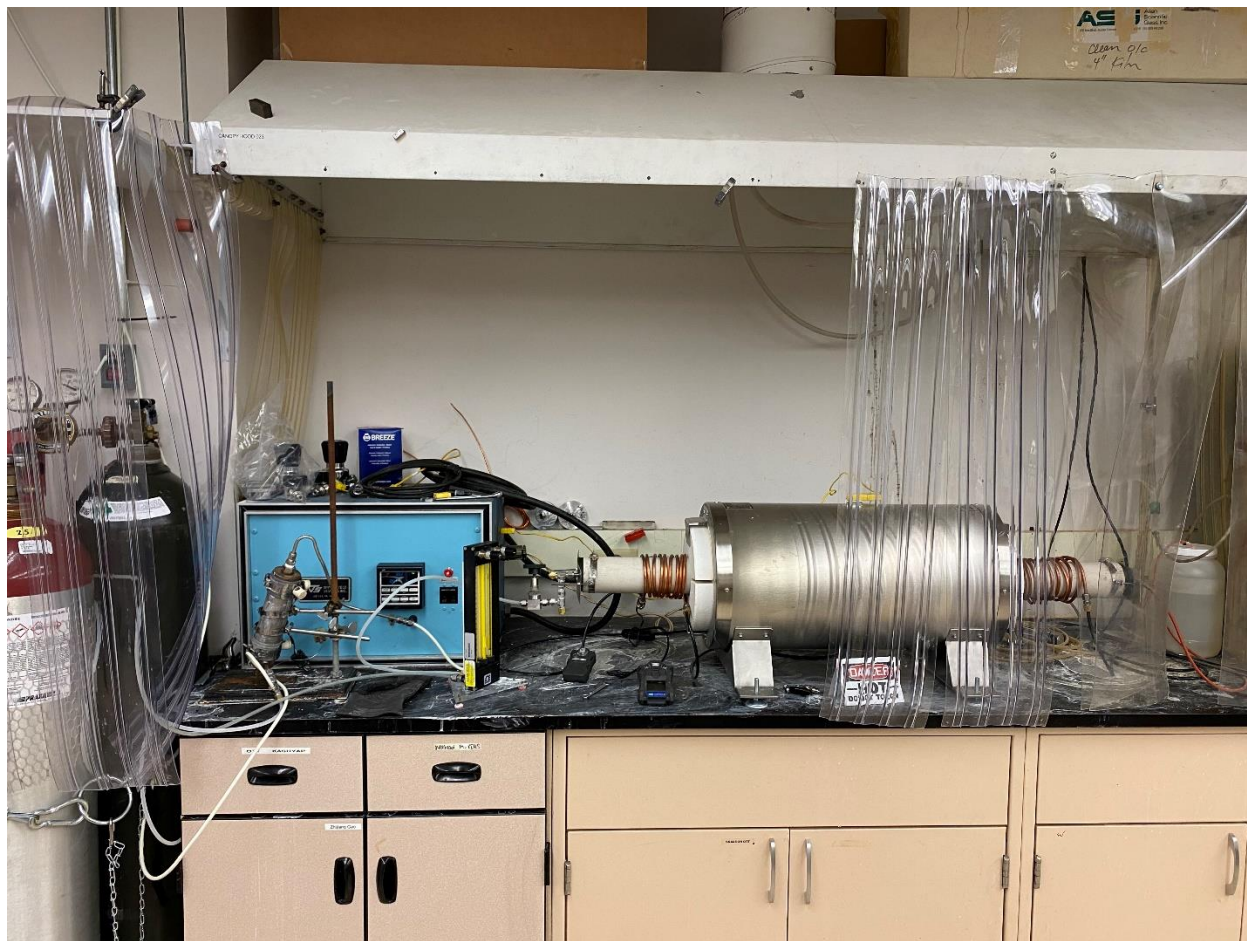


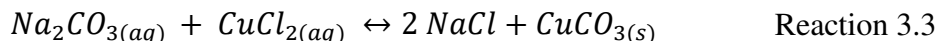
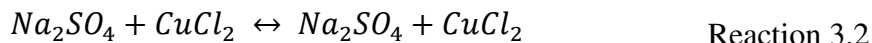
Figure 3.4: Furnace setup for acid regeneration testwork.

3.8 Design of Experiments and Statistical Methodology

Designed experiments are an approach to process improvement. It is hoped that the designed experiments herein can provide guidance on the influence of various process parameters for those unit operations most closely studied. Not all tests were conducted using a formal designed experiment as some amount of knowledge about the various parameters and the amount they should be modified is necessary for a properly designed experiment. The two main steps for designing of experiments is the choice of factors and levels, and the selection of the response variable. The first, choice of factors and levels, must be based on knowledge of the process. For example, in leach studies various parameters are understood to generally affect leach recovery, the magnitude of the change between two levels in these parameters must be decided by the researcher with understanding of the expected magnitude that will generate significant results. The determination of the response variable is based on knowledge of the flowsheet and the specific goals of the unit operation such that the appropriate metrics can be measured to determine the result of the test.

3.9 Wet Chemical Method: Copper Chloride Precipitation

A simple chemical reaction between sodium carbonate and copper chloride allows for a rapid analysis of the amount of sodium sulfate converted to sodium carbonate. The reactions important to this analysis are shown in reactions 3.2 and 3.3.



Sodium sulfate does not react with copper chloride in solution; However, sodium carbonate reacts with copper chloride to form sodium chloride salt and a solid copper carbonate precipitate. By filtering and massing the precipitate the amount of conversion from sodium sulfate to sodium carbonate can be determined.

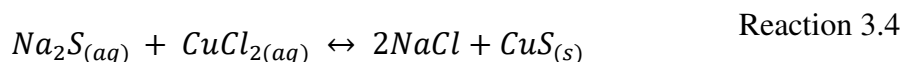
This technique is suitable to determine the amount of sodium carbonate in a mixture of sodium sulfate and sodium carbonate. Figure 3.6 shows the results of these reactions. It should be noted that there is a “blind spot” in this analytical technique in that it will not react with sodium sulfate carbonate double salt. This phase was observed to be present in the higher reaction temperature samples by XRD. This phase is discussed in the literature by Wang et al. [11], and is not expected to be stable under the conditions in the reactor but may have different reaction kinetics than the sodium sulfate direct conversion to sodium carbonate.

Modifications were made to this procedure for samples where ash could be observed. The samples were leached with water, usually overnight, until the salts had dissolved. The ash would generally be suspended in the water and could readily be filtered, the filtrate would then be mixed with copper chloride and the precipitates massed as described above.



Figure 3.5: Copper Chloride wet chem method for determining sodium carbonate amount (left is the copper chloride solution, middle is the solid white precipitate formed by the reaction of sodium carbonate and copper chloride, and right is the filtered precipitate for analysis).

In certain XRD results the presence of sodium sulfide was observed. Sodium sulfide reacts with copper chloride according to the reaction 3.4. The products are sodium chloride salt and an only slightly soluble copper sulfide. The precipitates from this reaction are easy to differentiate from those of reaction 3.3 above as they form a black precipitate rather than the white copper carbonate phase.



There is an observable difference in the appearance of copper sulfide and copper carbonate, however it is very difficult to differentiate them in this analytical methodology, XRD is used to differentiate these phases but cannot be used to conclusively identify the relative phase concentrations. A combined methodology was developed whereby the salt from the furnace was scanned by XRD to ensure that sodium sulfide was not present in significant quantities. If there was no sodium sulfide observed the copper chloride precipitate test could be used to quantify the sodium carbonate composition, if sodium sulfide was present this test was not effective in determining the percent conversion.

3.10 X-Ray Diffractometry

X-Ray diffractometry (XRD) is an analytical technique that uses an X-ray source to determine the interplanar spacing in crystal structures in a sample. The device takes advantage of

a source with a known frequency pointed at a surface. The x-rays can either reflect off of the external plane of the surface or from underlying layers of the crystal structure. At certain angles these reflections will interact constructively according to Braggs Law. At angles where the waves destructively interfere there is no ordered crystal plane.

Using this technique, the specific phases in a sample can be analyzed and determined. All of the XRD results herein were gathered using powder XRD techniques. With this technique pulverized or powder samples are presented to the XRD in a sample holder like that seen in

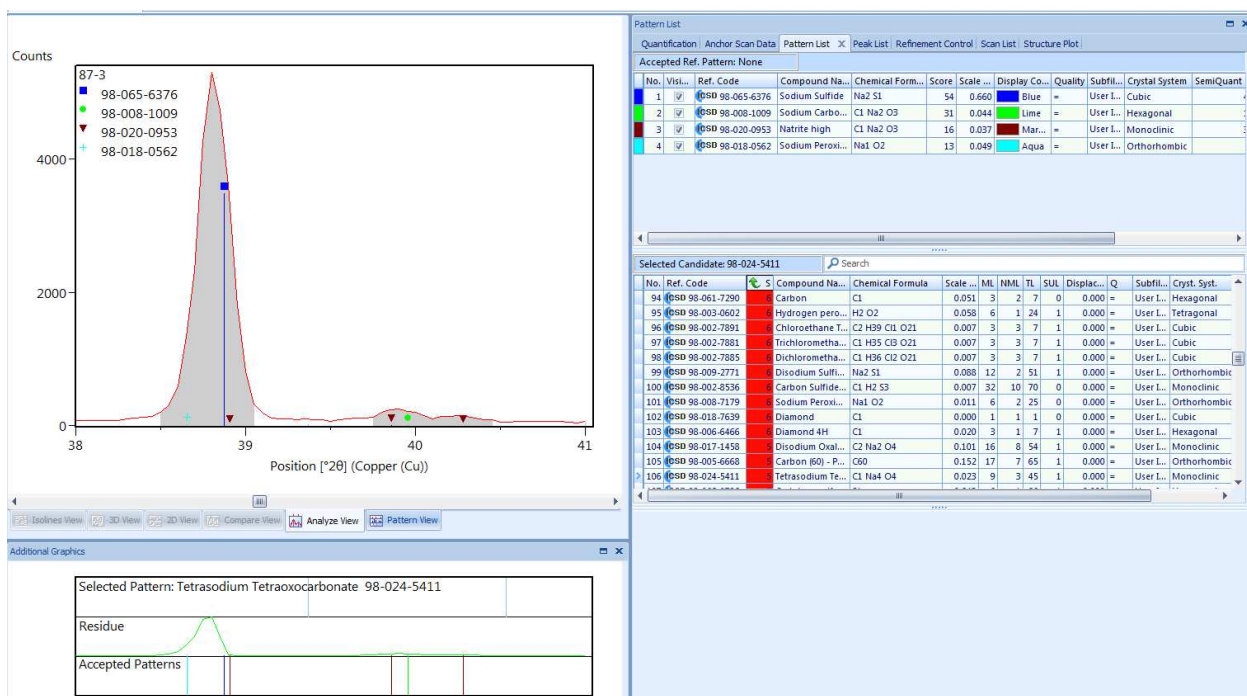


Figure 3.6: Example of XRD pattern, this one is for the CLP sample.

Figure 3.6. Samples must be pulverized to extremely small particle sizes on the order of 50 microns to produce useful XRD results, this is generally accomplished by mortar and pestle for small samples where loss of material is not tolerable or by ring and puck pulverizer if larger samples are available. The XRD instrument has various settings that can increase sensitivity and accuracy as a function of increased scanning time. After the XRD data is collected and interpretation is made with the assistance of software to determine the peaks and their relative intensities. Software can then be used to match the measured data with literature reference values of XRD peaks for various phases. The literature reference peaks are of well-known diffraction angle and relative intensity which enables both phase identification and quantification of relative phase amounts. The matching of phases relies on logical assessment of the phases that are likely

to be present. Matching phases for these tests was relatively easy as all elements other than sodium, sulfur, oxygen, carbon, and hydrogen could be eliminated from the matching software. An example of the matching procedure can be seen in Figure 3.7.

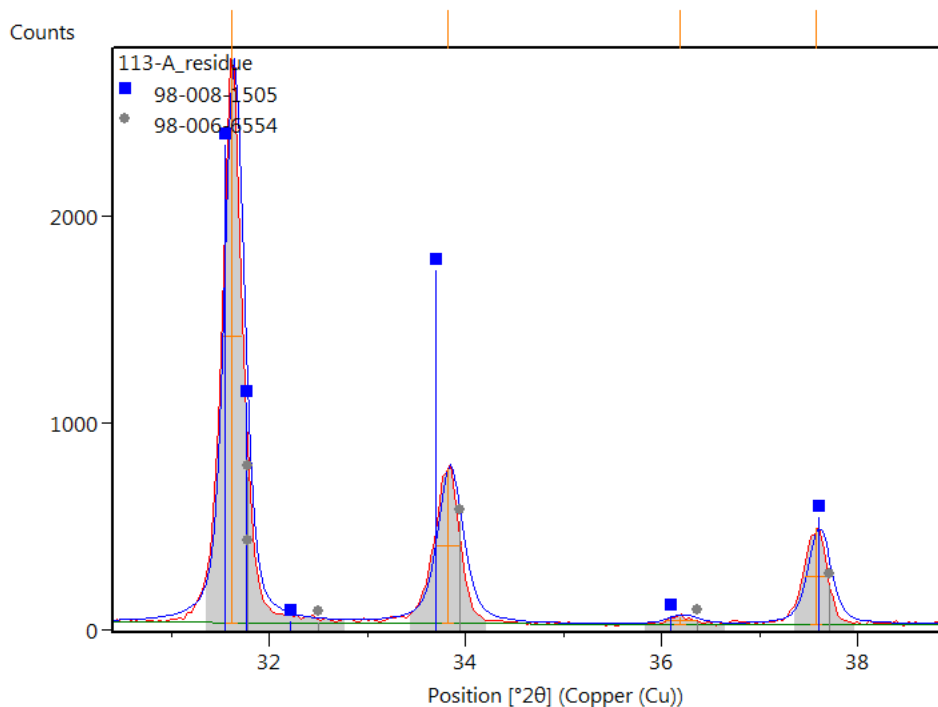


Figure 3.7: Overlapping XRD peaks can be seen with the broad peak at 34 degrees

The measured spectrum on the top left has been manipulated by the computer algorithm to eliminate noise and interference. This pattern is normally focused on small areas around distinct peaks to ensure fit with literature values for diffraction patterns. The patterns available are listed on the right pane with the top pane showing accepted patterns, and the bottom pane showing prospective patterns. The third column under the candidate patterns represents an algorithmic score for the pattern in question. High scores indicate a better match. The selection of phases is highly dependent upon the operator not only for selection of elements expected based on experimental conditions but also for identification of peaks, especially those where multiple peaks closely overlap. An example of overlapping peaks can be seen in figure 3.8. Knowledge of experimental conditions including for instance, temperatures, cooling rates, and atmospheric compositions can help identify phases that are likely present based on an understanding of phase stability. For example, in this research XRD results were mostly from

high temperature reduction test products, and the informed XRD operator could assess that hydrates are unlikely to have formed under these conditions.

XRD is typically not considered suitable for quantification of phases without significant data adjustment and standardization and is only useful in this case to identify major phases. For this reason, a combined XRD and wet-chemical method were developed to quantify phases observed in acid regeneration samples. This consisted of running a 1-hour XRD scan to detect and determine if sodium sulfide was present as a significant constituent (significant enough for XRD identification), only on samples where sulfide was not a major contributor were copper chloride precipitation reactions useful for analysis of reaction progress.

3.11 ICP-MS

Inductively Coupled Plasma Mass Spectrometry (ICP-MS) is used for quantitative elemental analysis of aqueous material. Most samples in this work for which ICP-MS was desired were aqueous samples (solvent extraction raffinates or feeds, & leach liquors) Samples that were not already in aqueous solution were digested for analysis. Samples are prepared by extracting a portion via pipet and subsequent dilution to reduce the total dissolved solids content to below 1ppm. The CSM ICP's sampling arm robot can carry out a dilution of up to 100:1 so samples must be prepared to below 100ppm before the ICP and its associated machinery can analyze them. Due to maintenance down time on the CSM ICP-MS some samples were analyzed at private laboratories using ICP-MS instruments. When possible, analyses were conducted in duplicate to confirm results. The ICP-MS results at CSM are conducted in triplicate with the machine drawing the same sample 3 separate times in a single test run.

3.11.1 ICP-MS Dilution Procedure

1. The necessary dilution is estimated using the known sample mass that is dissolved in the measured volume of sample. The ICP-MS requires an input below 1ppm total dissolved solids but the dilution robot can dilute up to 100x. Therefore, the dilution must reduce the dissolved solids amount to below 100ppm
2. The scale is tared with a 50ml sealable vial
3. the 1.0-liter sample prepared by digestion above is sampled using a pipet.
4. This sample is added by pipette to the empty 50ml vial
5. The mass of the sample is recorded and the necessary diluent volume is determined
6. The sample is tared again

7. The sample is diluted using analytically pure 2% nitric acid solution.
8. The mass of added diluent is recorded

3.12 ICP-AES, ICP-OES

Local outside laboratories operate both ICP-AES and ICP-OES different technologies to the ICP-MS. Both were shown to be suitable for base metal determinations at relatively high concentrations in the solution. The gallium, germanium, & indium were usually at concentrations too low to be analyzed by these techniques. One option used by these analytical laboratories is to determine the base metal composition on ICP-AES or OES and then use ICP-MS for the lower concentration critical metals. Samples for external laboratories were generally not diluted before delivery to those laboratories.

3.13 Total Digestion procedure

The feed material was analyzed by total digestion and analysis by ICP-MS, as follows: 60ml of aqua regia were prepared, nominally 0.5g sample of feed material was added to the aqua regia at 80°C, after 2 hours 2ml of HF were added to the solution, an additional 2ml of HF was added after 5 hours as there was some remaining residue observed in the sample. The mixture was allowed to continue digesting for ~18 hours at high temperature until there was no residue left in the sample, after which, the sample was diluted for ICP-MS chemical analysis.

CHAPTER 4 DISCUSSION OF SEPARATIONS RESULTS

4.1 Proposed flowsheets concepts

4.1.1 solvent extraction

The project definition originally proposed evaluating solvent extraction as a possibility for recovery of gallium from the zinc smelter residue. Previous studies available in the literature showed Kelex-100 as a potential extractant mostly used to separate gallium from Bayer process aluminum containing liquors, not high zinc/iron liquors. Other previous studies have studied Cyanex varieties for separating gallium from zinc residues. Other extractants in the literature include OPAP and TGAs. This research focused on Kelex-100 and Cyanex-923. Kelex was selected due to the thorough literature on its application and its availability. Cyanex-923 was recommended by contacts at Solvay Chemical as a potential extractant for this application.

The proposed flowsheet (Figure 4.1) included some leach of the CLP feed, probably with sulfuric acid, changing the pH to that required for the extraction to the organic phase, filtering if any solids precipitated during this pH adjustment, and then solvent extraction.

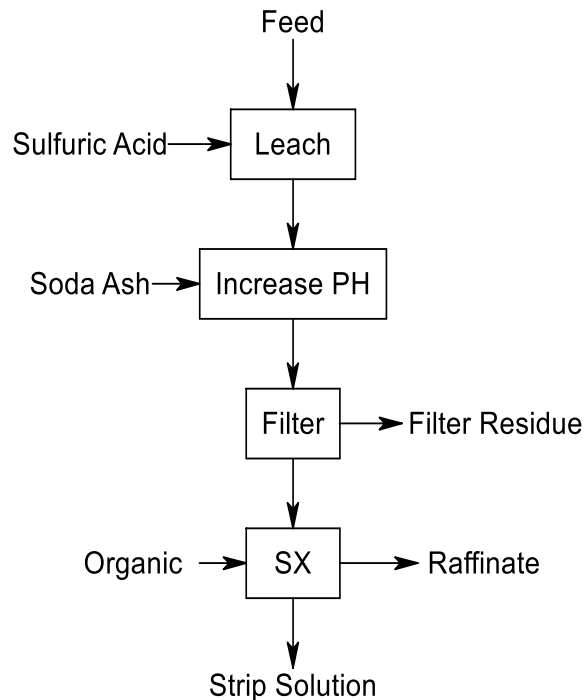


Figure 4.1: Proposed flowsheet for gallium recovery by solvent extraction

4.1.2 Precipitation

The precipitation of a gallium rich residue was first observed analyzing filter residues from initial solvent extraction experiments. Industry contacts suggested that further study of the precipitate was worthwhile as previous researchers handling this material had not paid appropriate attention to the precipitate residues instead focusing solely on SX/IX unit operations. The proposed precipitation process is illustrated in Figure 4.2.

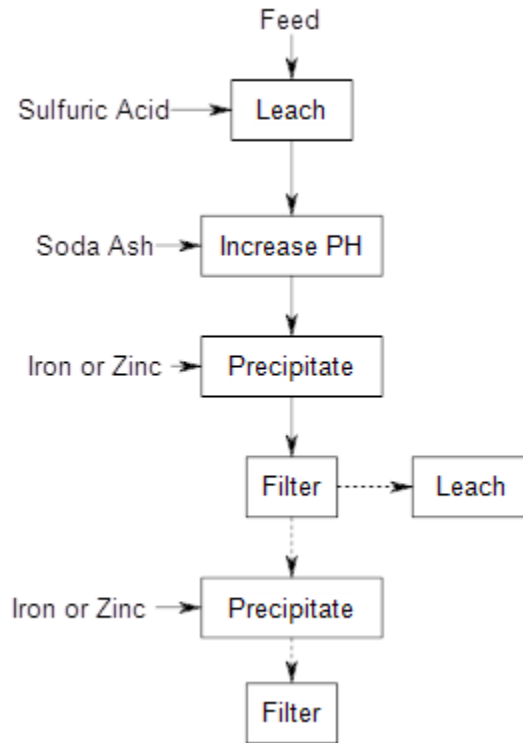


Figure 4.2: Conceptual flowsheet for gallium recovery via precipitation

4.1.3 Lixiviant Regeneration

Both of these process versions include a leaching unit operation and a subsequent adjustment of the pH to a point where the separation can be accomplished. This suggests that the lixiviant regeneration operation as part of this process may help reduce the costs of recovering material by either of these processes. The concept is shown in Figure 4.3. The valuable reagents recovered by the regeneration process include sodium carbonate that can be directly reused in the pH adjustment common to each process and sulfuric acid that can be directly reused in the leaching unit operation. Some development of each of these unit operations; The solvent

extraction, the precipitation or solvent extraction, and the lixiviant regeneration is developed in greater detail as part of the process development.

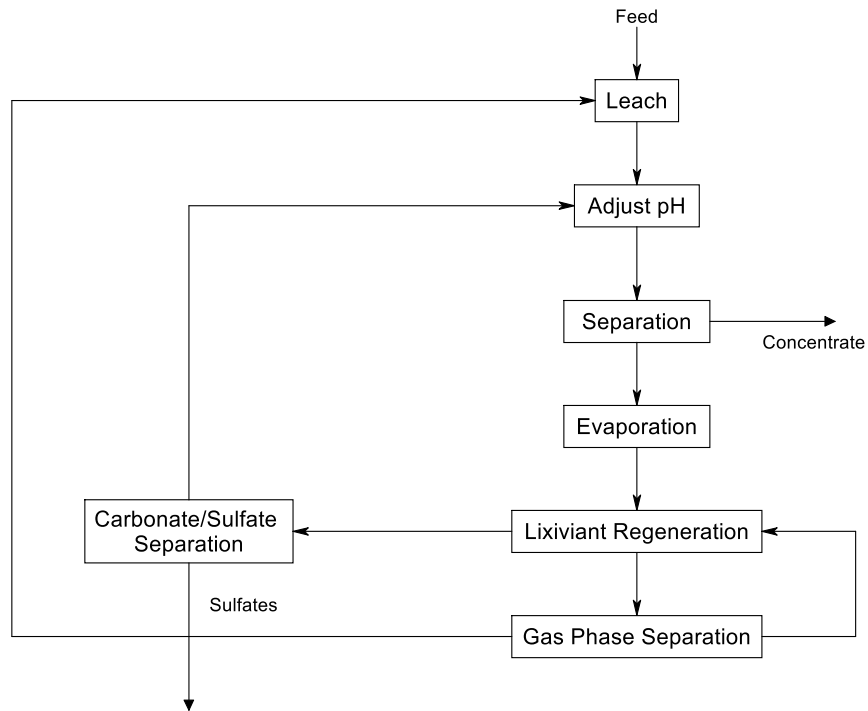


Figure 4.3: Conceptual flowsheet for acid regeneration as part of a gallium recovery process

4.2 Mineralogy and quantification of feed material

4.2.1 Summary of samples

There are 4 samples originally obtained as part of this and another project for critical materials recovery from this domestic resource. Initial research showed that the CLP sample had a concentration of gallium. This material was selected for further development of a process for gallium recovery. Other samples were considered and evaluated to various degrees but the primary focus was on this CLP material.

4.2.2 Sample Preparation

The CLP sample was delivered in 4-gallon buckets shown in Figure 3.1. The material was damp and formed agglomerations as are apparent in the image to the far left in Figure 3.1. For this reason, the sample was dried somewhat and crushed using a jaw crusher to break up the agglomerations such that splitting and sampling could be accomplished appropriately. The

crushed material looks like that in figure 4.4. Splits are made using a jones splitter to make congruent samples for various testing.



Figure 4.4: Picture of the CLP sample after crushing to break up large agglomerations

4.2.3 LA-ICP-MS

LA-ICP-MS results were obtained via partnership with ORNL. Data from these scans are shown in Figure 4.5. LA-ICP-MS is a potential tool for identifying the association of various metals. This instrument particularly is more useful than other options for mineralogical studies for extremely low concentration metals. The LA-ICP-MS results suggest that gallium is associated with the zinc phase.

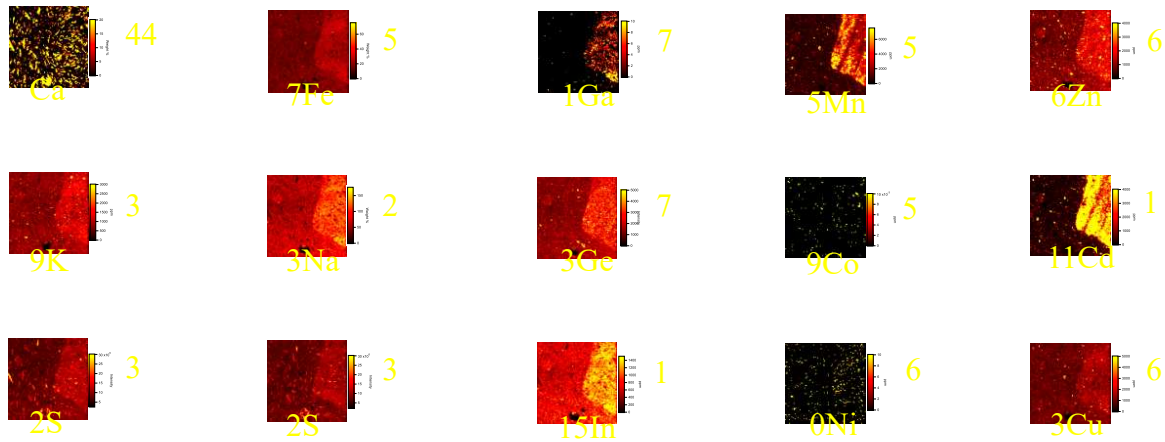


Figure 4.5: LA-ICP-MS results from the CLP sample

4.2.4 Digestion of CLP sample

Digestion of the CLP sample was necessary for determination of the grade of the feed material so that recoveries of various metals could be determined as part of the process. Sulfuric acid did not leach the majority of the material. The first attempt at digestion used aqua regia but significant solid residue remained. A procedure using HF was used to finally digest the sample with no solid residue. This procedure is detailed in the methods section (3.12). The solution was diluted with 2% nitric acid and concentrations were measured via ICP-MS. The composition of the sample determined by complete digestion is presented in Table 4.1.

Table 4.1: Metals composition of the CLP sample via complete digestion

Digestion Results (%)	
Al	6.79%
Fe	20.5%
Cu	1.32%
Zn	18.9%
Ga	0.62%
Cd	0.26%
In	0.0024%

4.2.5 CLP XRD Results

The Mineralogy of the CLP sample is determined by XRD to inform understanding of the materials behavior in both leaching and the proposed reduction process addition. In the light of this analysis, it is important to remember that the XRD is semi-quantitative only, any statements about the relative phase compositions are conjecture at best and only major phases would reliably be identified. The matching should include not just major peaks but also consider the minor peaks for each phase. It would be reasonable to summarize the XRD results as indicating the presence of metahohmannite, hydronium jarosite, Franklinite, and zinc sulfide.

4.2.5.1 Metahohmannite

Metahohmannite is a hydrated iron sulfate phase with lower hydration than hohmannite. In its pure form it has the composition $\text{Fe}_2(\text{SO}_4)_2\text{O} \cdot 4\text{H}_2\text{O}$. The matching of the characteristic peaks can be seen in figure 4.6. According to XRD this phase represents half of the material present in the CLP sample.

4.2.5.2 Hydronium Jarosite

Hydronium jarosite is an amber to brown mineral consisting of iron sulfate and hydroxide with the formula $(\text{H}_3\text{O})\text{Fe}_3(\text{SO}_4)_2(\text{OH})_6$. The iron is in the Ferric oxidation state. The

characteristic peaks are at angles of 17.5 and 29. These peaks can be seen in the sample in Figure 4.6. This phase, according to the XRD, makes up on the order of 1/4th of the CLP material.

4.2.5.3 Franklinite

Franklinite is an oxide spinel that may have both ferrous and ferric iron along with zinc forming a mixed oxide. Franklinite is a minor phase in the sample.

4.2.5.4 Zinc Sulfide

Zinc sulfide is among the most common natural forms of zinc in nature. A common mineral form is sphalerite. Zinc sulfide is a minor phase in the CLP material.

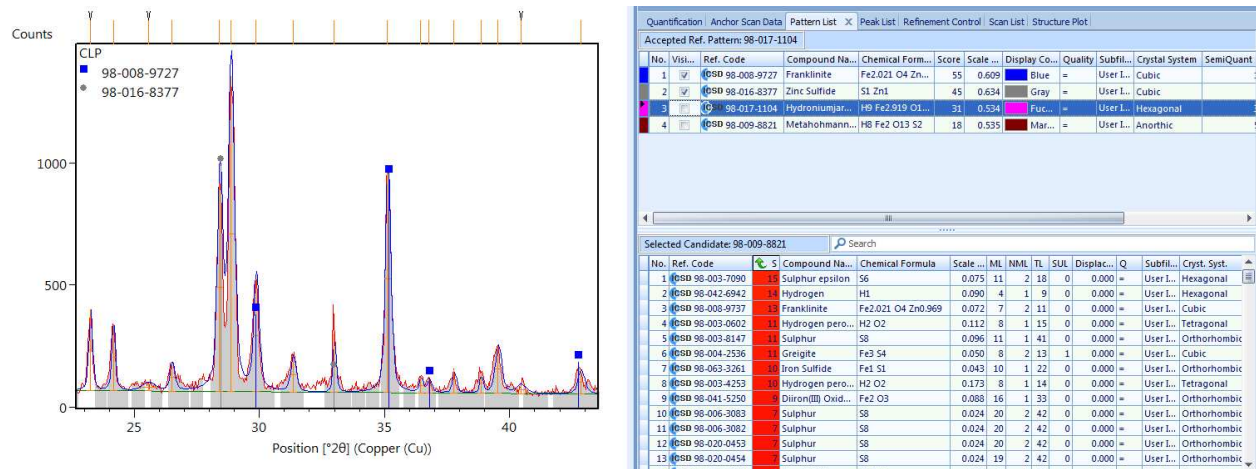


Figure 4.6: XRD result for the CLP sample along with major phases.

4.3 Leaching studies

Leaching studies were completed to determine the impact of various process parameters on the leaching results. The study is particularly interested in maximizing gallium recovery and in the ratio of gallium to zinc in solution. This is because subsequent unit operations particularly solvent extraction are limited by the activity of the ions in solution, in solutions where gallium is several orders of magnitude more dilute than zinc the low activity of gallium makes solvent extraction extremely difficult. In the precipitation work zinc recovery is considered positive as one of the products is a zinc concentrate that may be recirculated to the process. Iron is considered detrimental as it mostly reports to a waste product stream in that flowsheet.

4.3.1 Leaching Conditions Test work

The test work related to determining acceptable leaching conditions was initiated to determine parameters under which leach recovery could be improved. A simple conceptual flowsheet for these tests is shown in Figure 4.7.

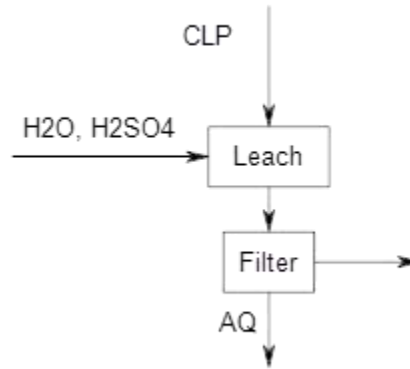


Figure 4.7: Flowsheet to illustrate leaching test procedure

Results are shown in Figure 4.8. The experiment was designed to determine the effect of various leaching parameters on the room temperature leach recovery for gallium and other key metals. The parameters for this test are presented in Table 4.2. The results are presented in the figure 4.8. For this graph the X-axis shows the acid concentration, Y-axis shows time, Color shows slurry density and the bubble diameter shows gallium recovery. This data is analyzed via statistical regression, the results of which are compiled in Appendix II.

Table 4.2: Parameters for sulfuric acid leaching tests

Experiment	Acid Con	Time	Slurry Density	Temperature
1	5	2	10	25
2	50	4	15	25
3	150	6	20	25
4	5	4	20	25
5	50	6	10	25
6	150	2	15	25
7	5	6	15	25
8	50	2	20	25
9	150	4	10	25

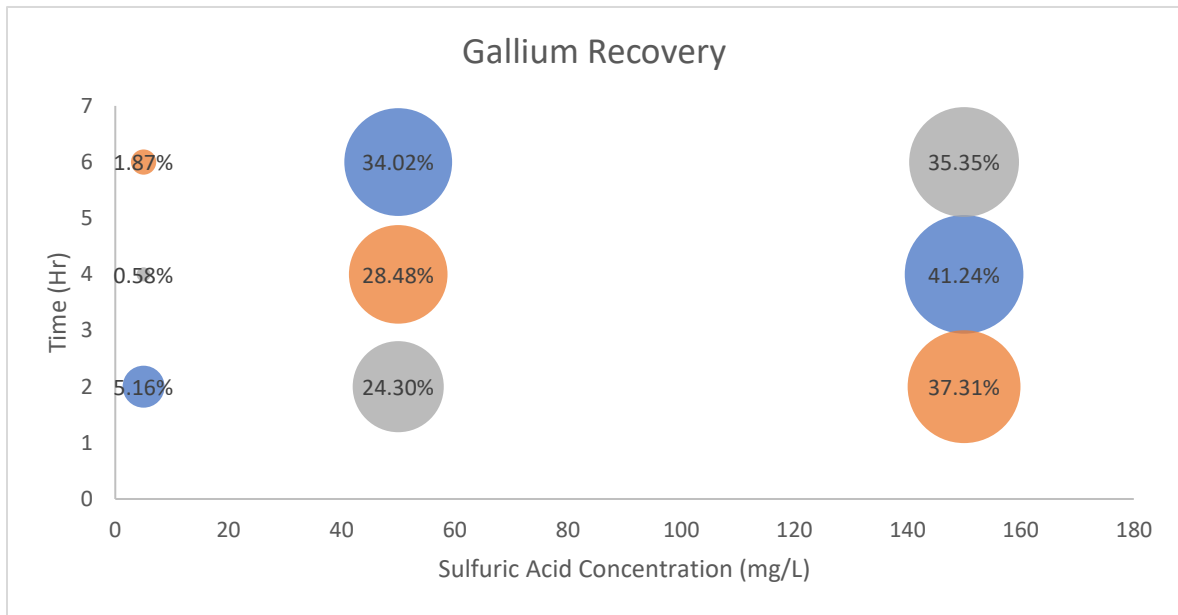


Figure 4.8: graphical illustration of gallium recovery (circle diameter) as a function of acid concentration and leaching time

These analyses show the parameters that affect recovery for the metals of primary interest in the CLP sample, these analyzed effects are limited by the mineralogy of the CLP sample so this data cannot be extrapolated to predict a condition for 100% gallium leach recovery, that practical limit for gallium recovery is not discussed herein. However, this analysis can be used to determine whether parameters may be changed (perhaps to improve plant economics discussed in chapter 5) and not experience loss of recovery. For the SX process the maximization of gallium recovery and minimization of zinc recovery was desirable, however for the precipitation process zinc is a positive contributor to process economics and so recovery of zinc is desirable. The iron is primarily a waste product but its positive or negative contribution to the process is generally negligible. The copper recovery may be interesting as it generally represents a valuable commodity but, in the fractions where copper is concentrated, it is difficult to separate from the main diluents (mostly iron).

The designed experiments reduced the total number of tests run (and the cost associated with achieving these results). The three parameters shown in the chart are acid concentration (A), time (B), and slurry density (C). The analysis also considers whether the interaction of two or all three of these parameters is influential over the independent variable (recovery in this study). The primary statistical test used to make a conclusion about the significance of the affect is the p-value. In the case of the p-value being less than alpha (the significance level) the parameter is

considered significant, if the p-value is greater than alpha, the parameter is considered insignificant. In this discussion significance is used specifically to refer to statistically significant results. The value of alpha is defined for this study as 0.05 based on a 95% confidence that parameters outside of this range will be insignificant to the signal parameter.

The analysis shows that the acid concentration is a significant contributor to the recovery of gallium, zinc, and iron. Other parameters did not strongly influence the metals recovery for any of the three metals. And there are no interactions between any of the parameters that may be considered affectual to the confidence level required.

4.3.2 Temperature dependence of leach behavior

The leaching behavior is studied at several temperatures to identify parameters under which recovery could be improved the recovery of various metals of interest at several temperatures is shown in figure 4.9. These tests were two hour leaches of CLP material with a slurry density of 10% and a 100g/l sulfuric acid composition.

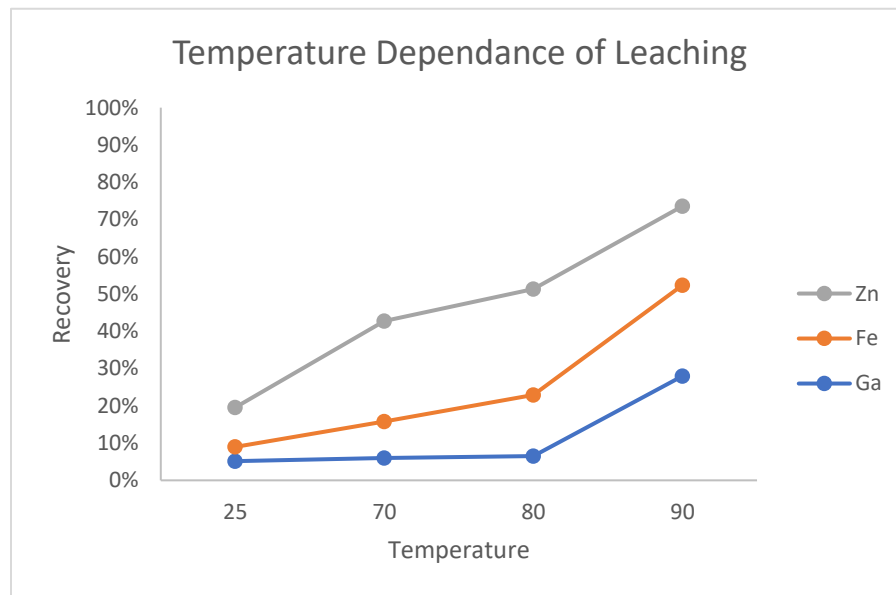


Figure 4.9: Effect of temperature on leach recovery.

These tests were conducted prior to the other tests for leaching behavior and so were 2-hour tests to keep testing short and allow easier monitoring of temperature over a short time period. The results show that recovery of all three metals of interest are improved with higher leaching temperatures, the zinc recovery was higher for all samples than the iron and the gallium. At very high temperatures (near the boiling point of the aqueous acid solution) the leach

recovery jumped to very high levels including 80% zinc recovery. Ambient temperature leaching was used for the integrated flowsheets as high temperature leaching is generally speaking more expensive, the possible changes to process performance are evaluated as part of the sensitivity analysis in section 5.3.1.

4.3.3 Alternative Leach Strategies

4.3.3.1 Caustic Leach Study

Caustic leaching was originally interesting as part of a solvent extraction process utilizing Kelex-100 to concentrate gallium in caustic liquors. though this study was mostly unsuccessful the results influenced the design of the sequential precipitation flowsheet. The test work tried to recover gallium from the CLP sample at a range of caustic compositions during overnight stirred leach tests. The data in Table 4.3 is based on these stirred vat leach tests completed over 16 hours with a slurry density of 10% at room temperature.

Table 4.3: Metal recovery results for caustic leach tests

pH	Recovery (%)					
	Ga	In	Fe	Zn	Al	Cu
14	29.8%	0.0%	0.0%	100.0%	100.0%	0.0%
13.5	15.9%	0.0%	0.0%	100.0%	97.0%	0.0%
13	1.0%	0.0%	0.0%	100.0%	0.8%	0.0%
12.5	0.6%	0.0%	0.0%	100.0%	1.9%	0.0%
11.94	0.0%	0.0%	0.0%	100.0%	0.3%	0.0%
11.5	0.0%	0.0%	0.0%	100.0%	0.2%	0.0%
10.98	0.0%	0.0%	0.0%	100.0%	0.3%	0.0%
10.61	0.0%	0.0%	0.0%	100.0%	0.2%	0.0%

The results showed a recovery of aluminum, zinc, and gallium to the caustic liquor phase with iron, copper, and some other metals staying in the solid. Aluminum is not considered problematic for the Kelex solvent extraction work as it is not extracted by Kelex-100, zinc however is extracted by Kelex and so will interfere with making a clean gallium concentrate. It is notable that caustic leaching may be used to recover gallium preferentially from iron.

4.3.3.2 Sequential Leach Study

An additional leach study was completed to show metal recovery by means of multi-step leaching, if particular interest were the results of combined caustic and sulfuric acid leaching, and leaching with different acid concentrations in sequence. All of these leaches were 24-hour leaches at room temperature.

Table 4.4: Sequential leach results

	Total Recovery			First Leach			Second Leach		
	Zn	Ga	Fe	Zn	Ga	Fe	Zn	Ga	Fe
150 g/l H2SO4	15.41%	34.71%	25.03%						
150 g/l H2SO4 + 150 g/l HCl	21.97%	49.95%	40.56%	15.41%	34.71%	25.03%	6.56%	15.24%	15.53%
150 g/l HNO3 + 150 g/l H2SO4	22.61%	52.23%	44.19%	17.88%	40.67%	31.48%	4.73%	11.56%	12.71%
150g/l NaOH + 150 g/l H2SO4	17.86%	55.74%	41.03%	6.53%	27.43%	0.06%	11.33%	28.31%	40.96%
150 g/l H2SO4 + 150g/l NaOH	16.93%	40.52%	28.91%	16.06%	37.00%	28.92%	0.87%	3.52%	0.00%
150 g/l HNO3 + 150 g/l NaOH	26.22%	55.57%	34.46%	22.72%	42.41%	34.39%	3.50%	13.16%	0.08%

The most interesting results are that for caustic and sulfuric acid combined. Particularly the caustic leach followed by sulfuric leaching yielded very high gallium recovery higher than those for just sulfuric leaching. The caustic leach does not recover iron and so it may lead to easier separation of the gallium from the base metals. The caustic leach liquors for the fourth, fifth, and sixth leach series showed gallium grades of 11, 11, and 10 percent respectively. These might need very limited upgrading to produce a saleable product. This is most likely possible via Kelex-100 solvent extraction. Interestingly re-leaching with additional sulfuric acid, even higher concentration sulfuric acid, did not improve recovery of these three primary metals. The integrated flowsheet and subsequent economic model are based on single step sulfuric acid leaching nitric showed slightly improved zinc and gallium recovery than sulfuric but is considerably more expensive on the order of \$265/ton compared to \$135 for sulfuric acid. Caustic re-leaching of the residue may contribute to higher yields with additional test work to determine optimize those leach conditions to some degree.

4.3.3.3 Roast-Leach Study

Another researcher at CSM has been doing simultaneous work on a similar feed containing indium in a zinc ferrite lattice. He has shown that a pyrometallurgical reduction of the zinc ferrite to zinc oxide and iron oxides has improved leach recoveries for zinc and the critical materials in the ferrite lattice. The success of his work motivated a similar test on the CLP material studied here. Two samples were prepared of equivalent mass. One was reduced according to a procedure developed by Vivek Kashyap at CSM and then both were leached with 100 gram per liter sulfuric acid. The flowsheet for this test can be seen as figure 4.10.

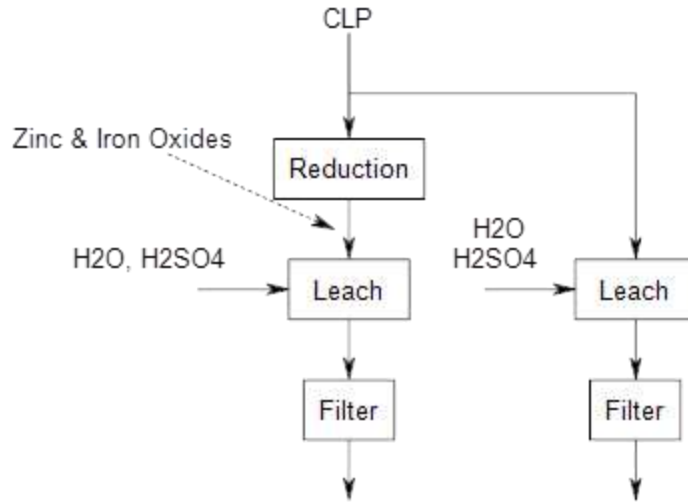


Figure 4.10: Roast leach study flowsheet

The results of this test work show improved gallium recovery from the sample via the reduction roasting process. The gallium however was recovered at lower grade in the reduced sample as zinc, copper, and manganese recoveries increased drastically along with the gallium recovery. Additional downstream test work using the reduction process would be interesting but the current experimental setup is not developed well enough to be conducive to large volume tests. Small leach-precipitation tests in this work are generally accomplished with 100g samples and the mass balance is based on a 1kg sample whereas the reduction tests were designed for less than 10g samples. The leach-precipitation tests show on the order of 12% of CLP feed is leached, so with a 100g sample some of the precipitates are on the order of five grams or less, a 10-gram feed would be quite difficult to work with as the total dissolved material would be 1gram and the concentrate for example would be on the order of 0.05 grams. It is very difficult to analyze fractions this small particularly for the minor elements such as gallium. The leach recovery for various metals is shown in Table 4.5. The recoveries in table 6 for the CLP leach are noticeably lower than those supported by other research.

Table 4.5: Comparison of recoveries for various metals of interest for the reduced sample from the CLP leach.

		Recovery							
		A	M	F	C	Z	G	C	I
		l	n	e	u	n	a	d	n
CL		1	8	3	1	1	2	2	2
P Leach		.4%	.9%	.7%	4.2%	3.2%	8.3%	0.3%	5.2%
Re		2	3	1	5	3	5	3	5
duced		.5%	4.4%	.7%	6.9%	5.9%	5.6%	1.4%	5.7%
Sample									

The metals grade of the leach liquor for each of these leach liquors is shown in Table 4.6.

Table 4.6: Metals grades of the leach liquors for the reduction-leach test

		Grade							
		A	M	F	C	Z	G	C	I
		l	n	e	u	n	a	d	n
CL		2	0	2	4	6	4	1	0
P Leach		.4%	.8%	0.0%	.9%	5.8%	.6%	.4%	.0%
Re		2	1	4	8	7	4	1	0
duced		.0%	.4%	.1%	.7%	8.8%	.0%	.0%	.0%
Sample									

The results show that gallium recovery is improved by 27% in absolute terms and 95% in relative terms. Zinc recovery is improved from 13% to 36% representing a rough tripling of the zinc recovery.

The XRD results on the reduced sample show the phase changes from the CLP material discussed in section 4.2. The phases indicated by the XRD as possibly present in the reduced sample include; zinc sulfide, zincite, and franklinite. It appears that the hohmannite and jarosite phases of the CLP sample were reduced to zincite.

4.3.4 Summary of Leach results

Leach results show gallium recovery in the range of 35-50% and zinc recovery in the range of 20% This is supported by empirical data from tests with 10g to 1kg of sample. It is shown that a reduction roasting process may enable improved leach recoveries. It is shown that acid concentration significantly affects the gallium and zinc recovery indicating that reduction in acid concentration (to reduce sulfuric consumption) would result in lost recovery of gallium.

This initial work certainly does not constitute an optimization of the process but could be used to indicate help design tests for process optimization. The economic assessment of the process will be based on the empirical data from the 1kg sample test.

The leaching recovery can be explained in the context of the sample mineralogy in that the zinc ferrite did not leach, the other major phases (hohmannite and jarosites) did leach but represent a minority of the gallium and zinc present.

4.4 Solvent Extraction Studies

4.4.1 Cyanex-923

Cyanex-923 test work was based on literature particularly that published by Mishra. The initial tests were designed as 5-minute shakeout tests at a 4.5 pH. The initial results did not show the separation expected and so additional experiments were designed to determine the pH range where a separation could be achieved. This was first done with synthetic samples and then duplicated with samples from ore leach liquors. The synthetic samples were used to determine conditions where gallium may be absorbed to the organic preferentially over the other major metals particularly zinc. Most of the literature suggested reducing iron in solution to the ferrous oxidation state to allow selection of gallium over iron. The zinc added to do this usually motivated the precipitation of iron, gallium, and other metals. With iron in the ferric oxidation state (or mostly in the ferric state). Cyanex is a neutral extractant that extracts metals as complexes under certain conditions. At low pHs gallium forms the trivalent gallium ion in aqueous solution according to the phase stability diagram in figure 2.1. The absorption isotherm for Cyanex is shown in figure 4.11 for various metals of interest in the system. The results in figure 4.12 are for extraction from leach liquor with mixed metals in solution.

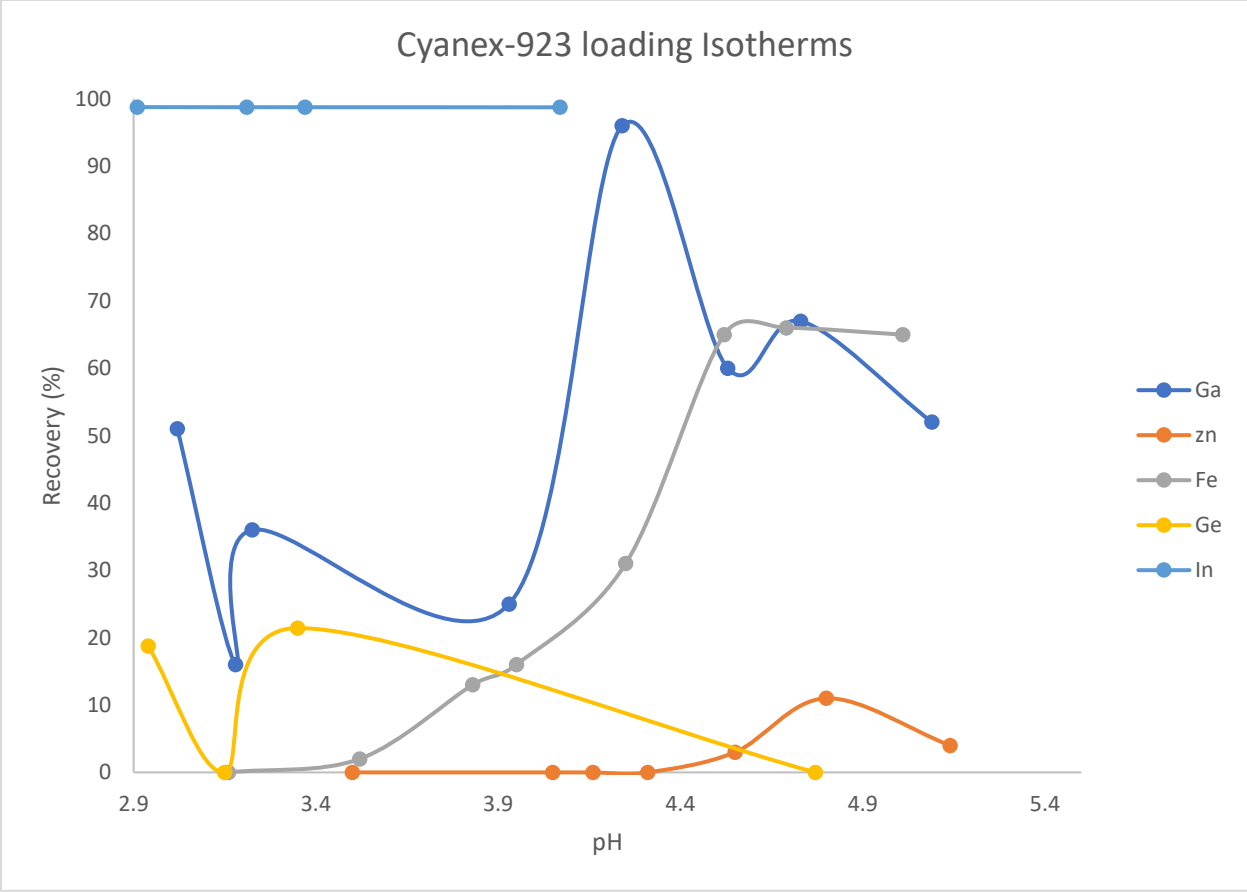


Figure 4.11: Cyanex loading isotherms based on ore leach samples

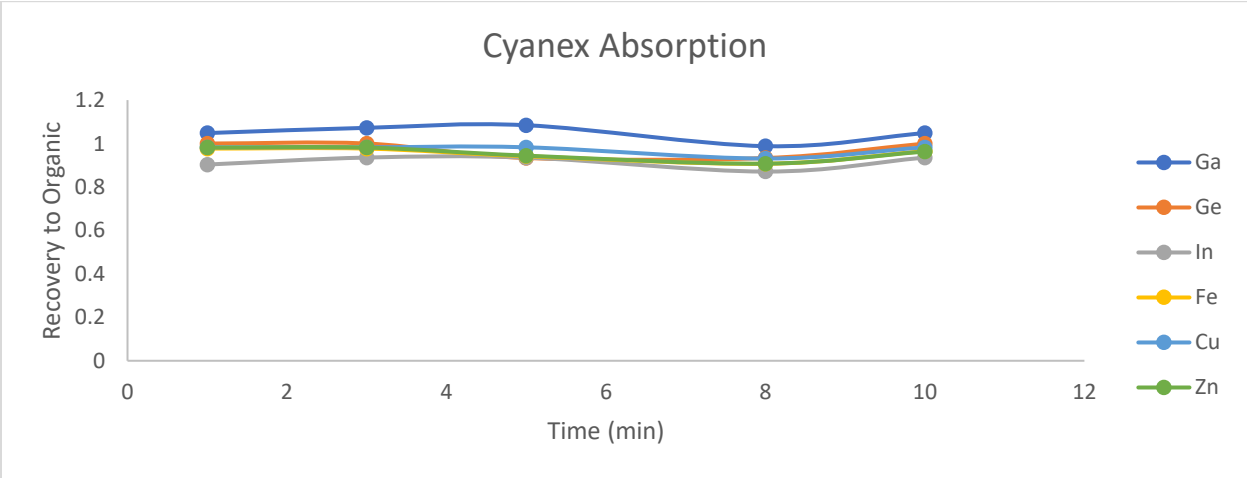


Figure 4.12: Cyanex loading at several temperatures with ore leach samples

4.4.2 Kelex-100

Kelex-100 is primarily used in extraction under alkaline conditions. The Kelex-100 is most interesting in a complimentary application to the precipitation work as a caustic leach seemed to contribute to the recovery of a gallium concentrate. Kelex is a chelating extractant. The results for Kelex loading are shown in figure 4.13. These are based on multistage tests using 10% Kelex in kerosene.

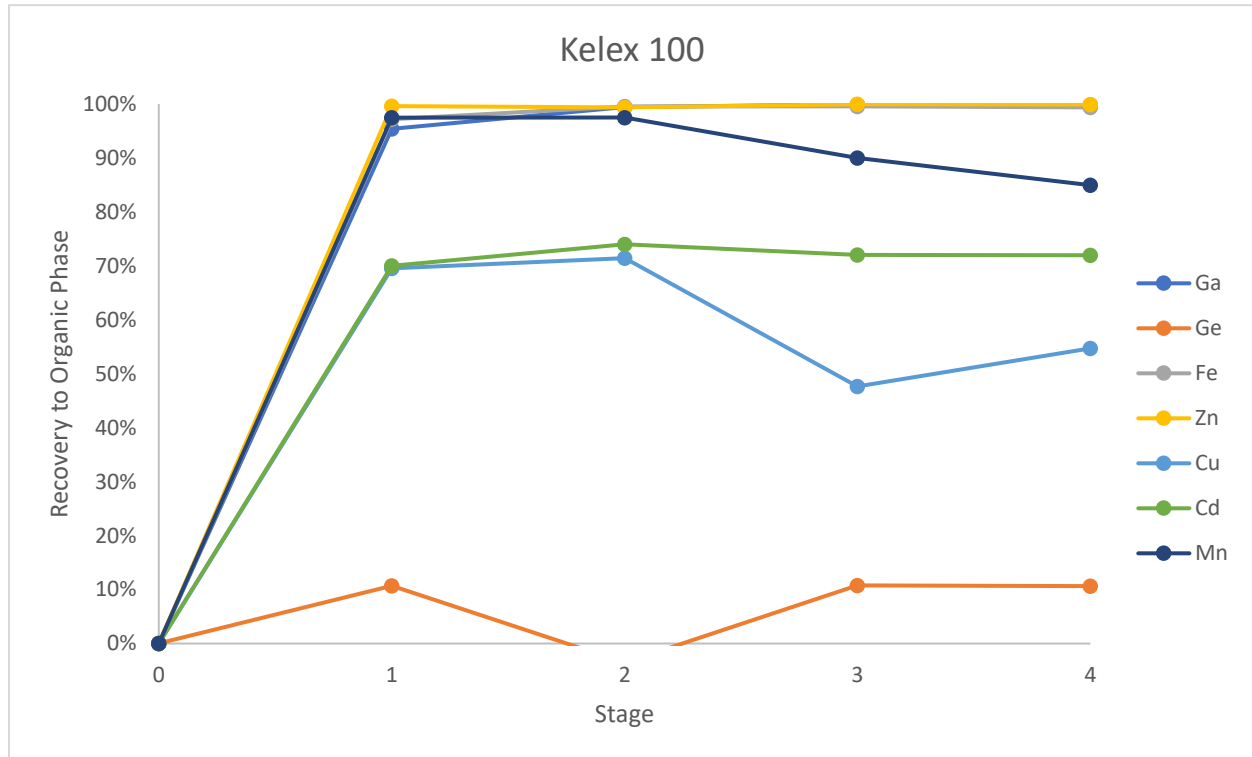


Figure 4.13: Kelex loading for metals of interest

4.4.2.1 Stripping Results

Kelex loading tests showed little selectivity for gallium but showed absorption of several metals. Stripping tests were designed based on the literature. Kekesi listed various concentration of HCl for stripping Kelex, and Puvvada et al used a combination of 2M and 6M HCl to achieve selectivity for gallium. The nitric acid solution did not strip iron from the Kelex and so, showed some selectivity. The Gallium/zinc recovery are low and desorption isotherms should be developed to determine the proper aqueous to organic ratio. Caustic did not yield a significant result, perhaps with much longer stripping times or a different organic to strip solution ratio. The combination of two different hydrochloric strip solutions showed a preference for stripping gallium in the higher concentration acid and a preference for zinc in the lower concentration

hydrochloric acid. The literature suggests that 2M HCl should strip zinc and then 6M HCl could be used to subsequently strip a gallium concentrate.

4.4.3 Novel Extractants

Three novel extractants were provided by CMI partners at ORNL. These extractants were TODGA based extractants including TODGA, T2EHDGA, and DEDODGA. Very small samples of each were made available so simple tests were designed based on literature and discussions with ORNL. The extractants were mixed with Isopar as an organic diluent. Isopar was selected for its availability and its ease of use. The other common diluents for TODGA type extractants included chlorinated hydrocarbons that had more serious safety concerns related with their use. Isopar had much simpler safety procedures and was preferred for initial studies for this reason. It is also commercially available in large quantities; other solvents may be explored to further develop this study. The conditions and results for the primary metals are shown in table 4.7.

Table 4.7: Kelex strip results

	Recovery to strip solution		
	Zn	Ga	Fe
3M HNO3	4%	5%	0%
NaOH	0%	0%	1%
6M HCl	0%	1%	1%
2M HCl	2%	0%	0%
2M HCl	5%	0%	1%
6M HCl	0%	4%	1%

All three reagents were first tested with a 5-minute mixing time before phase separation. The concentration for these extractants in Isopar was 0.1M, the acid concentration in the aqueous phase was 3M. Shakeout tests were designed similar to those for Cyanex-923 with 5-minute mixing times. One of the three extractants showed absorption in that test. Additional tests with longer mixing times were completed for the other two extractants. The results and details of these tests are shown in table 4.8.

The feed to these tests was a CLP leach liquor containing gallium, zinc, iron and other metals in the leach solution. The recovery is based on analysis of the feed liquor and the raffinate.

These absorption tests show that these extractants (generally talking) were selective for iron over gallium. It is perhaps possible that these extractants could be used to remove iron from solution first prior to extraction of the gallium under different conditions. Further work is warranted on these extractants if larger samples of each could be obtained. There was a single strip test completed with the loaded TODGA extractant according to conditions used in the literature with a 3M nitric acid strip solution, but there was no desorption in this test. In order to develop a flowsheet using these extractants significant additional work is needed including development of absorption isotherms, this would require larger samples of each extractant. All three may be interesting for additional study based on these results.

Table 4.8: Recoveries and extraction conditions for several novel extractants

	Recovery to Organic Phase			Time (min)	Extractant Concentration M	Diluent	Aqueous pH
	Zn	Fe	Ga				
DEDODGA	0	0	0	5	0.100	Isopar	0.5
DEDODGA	8.9%	76.4%	0.0%	120	0.100	Isopar	0.5
T2EHDGA	0.0%	0.0%	0.0%	5	0.099	Isopar	0.5
T2EHDGA	9.1%	76.1%	0.0%	120	0.099	Isopar	0.5
TODGA	100%	100%	100%	5	0.106	Isopar	0.5

4.4.4 Summary of Solvent Extraction Results/Solvent extraction flowsheet

Solvent extraction test work showed poor separation for all the extractants tested across a broad range of conditions. Cyanex-923 showed the most interesting separation with gallium preferentially absorbed to some degree. Kelex-100 did not show concentration of gallium during absorption but may have shown indication of concentration via stripping with differing sulfuric acid concentrations. One of the major challenges for preferential absorption from the leach liquor is the low relative activity. This is probably due to low activity of gallium in the solution relative to zinc and iron in the leach liquor. The results for Cyanex loading showed that at a pH around 4.3 gallium and iron could be selectively solvated to the organic phase. The separation between gallium and iron was difficult as zinc addition to reduce the iron to the ferrous valency caused precipitation of gallium. There are two operating challenges with this pH in the leach system. The first is that upon raising the pH to this range most of the gallium and significant iron begins to precipitate this is explained in section 4.7 more thoroughly with reference to the phase stability in the aqueous sulfate system. Additionally, the pH change is relatively slow (consuming large quantities of soda ash) and so is easily controlled up to a pH of about 3.0,

adjustments above that are much more sensitive and it is very difficult to neutralize sulfuric with soda ash to exactly 4.5. this is simple enough to perform in the lab with patience but is impractical for operating scale. Changing the pH with caustic would be more easily controlled as the titration curve is gradual up a pH well above the operating condition. The Challenge with caustic is the formation of a gel that makes both filtering and subsequent solvent extraction difficult.

The novel extractants are interesting for future work, they showed some selectivity under conditions that may be reached realistically for the process. Larger samples of these extractants would be useful for testing to compare to the precipitation results.

4.5 Precipitation studies

The initial precipitations studies were a simple analysis of the residue precipitated from the leach liquor as part of the preparation for solvent extraction test work. It was observed that a significant mass of material formed a solid precipitate as pH was changed from very low ranges for the leaching (100g/l H₂SO₄) to more moderate ranges for Cyanex solvent extraction (pH = 3.5-4.5). The initial Cyanex procedure called for zinc dust addition to the liquor to reduce ferric ions to ferrous ions, this reduced some of the metals in solution to allow precipitation. The analysis of this precipitate showed significant recovery of the gallium from the leach liquor to

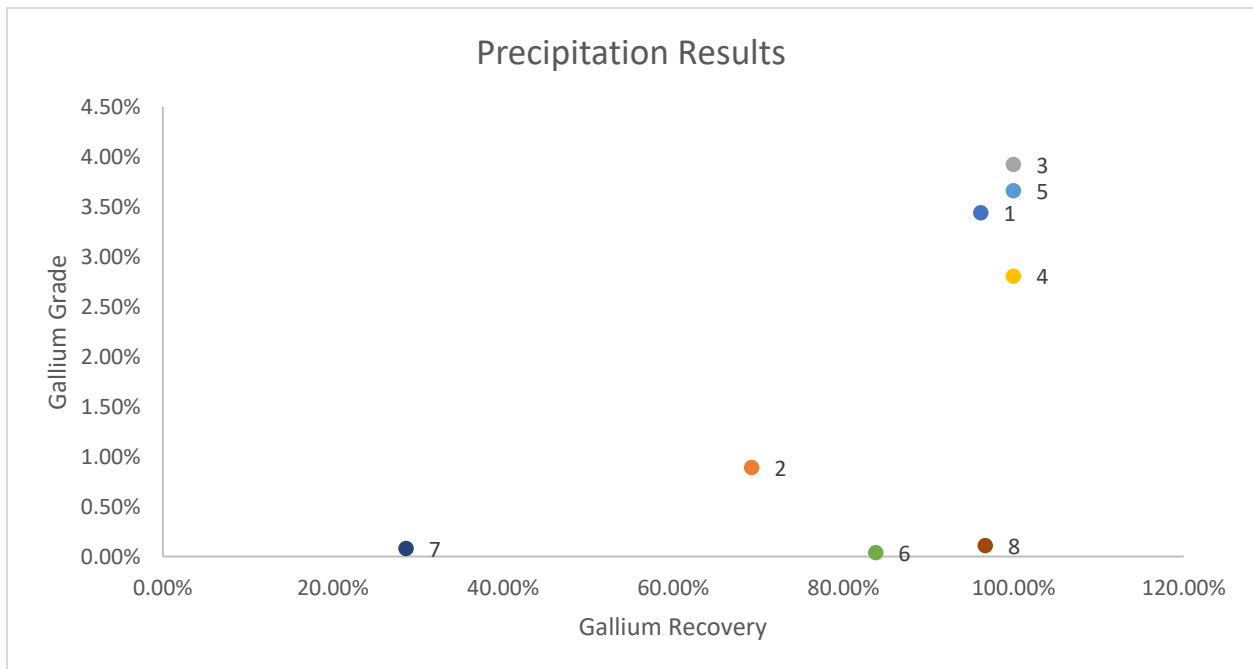


Figure 4.14: Gallium grade and recovery for various precipitation tests.

this precipitate and an upgrading relative to the other metals in the process feed. The composition of some samples of this initial assessment are shown in figure 4.14. The conditions for these tests are shown in Table 4.9.

4.5.1 pH Precipitation

The results of this initial assessment inspired a designed test to determine conditions under which gallium would preferentially report to the precipitate phase to enable concentration. The test work focuses on performing the precipitation at several different hydronium concentrations as well as by different zinc additions. The results for precipitation at different pHs can be seen in figure 4.15. The pH shown on the X-axis was achieved via partial neutralization with soda ash. The tests are run in triplicate. The drawn lines represent the trend for the percent of the material in the leach reporting to the precipitate fraction.

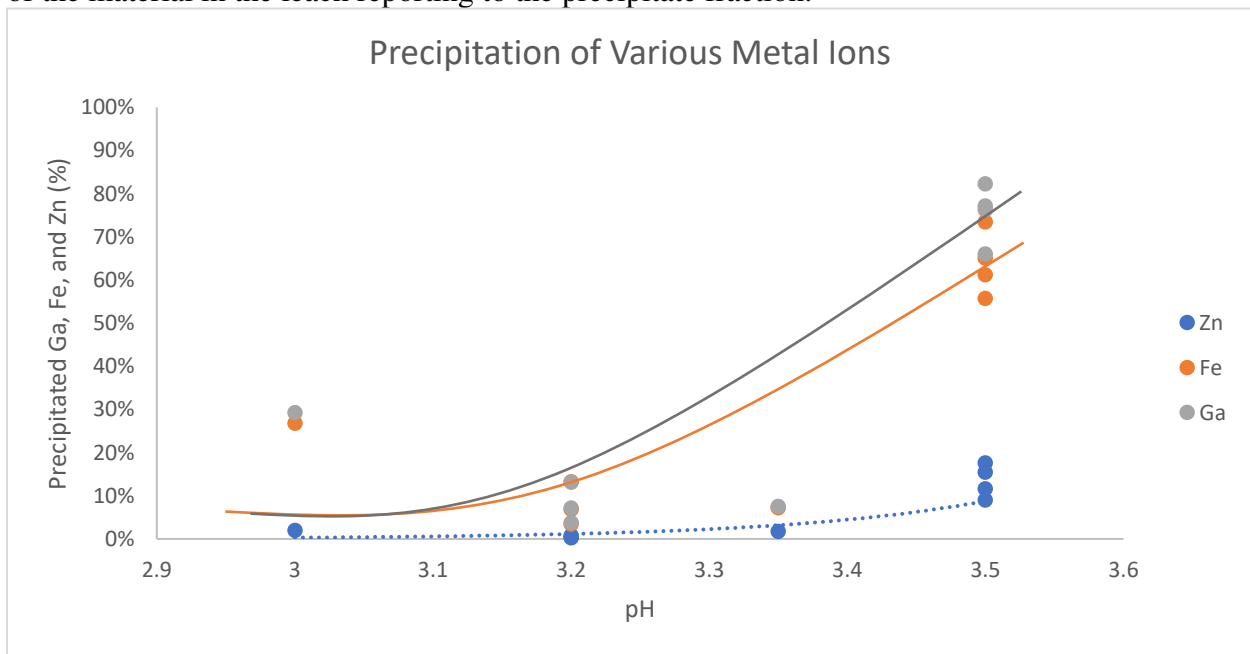


Figure 4.15: Precipitation behavior of major metals upon change in pH.

Table 4.9: Conditions for test results in Figure

Number	Zn addition	pH
1	50	3.2
2	100	3.2
3	100	3.2
4	50	3.5
5	50	3.5
6	100	3.5
7	50	3.2
8	100	3.5

The primary components of the precipitate were iron and gallium with zinc mostly remaining in solution and remaining a minor component of the precipitate. This represented a significant upgrade of gallium from the solution. The precipitation of nearly all of the gallium in solution was possible via simply change in the pH.

4.5.2 Precipitation by zinc addition

Zinc can be used to reduce the ions in solution and thereby precipitate a gallium-iron rich residue. This is done in other hydrometallurgical processes in order to recovery metals more noble than zinc. In this work gallium and iron are to be precipitated by reduction via addition of zinc dust to the liquor. The results from some test work to this effect are presented in figure 4.16.

This test was accomplished by adjusting the pH of the leach liquor to 3.5. The liquor was then sampled to provide a basis and split for the various tests. The recovery to the precipitate is in terms of the metal composition in the feed to this unit operation. The zinc recovery accounts for the zinc dust that is added though this quantity is relatively minor. The test work shows that gallium and iron can be precipitated from the leach liquor by zinc addition to recover a gallium con. This work contributed to the design on an integrated flowsheet.

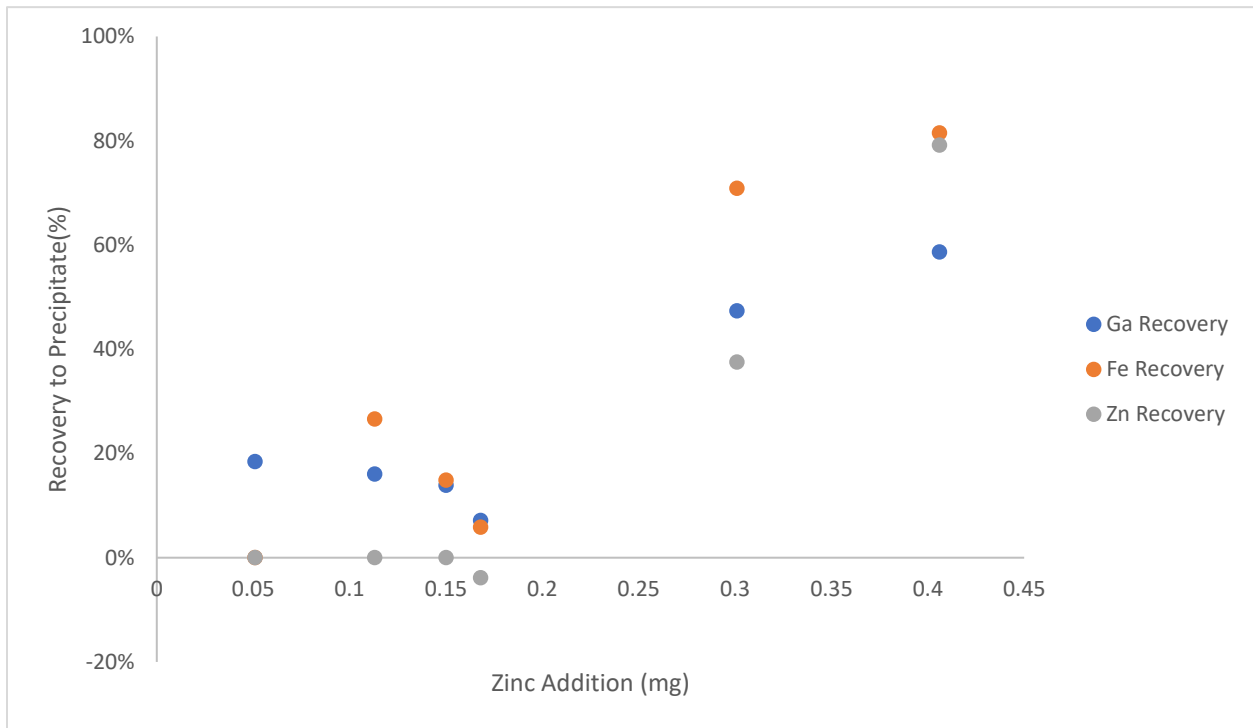


Figure 4.16: Precipitation behavior upon zinc addition

4.5.3 Iron Precipitation

Just as is done for precipitation by zinc addition, the addition of iron to precipitate metals with higher nobility is possible. The expectation was to achieve a concentration of germanium and indium by iron addition, this was shown to be possible but more than half of the cadmium also precipitated making this concentrate less than useful for germanium/indium recovery. It is possible that precipitation of a major fraction of the cadmium is beneficial to remove cadmium from the system if that may result in a smaller cadmium containing waste fraction. The potential value of this concept is discussed in section 5.3.1.8. The results of grade and recovery are shown in figure 4.18 for precipitation by iron addition.

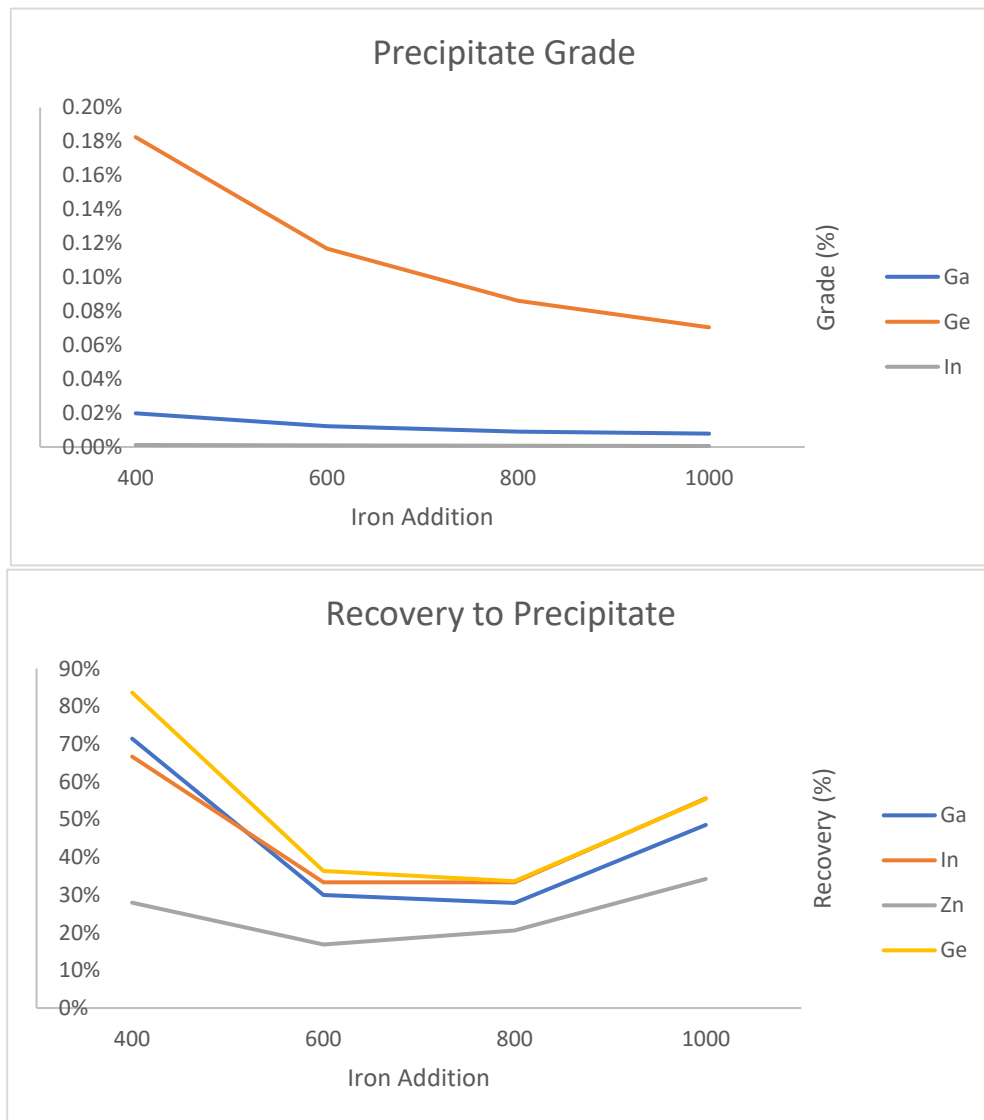


Figure 4.17: Precipitation behavior upon iron addition

4.5.4 Combined Precipitation test work

Based on the results from that test work additional precipitation tests were designed to show the relationship between pH and zinc addition and gallium recovery. The data from that test is shown in figure 4.18.

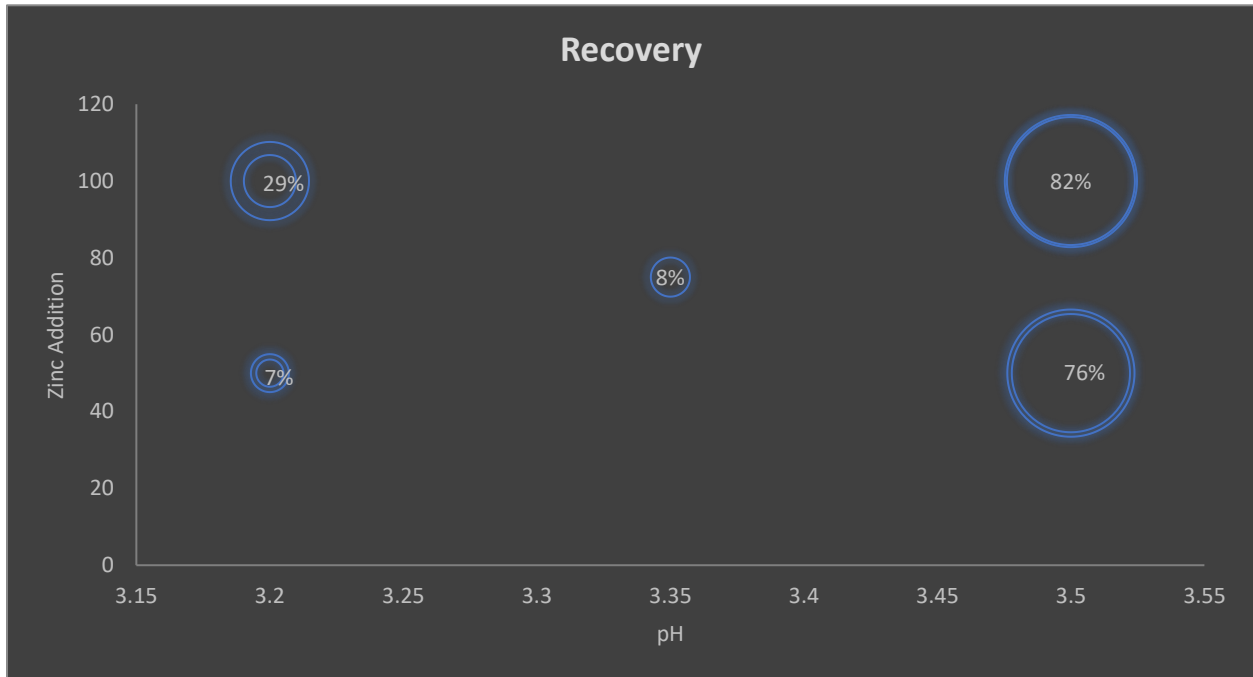


Figure 4.18: Precipitation behavior presented as gallium recovery (circle diameter) in relation to pH and amount of zinc addition

This data was analyzed via simple statistical tests similar to those in section 4.3.1. The statistical test suggests that pH may be the more affectual variable for gallium (or zinc recovery). The p-test for the data was not below alpha for the 95% confidence interval and so no concrete conclusions can be drawn from this statistical analysis. Additional test work with duplicate tests may enable better design of the precipitation unit operation. The statistical test supports that there is not a strong correlation between gallium recovery and zinc addition.

4.6 Precipitation flowsheet and summary

4.6.1 Initial sequential precipitation test work

Noticing the precipitation and leaching behavior it was suggested that a gallium concentrate could be made by precipitating gallium and iron via change in pH and zinc addition

and then leaching with caustic. The flowsheet for this process is shown in figure 4.20. The grade and recovery to various fractions is presented in table 4.11.

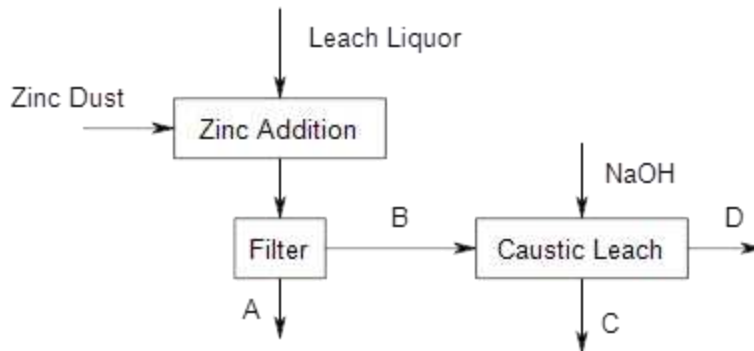


Figure 4.19: Precipitation-Leach flowsheet concept

Table 4.10: Details on the various fractions recovered as according to the flowsheet in Figure

Fraction	Grade			Recovery
	Ga	Zn	Fe	Ga
A	0.01%	49.3%	45%	41%
B	0.15%	5.5%	84%	59%
C	0.09%	2.4%	92%	37%
D	4.27%	17.2%	41%	22%

The first consideration is the separation of fractions A and B via precipitation. Fraction B is the solid precipitate formed upon partial neutralization of and zinc addition to the leach liquor, this fraction contains greater than half of the gallium in the system at a grade of 0.15%. The fraction A contains a minority of the gallium at a low metals grade. Fraction B also contains the majority of the iron in the leach liquor while zinc is partitioned to the aqueous fraction. The mass balance for this test did not “close” meaning that the accountability of various metals was not 100%. Some of the difficulty with the mass balance was caused by the very small sample for this test. The feed was 50ml of leach liquor which yielded a precipitate of ~0.4g. The precipitate was split for composition analysis and so only half was leached with caustic. Further tests were designed with the understanding of the amount of precipitate that may be expected from a given volume of leach liquor.

This test was duplicated in large part with a larger sample of leach liquor in order to provide enough precipitate to perform analytical digestion of various fractions as well as feed the caustic leach unit operations. The precipitate formed during pH adjustment is kept separate from that formed after zinc addition for this test. The process is illustrated by figure 4.20.

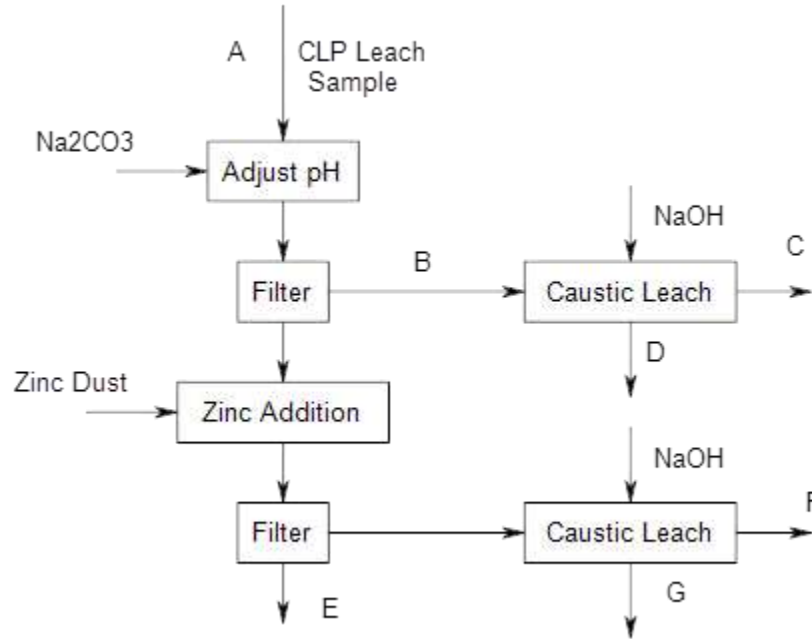


Figure 4.20: Flowsheet for larger test with stock CLP leach sample

The CLP leach sample was part of a several liter leach solution prepared for a range of precipitation and solvent extraction work. This experiment used 1 liter of leach liquor (larger than the 50ml sample used for the test shown in figure 4.19) The recoveries and grades of various metals are shown in table 4.11.

Table 4.11: Analysis results from various materials sampled from the flowsheet in figure 4.20.

	Recovery			Grade		
	Ga	Zn	Fe	Ga	Zn	Fe
A				2.3%	30.2%	2.2%
B	81.2%	36.4%	81.2%	2.8%	17.0%	76.7%
C	12.0%	19.2%	78.5%	0.5%	10.4%	86.2%
D	57.1%	13.0%	1.0%	19.8%	60.8%	9.9%
E	0.1%	57.4%	1.0%	0.0%	88.7%	3.2%
F	0.1%	0.7%	1.2%	0.2%	18.1%	66.6%
G	0.2%	0.5%	0.0%	0.9%	32.6%	3.6%

The basis for the recoveries presented in table 4.12 is the composition of the leach liquor. This does not represent total process recovery as leach recovery is neglected in this test. The partitioning of leached metals to the various fractions is still interesting as part of the process development. 81% of the gallium is shown to report to the first precipitate with very little additional gallium in the second filtrate. The second filtrate is not directly analyzed as there was not enough to split for an appropriate sample and provide material for a caustic leach. The filtrate E contains the majority of the zinc with a minority partitioned to the precipitate phase B. About half of the precipitated zinc reported to the caustic leach liquor. Iron mostly reported to the first precipitate but was not leached by the caustic leach. Fraction D is the gallium concentrate with a grade on the order of 20% gallium. The major diluents are zinc and iron. The fraction C is an iron concentrate with some zinc present. The fraction E is a zinc concentrate that could probably be recycled to the plants zinc processes. The caustic leach G did not recover significant additional gallium in addition to the gallium recovered in fraction B (and subsequently D). For this reason, the zinc precipitate was added to the precipitate formed by pH adjustment in later test work. Additional leaching operations are probably the most interesting question of this research as 12% of the gallium is lost to fraction C, the larger experiment discussed in the next section used scavenger leach unit operations to capture this lost gallium.

4.6.2 Preliminary complete flowsheet test work

The next test integrated the knowledge developed as part of the previous test work to develop a complete flowsheet that may be used to recover gallium from the CLP feedstock. The flowsheet for this work was based results from the sulfuric leaching test work, caustic leaching test work, and precipitation test work. The test used a 1kg sample of CLP material to provide a sufficiently large precipitate fraction for caustic leaching and analytical test work.

4.6.3 Large sample test work

Figure 4.21 illustrates a test that included leaching as part of the full process. The leach unit operation was accomplished with a slurry density of 10%, for 6 hours, and an acid concentration of 100g/l. The leach was filtered and pH adjusted to form the first precipitate. This was filtered before zinc was added. The second filtrate was produced by filtering across the same

filter so that the built-up cake from the first filtering operation aided in filtering the zinc precipitate. The combined filtrates were then leached with caustic.

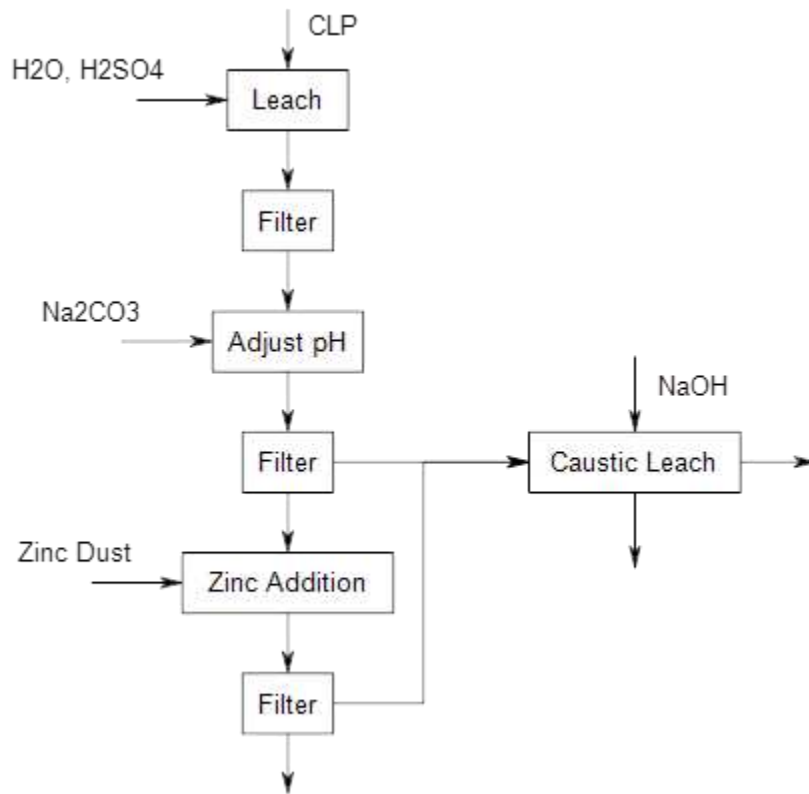


Figure 4.21: Flowsheet for first leach-precipitation test

The results of this test are summarized in the flowsheet. The partitioning of various metals roughly matches that for tests previously discussed. The leach recovery is notably low with significant gallium remaining in the leach residue. Additional work on leach recovery is necessary, but only in context of economic analysis, it is considered probable that most methods for improving leach recovery (for instance high temperature leaching) will prove too costly for the process to be viable. This is discussed in greater detail in section 5.13. This test is duplicated with some additional post processing to develop a final flowsheet shown in figure 4.22.

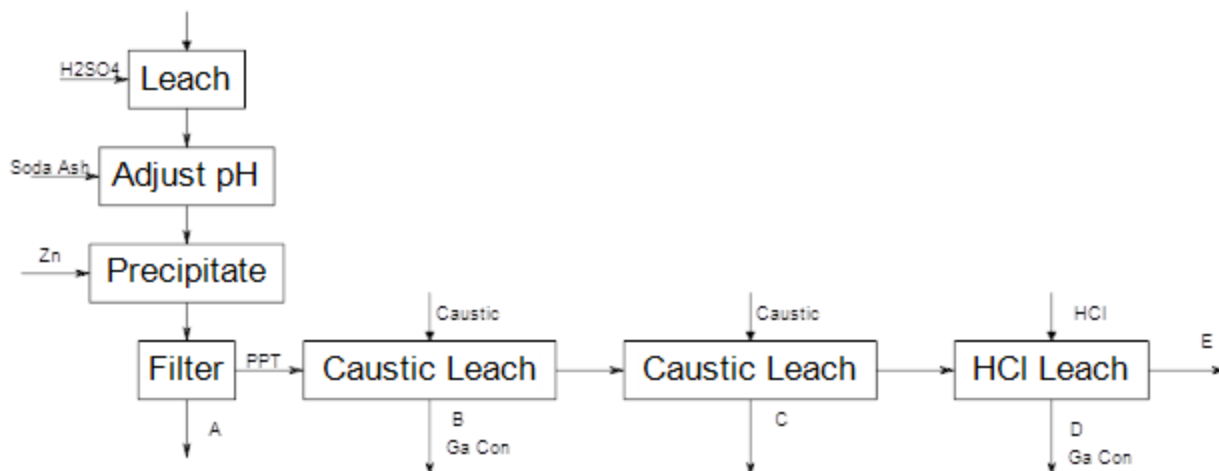


Figure 4.22: Flowsheet for 1kg sample

The leach recovery is similar to that shown in the other test work with 45% of the Ga recovered to the leach liquor. The gallium recovery was slightly higher than that observed for the small-scale tests, this is probably due to longer leach times resulting from the time required to filter these samples being significantly longer than the designed leach time. There was also a more powerful impeller type agitator that may have broken up agglomerations of CLP material more effectively than the magnetically stirred bars. The fraction A is a zinc concentrate that can be recycled to the process. Fraction B is the first gallium concentrate, fraction C is most likely a waste product, fraction D is a second gallium con, and fraction E is the major waste stream.

Table 4.12: Recovery for leach-precipitation flowsheet

	Recovery to product streams					
	Ga	Zn	Fe	Al	Cu	Cd
A	0.1%	20.0%	13.0%	24.0%	10.0%	45.0%
B	22.0%	0.6%	0.0%	0.9%	0.0%	0.0%
C	0.3%	0.1%	1.3%	0.1%	5.5%	2.2%
D	6.8%	0.5%	0.0%	0.5%	0.1%	0.0%
E	16.7%	0.0%	32.5%	0%	29.5%	0.0%

Table 4.14: Grade of various products of leach-precipitation flowsheet.

	Composition of product streams					
	Ga	Zn	Fe	Al	Cu	Cd
A	0.0%	74.0%	20.7%	1.2%	1.1%	0.7%
B	45.9%	36.8%	1.9%	21.6%	0%	0.0%
C	0.5%	7.1%	69.7%	1.2%	19.2%	1.5%
D	25.0%	53.3%	0.5%	18.9%	0.8%	0.1%
E	1.8%	0%	90%	0%	7%	0%

The cost model developed in the next chapter is based on these results and chemical/mineralogical analysis of the fractions shown here. Economic discussion of the value of these fractions is found in section 5.1. In this section the fractions will be discussed in terms of further processing.

4.6.3.1 Fraction A

Fraction A is the aqueous filtrate produced by the combined filtration steps, It represents five percent of the feed mass or 45% of the total leached mass. The fraction is mostly zinc metal in solution with some minor impurities including iron, aluminum, copper, and cadmium.

4.6.3.2 Fraction B

Fraction B is the first gallium concentrate in the form of gallium metal with other metals and metal hydroxides including iron and zinc. Fraction B represents 0.3% of the feed mass or 3% of the leached mass.

4.6.3.3 Fraction C

Is an iron-copper mixture and also contains the majority of the cadmium in the feedstock. This is probably sufficient to make it a hazardous waste. Additional expenditure to remove the cadmium is probably not interesting as the amount of this product produced by the processes is very low the total mass reporting to this product is 0.4% of the feed mass and only 3.3% of the leached material.

4.6.3.4 Fraction D

Fraction D is the second (and lower grade) concentrate produced by the leach-precipitation process. The fraction also contains significant zinc. Some gallium refiners would actually prefer this material to the higher-grade fraction as they expect to make revenue from both gallium and zinc production. Fraction D represents 0.2% of the feed mass and 1.5% of the leached material.

4.6.3.5 Fraction E

Fraction E is also considered a waste. And is potentially more interesting in terms of the development of additional separations. The material is an iron-copper rich fraction mostly consisting of goethite (an iron hydroxide) and mixed copper oxides. The entrained value of copper is very interesting but the separation of these phases is not considered viable. Copper-goethite mixtures are relatively common in zinc operations but they represent a waste as a viable separations process has not been developed. This is a non-hazardous waste and so the disposal

cost is relatively small but the opportunity cost of lost copper value (and maybe iron) is significant. This is especially significant as fraction E represents 48% of the leached material and 5.5% of the feed mass meaning significant energy and operating expenditure associated with this product have been input to this point in the process.

4.6.4 Alternative feedstock test work

An additional test was completed on another fraction called the “ferrite sample” this sample was tested with a very similar process to that discussed in section 4.5 for the CLP sample. The results showed that there was not significant gallium recovered to the leach liquor. The primary metal of interest recovered to the leach liquor was zinc which is probably not sufficiently valuable to motivate recovery just for the zinc value. The reduction roasting of zinc ferrite has been tested on this material and may improve critical materials leach recovery sufficiently for additional research to be interesting.

Table 4.15: Leach liquor composition for ferrite sample.

Metal	Al	Mn	Fe	Cu	Zn	Ga	Cd
mg in leach liquor (mg/l)	137	724	4961	497	6988	33	149

4.7 Discussion of precipitation thermodynamics

There are two mechanisms by which the metals are precipitated from the leach liquor and the separation is made. The governing thermodynamics for these phenomena are illustrated best via the Eh-pH diagrams shown as figures 4.23 through 4.26. The first figure, figure 4.23, shows that gallium is stable as an aqueous ion only at extremely low pHs in aqueous solution, while at higher pHs gallium forms insoluble oxide-hydroxides. This is quite similar to the stable phases for iron shown in figure 4.25. The iron forms iron ions in solution at low pH values, above which a stable oxide-hydroxide phase is formed. In contrast, zinc has a very wide range of stability in solution particularly associated with the phase $Zn(HS)_3$. By raising the pH from <1 to 3.5, both iron and gallium are precipitated as the oxyhydroxide phase.

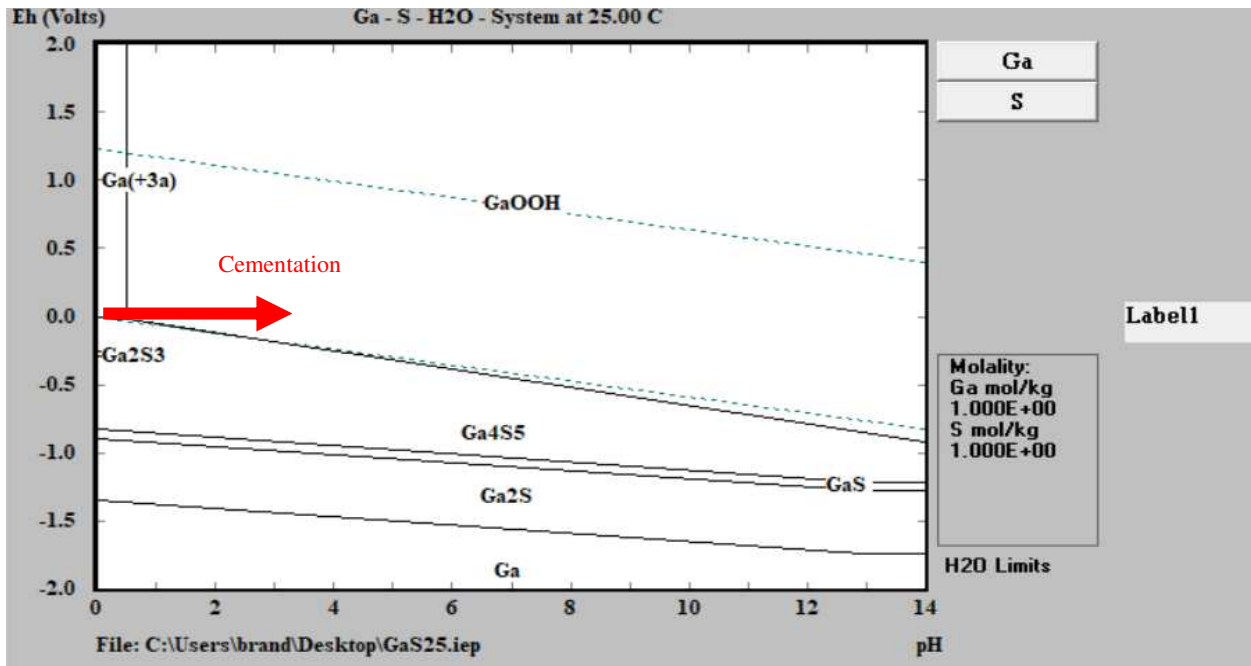


Figure 4.23: Eh-pH diagram for gallium.

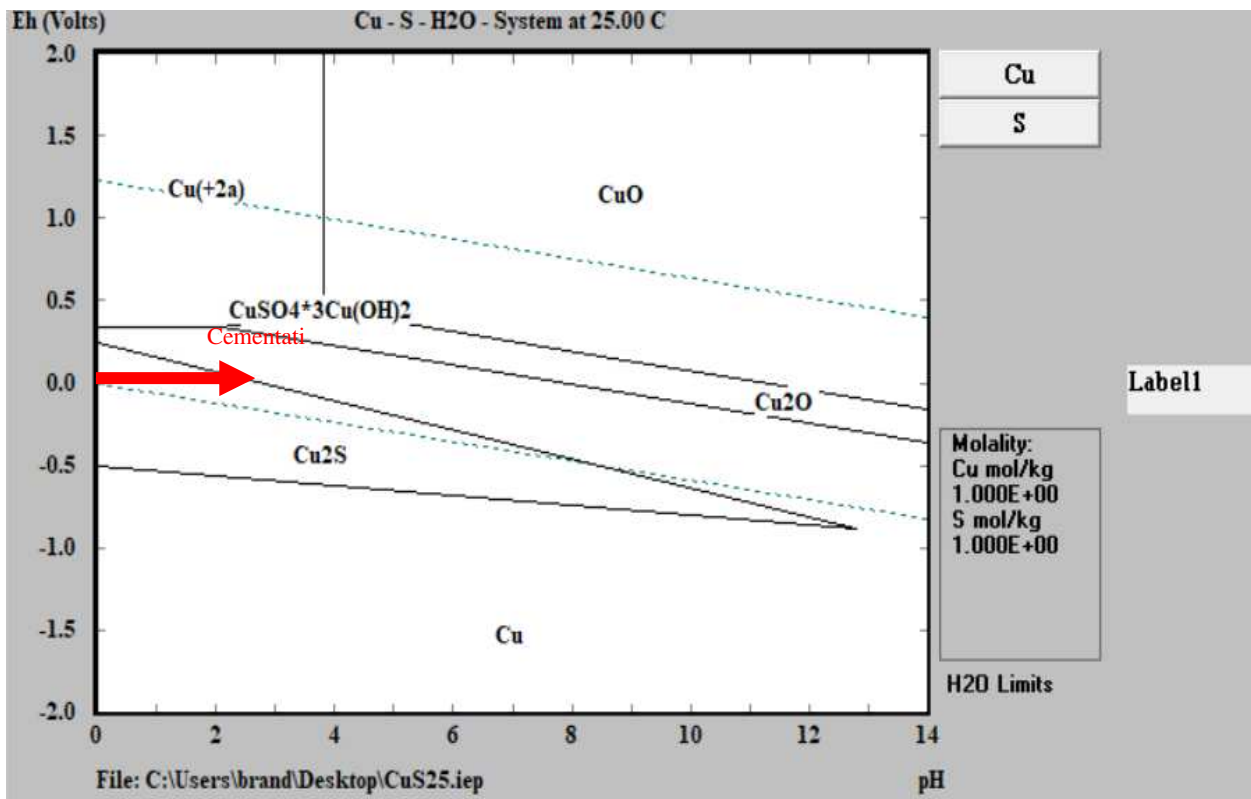


Figure 4.24: Eh-pH diagram for copper

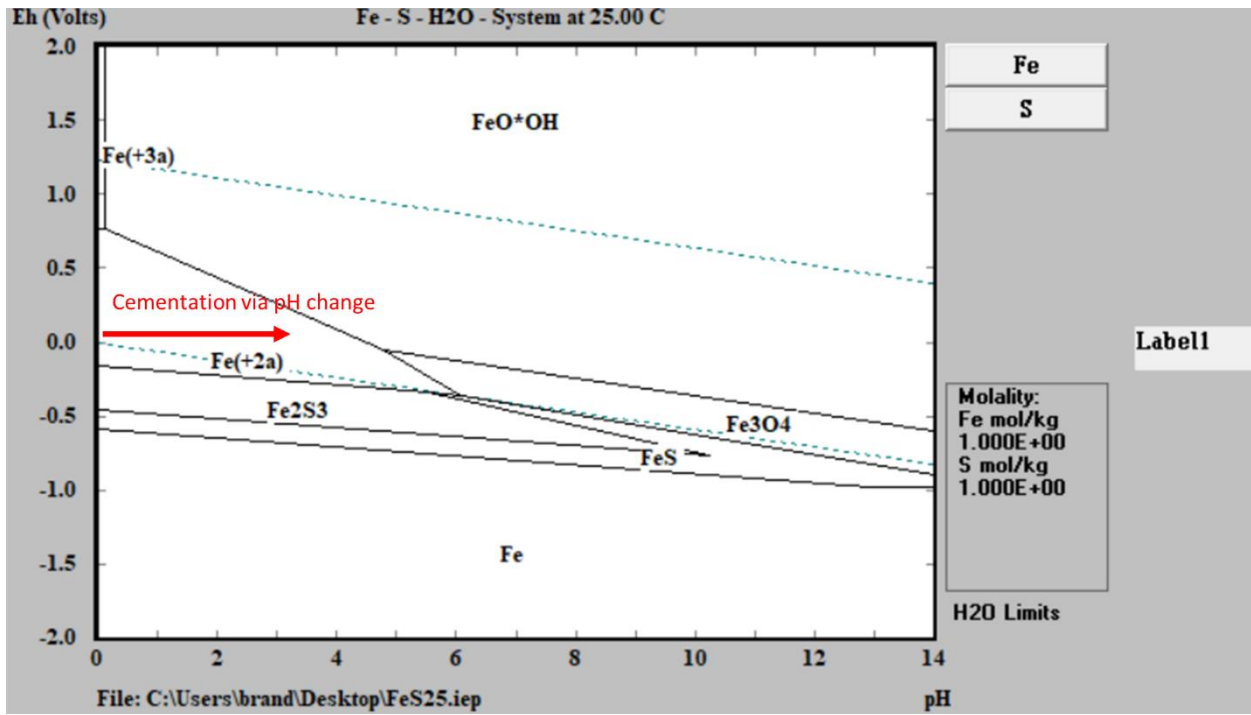


Figure 4.25: Eh-pH diagram for Iron

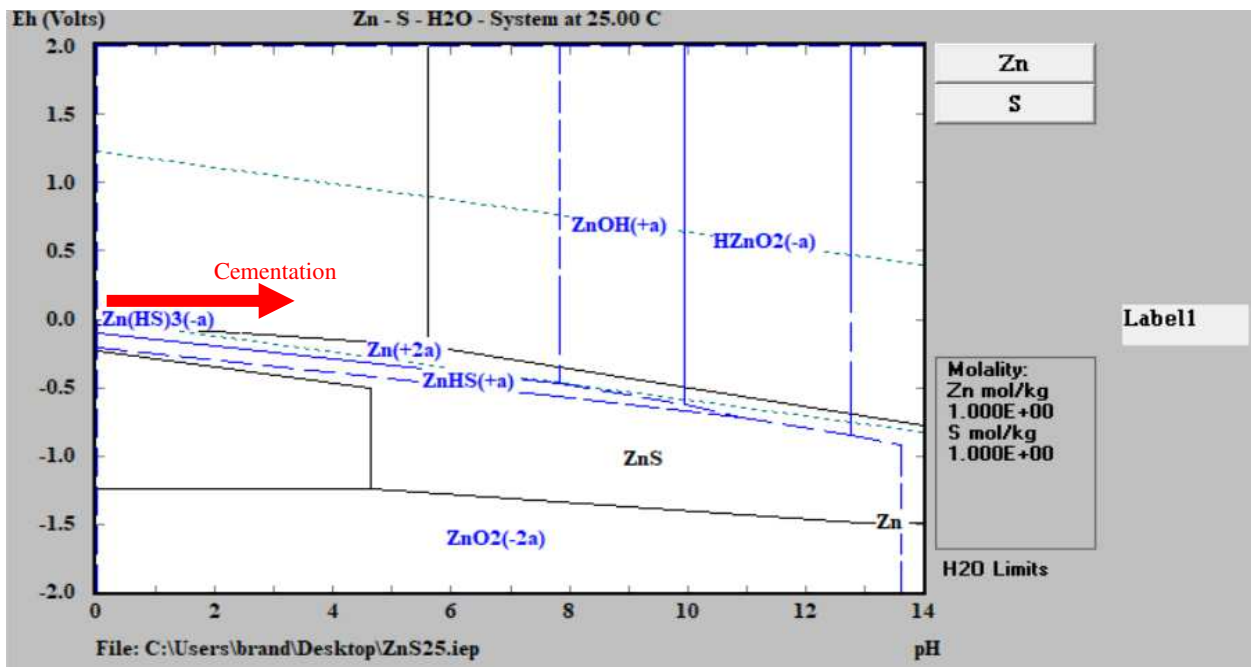


Figure 4.26: Eh-pH diagram for zinc

This is confirmed by the XRD results that show goethite as the primary precipitated phase. The additional phases identified are mostly copper oxides. The semiquantitative XRD analysis of the composition estimated the composition on the order of 85% goethite with minor copper oxide content. The copper oxide formation is explained via reference to the stability diagram for copper in the sulfate system (figure 4.24). At the pH 3.5, the reaction begins to shift from sulfide stability to oxide stability. This yields a stable copper oxide phase.

Upon zinc addition the metals are reduced to form stable and insoluble sulfides including Cu_2S , Fe_2S , Ga_4S_5 and Ga_2S ; there are multiple mineralogies of mixed sulfides, but they are not identified by the XRD as their relative composition is low in the solid fraction. Most of the metals of interest are precipitated as oxyhydroxides, but may also yield some sulfides particularly of gallium. The figure, figure 4.27, shows a combined stability diagram for iron and gallium.

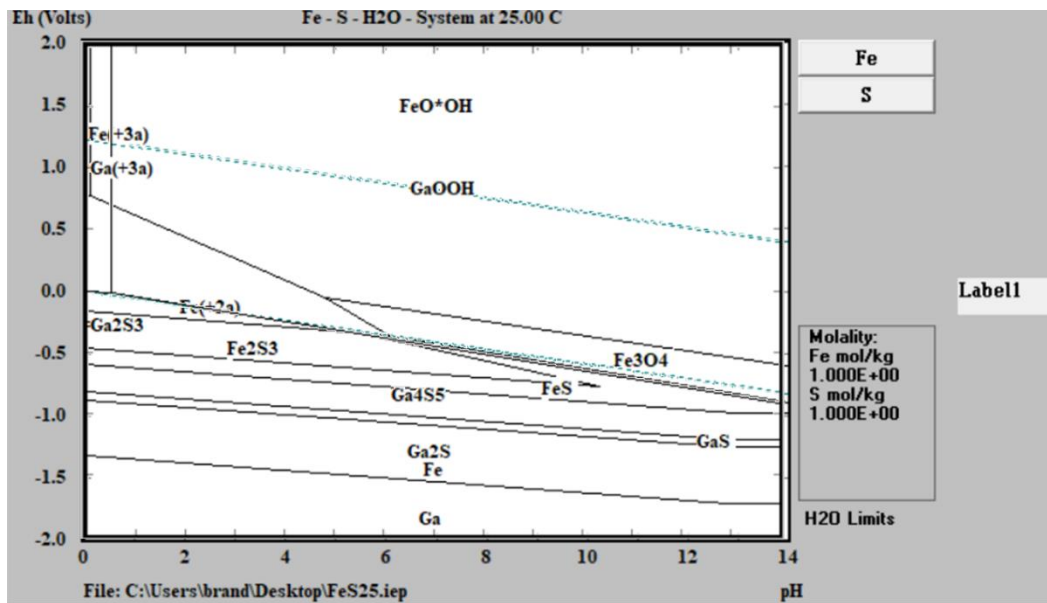


Figure 4.27: Eh-pH diagram for gallium and Iron

When zinc is added to reduce ferric iron to the ferrous oxidation state, several metals are precipitated including gallium as Ga_2S_3 . This can be seen via the Eh-pH diagram in figure 4.27. This is one of the difficulties of solvent extraction for recovery of gallium from this system. The extractants (particularly Kelex) are expected to be selective for metals with different valences, but any reduction of iron, such that it is not absorbed to the extractant, is not possible without beginning to precipitate gallium from the leach liquor.

CHAPTER 5 ECONOMICS OF GALLIUM SEPARATION

5.1 Cost model

The mass balance for the various fractions is based on empirical results from a leach-precipitation test using 1kg of CLP feed. The sizing of various equipment is based on this mass balance. There are some cases discussed in this section that are not based on experimental results which is noted specifically when they are referenced. The flowsheet with its products is illustrated in Figure 5.1.

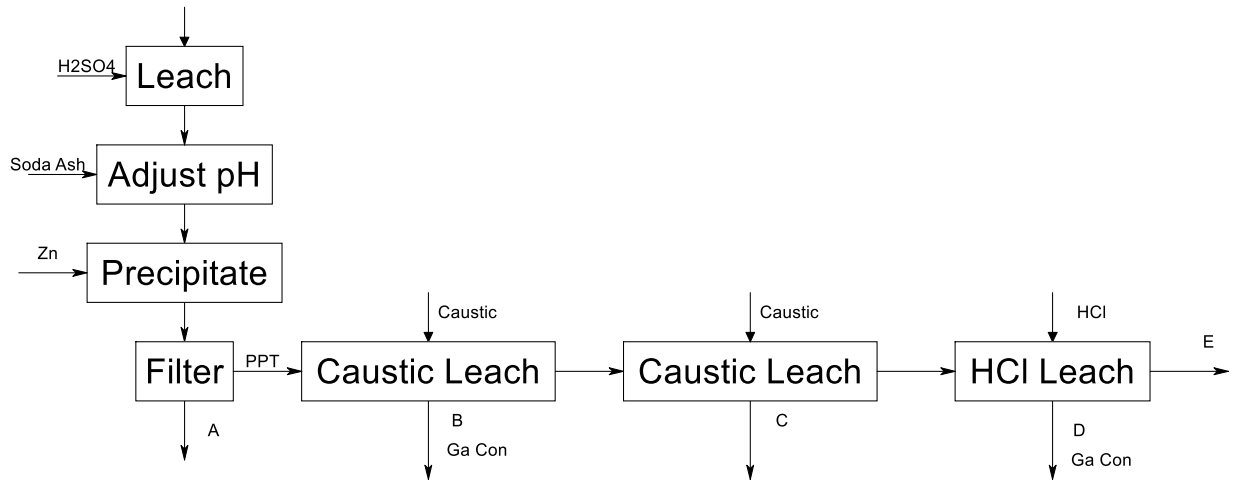


Figure 5.1: Gallium recovery flowsheet used for the economic model

5.1.1 Gallium market and value of products produced

The value of gallium has been volatile as of the time of this writing. The spot price is on an upward trend over the past few years rising from below \$200 per kilogram five years ago to the mid \$300s at the start of this project. Over 2019 and 2020 the gallium price stayed between \$340 and \$280 per kilogram before recently rising dramatically to greater than \$530 over the past several months. The spot price presented here is for gallium metal ingots with a purity of 99.995%. This is an altogether different product than the material produced by the process described in section 4.6.3. Although both contain gallium the purities make them suitable to a very different customer. The buyer of 99.995% gallium can directly or with minimal additional processing use this metal in gallium arsenide chips or light emitting diode devices. The material recovered by this process is a nominally 45% gallium concentrate that would be sold to a refiner rather than a gallium user. The price the refiner is willing to pay is based on the market price of gallium and the costs they would incur to realize that price. This is true not just for the gallium

concentrate but also for the several other fractions produced by the process that may be sold. Values of the various product streams presented herein are based on conversations with industry contacts. The value to refiners of various products are presented in Table 5.1.

Table 5.1: Summary of values of each fraction produced by the sequential leach-precipitation process

Summary of Values for Various Output Streams						
Name	Main value component	Composition	Value per ton	Tons recovered annually	annual value	percent of annual value
Fraction A	Zinc	74%	\$1,320.35	350	\$462,120.75	51%
Fraction B	Gallium	46%	\$35,000.00	22.092	\$354,907.98	39%
Fraction C		0%	-\$300.00	26.46	-\$7,938.00	0%
Fraction D	Gallium	25%	\$35,000.00	11.704	\$102,410.00	11%
Fraction E	Iron/Copper	0%	-\$20.16	385	-\$7,761.60	0%

Fraction A

Fraction A is the aqueous fraction of the precipitate phase, the subsequent processing would include precipitation by adjusting pH to neutral. This would result in a solid zinc containing fraction and a relatively clean sodium sulfate containing aqueous solution. The solid zinc fraction would be interesting to a smelter based on the zinc content. As discussed for gallium the value to a smelter represents the processing costs for the smelter as well as a profit margin. The five-year chart of the spot price for zinc is shown in figure 5.2.



Figure 5.2: Five-year spot price for zinc metal [20]

The price for this concentrate is calculated as follows:

1. Deduct 8% from the zinc assay and pay for the resulting zinc content at 85% of listed LME price
2. Deduct a treatment charge
3. Deduct additional penalties for high levels of As, Fe, Mg

The ratio of zinc to iron is important, in this material the ratio is ~3.7 which is lower than the 5-7 range for zinc smelters. This would probably result in a penalty on the order of \$5-\$15 per ton.

The treatment charge is generally representative of the operating cost of a smelter; however, it is often negotiated between smelters and producers of concentrate and can be quite volatile based on market conditions. Treatment costs have been quite volatile recently ranging from a benchmark of \$299 per tonne for 2020 and falling as low as \$65-\$75 per tonne in March 2021. The treatment cost at present and used for calculations herein is expected to be no more than \$200 per tonne. The price for zinc since 2019 has maintained a range between \$2550 and \$2895 per tonne. For this work a price of \$2745 is used which represents the Q1 2021 average price.

The calculation of fraction A's value is shown below.

Payable Zinc in 1 Tonne	$(0.74-.08) *.85 = \$1540$
Subtract TC of \$200	$\$1540-\$200 = \$1340$
Subtract Penalty of \$10	$\$1340 - \$10 = \$1330$

The value then of Fraction A that is used in this economic analysis is \$1330 per tonne.

5.1.2 Fraction B

Fraction B is the first gallium concentrate produced by the process and is a higher grade than the second concentrate (Fraction D) the material is 45% gallium by weight. The value used for the concentrate is based on a pricing criterion from a North American gallium refiner. The value used for this study is \$3500 per tonne.

5.1.3 Fraction C

Fraction C is a mixture of copper and iron. The copper is probably not interesting to a copper smelter without significant gold and/or silver components. The material is most likely considered a waste. For this economic assessment it is assumed that the cadmium content would qualify this fraction as a hazardous waste via TCLP. The costs of disposal are estimated considering this classification. The Material would be classified by the EPA as a high volume, low characteristic waste. The cost of disposal includes; freight to send to landfill, permit fees, testing fees, stabilization fees, and record fees. All of these fees are known to vary from case to case. \$300 per tonne is used as an approximation of the disposal cost for this material.

5.1.4 Fraction D

Fraction D is the second concentrate produced by the process. It is a 25% gallium concentrate with significant (greater than 50% by mass) zinc. Some refiners particularly one in china would offer up to 40% of the contained gallium value as their flowsheets are designed to recover value simultaneously from zinc and gallium. As the focus of this project is a contribution to a domestic supply chain a pricing structure from a North American refiner was used to determine a value for this concentrate. Their pricing shows support for a product ranging from \$20-\$35 per kg of concentrate.

5.1.5 Fraction E

Fraction E is an iron-copper material mostly consisting of Goethite (iron hydroxide) and mixed copper oxides. The entrained value of copper is higher than the entrained iron value but realizing value in either case is quite difficult. Goethites have long been considered as iron feeds but their minerology is not conducive to iron/steelmaking. Goethite is also quite difficult to separate from copper so recovery of copper value is not considered economically viable particularly on a relatively small material stream. This material is to be disposed of as non-hazardous mineral waste. The cost for disposing this material is estimated at \$20.16 per ton. [21]

5.1.6 Estimation of major costs

The major cost items for the processes presented in this research can be broken into two main categories those being; operating expenditures and capital expenditures. The engineer must consider a model of the plant including data from the mass and heat balance to understand the sizing of various equipment. With data about the size of equipment needed the cost of each line item can be estimated using either budget prices provided by industry contacts, or from collections of cost information such as costmine. Data for this project is mostly sourced from costmine unless otherwise noted.

CAPEX

The estimation of various capital items are presented in Table 5.2. The first subtotal represents the sum of the prices for these items. Subsequent prices for Delivery, Engineering, Installation, Electrical, and Instrumentation are based on published fractions of the capital item total. These costing coefficients are generally published as a range. Generally speaking, larger projects can expect to be at the lower end of the range as they tend to have pricing power and an economy of scale. The second subtotal represents the sum of all equipment in addition to these

calculated costs. The total represents these along with operating capital (3 months of operating expenditures) and a contingency also calculated as a fraction of the capital item subtotal.

Table 5.2: CAPEX model for plant

CAPEX	
Vat Leach (Vat+mixer)	\$40,400
Filter	\$137,700
Cementation tank	\$40,400
Filter	\$73,346
Caustic vat leach	\$23,100
Filter	\$73,346
Caustic vat leach	\$23,100
Filter	\$73,346
HCL Leach	\$23,100
Filter	\$73,346
Subtotal	\$581,183
Delivery	\$17,435
Engineering	\$191,790
Installation	\$145,296
Electrical	\$145,296
Instrumentation	\$58,118
Plumbing	\$116,237
Subtotal 2	\$1,255,355
Operating Capital	\$888,500
Total with contingency	\$2,583,000

OPEX

Operating Expenditures or OPEX represent the operating or ongoing costs of running the plant. These include labor, consumables, and electricity. Water was not considered a significant contributor to the cost especially considering the ability to precipitate metals from solution and reuse most of the process water and so was left out of the OPEX estimate. The OPEX for the designed plant according to the flowsheet in Figure 5.1 is presented in Table 5.3.

Table 5.3: OPEX model for the complete processing plant

Cost Item		per unit cost	units per year	Total per year:
LABOR:	Quantity	cost per hour	Hours per year	\$723,173
Mill Labor	8	\$24.00	2000	\$556,800.00
Mill Operator	1	\$28.50	2000	\$82,650.00
Mechanic	1	\$28.87	2000	\$83,723.00
ELECTRIC POWER	QNTY per Hr (Kw)	cost per KwHr	KwHr per year	\$12,632
Vat Leach Vat+mixer	4.45	\$0.07	8400	\$2,698.84
Filter	3.73	\$0.07	8400	\$2,262.17
Cementation tank	2.98	\$0.07	8400	\$1,807.31
Filter	1.3	\$0.07	8400	\$788.42
Caustic vat leach	1.49	\$0.07	8400	\$903.66
Filter	1.3	\$0.07	8400	\$788.42
Caustic vat leach	1.49	\$0.07	8400	\$903.66
Filter	1.3	\$0.07	8400	\$788.42
HCL Leach	1.49	\$0.07	8400	\$903.66
Filter	1.3	\$0.07	8400	\$788.42
CONSUMABLES	Quantity	Cost per Ton	Tons per year	\$2,818,200
Sulfuric Acid	1	\$135.00	7000	\$945,000.00
Sodium Carbonate	1	\$150.00	7000	\$1,050,000.00
Sodium Hydroxide	1	\$300.00	1960	\$588,000.00
HCl	1	\$240.00	980	\$235,200.00
Total:				(\$3,554,000)

Cashflow Models

The prior economic data is combined to construct a cashflow model. The OPEX and CAPEX are included as costs. The material values in combination with the mass balance are used to predict revenues based on empirical results for process throughput and recovery. The cashflow model for the process illustrated by Figure 5.1 is shown in Table 5.4.

Table 5.4: Cashflow model for the gallium recovery process

		Cashflow	\$ (2,583,000.00)	\$ (2,650,260.87)	\$ (2,650,260.87)	\$ (2,650,260.87)	\$ (2,650,260.87)	\$ (2,650,260.87)	\$ (2,650,260.87)	\$ (2,650,260.87)	\$ (2,650,260.87)	\$ (2,650,260.87)	\$ (2,650,260.87)	Sum
		Year	0	1	2	3	4	5	6	7	8	9	10	
		CAPEX	\$ (2,583,000.00)											
Zinc Price \$/Tonne	\$2,745	OPEX		\$ (3,554,000)	\$ (3,554,000)	\$ (3,554,000)	\$ (3,554,000)	\$ (3,554,000)	\$ (3,554,000)	\$ (3,554,000)	\$ (3,554,000)	\$ (3,554,000)	\$ (3,554,000)	
Value of A per ton	\$1,320	Value of Fraction A	\$ -	\$ 462,121	\$ 462,121	\$ 462,121	\$ 462,121	\$ 462,121	\$ 462,121	\$ 462,121	\$ 462,121	\$ 462,121	\$ 462,121	
Value of B per ton	\$35,000	Value of Fraction B	\$ -	\$ 354,908	\$ 354,908	\$ 354,908	\$ 354,908	\$ 354,908	\$ 354,908	\$ 354,908	\$ 354,908	\$ 354,908	\$ 354,908	
Value of C per ton	-\$300	Value of Fraction C	\$ -	\$ (7,938)	\$ (7,938)	\$ (7,938)	\$ (7,938)	\$ (7,938)	\$ (7,938)	\$ (7,938)	\$ (7,938)	\$ (7,938)	\$ (7,938)	
Value of D per ton	\$35,000	Value of Fraction D	\$ -	\$ 102,410	\$ 102,410	\$ 102,410	\$ 102,410	\$ 102,410	\$ 102,410	\$ 102,410	\$ 102,410	\$ 102,410	\$ 102,410	
Value of E per ton	-\$20	Value of Fraction E	\$ -	\$ (7,762)	\$ (7,762)	\$ (7,762)	\$ (7,762)	\$ (7,762)	\$ (7,762)	\$ (7,762)	\$ (7,762)	\$ (7,762)	\$ (7,762)	
Ga Grade	Fraction of Input Mass	Feed Processed (Tons)	0	7000	7000	7000	7000	7000	7000	7000	7000	7000	7000	70000
0%	0.05	Fraction A Recovered (Tons)	0	350	350	350	350	350	350	350	350	350	350	3500
46%	0.0032	Fraction B Recovered (Tons)	0	22	22	22	22	22	22	22	22	22	22	221
0%	0.0038	Fraction C Recovered (Tons)	0	26	26	26	26	26	26	26	26	26	26	265
25%	0.0017	Fraction D Recovered (Tons)	0	12	12	12	12	12	12	12	12	12	12	117
0%	0.055	Fraction E Recovered (Tons)	0	385	385	385	385	385	385	385	385	385	385	
		Gallium Recovered (lb)	0	26132	26132	26132	26132	26132	26132	26132	26132	26132	26132	261325
NPC	(\$22,200,720)	NPC/lb Ga	(\$84.95)											
NPV	(\$13,812,214)	IRR	#NUM!											

5.2 Base Case Incremental analysis

The cashflow model and net present value discussed above is interesting only insofar as business decisions can be informed by the analysis. To better summarize the possible business decision making in this project an incremental analysis is completed considering each process product and the costs for its recovery independently. To accomplish this four separate OPEX, CAPEX, and cashflow models are developed to represent the additional OPEX, CAPEX and independent cashflow related to each part of the total flowsheet (Figure 5.1). This incremental analysis is not as abstract as it may appear at first glance, the concept is simply considering each additional optional processing operation as additions to an existing process. This project is actually conceived as an optional additional processing route to treat a waste product from the primary zinc process. The CAPEX for each additional increment is easy to determine as each increment utilizes independent apparatus in the original cashflow model and so the costs associate with each incremental part of the flowsheet can be assigned. The OPEX, particularly labor, is somewhat more difficult to accurately distribute across the various operations. For this analysis the labor is distributed according to the number of unit operations in each increment.

5.2.1 Increment A

Fraction A is the first fraction extracted; it is possible to recover fraction A without recovering any of the subsequent gallium concentrates this concept is illustrated with Figure 5.5. Another fraction very similar to fraction E would be produced even without subsequent processing steps, the value of E should be considered as part of this process as chemically and mineralogically this precipitate is very similar to E. The precipitate mass here is on the order of 6% of the feed mass, Fraction E previously represented about 5.5% of the feed mass. The total mass extracted via the additional operations is on the order of 0.7% and so will not make a significant difference in the metals value for fraction E, at least to the resolution available in this early level economic analysis.

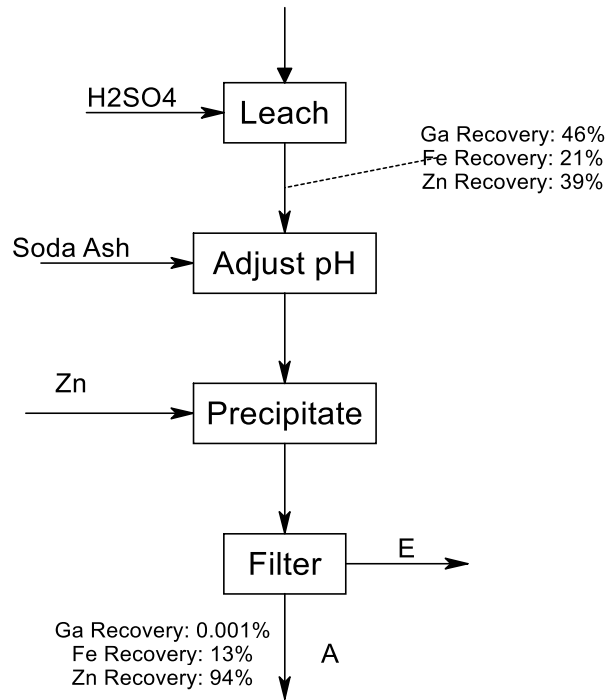


Figure 5.3: Incremental flowsheet A

The CAPEX for this flowsheet is shown in Table 5.5.

Table 5.5: Capex for Increment A

CAPEX	
Vat Leach Vat+mixer	\$ 40,400.00
Filter	\$ 137,700.00
Cementation tank	\$ 40,400.00
Filter	\$ 73,345.72
Subtotal:	\$ 291,845.72
Delivery	\$ 8,755.37
Engineering	\$ 96,309.09
Installation	\$ 72,961.43
Electrical	\$ 72,961.43
Intrumentation:	\$ 29,184.57
Plumbing:	\$ 58,369.14
Subtotal 2	\$ 630,386.75
Operating Capital	\$ 604,000.00
Total with contingency	\$ 1,455,000.00

The OPEX for this flowsheet represents the energy and consumables consumption based on the mass balance as well as 4/7^{ths} of the total labor costs (proportion of the unit operations

included in increment A). This is presented in Table 5.6. The cashflow model is detailed as Table 5.7. The cashflow model also presents the recovery of various materials.

Table 5.6: OPEX for increment A

Cost Item:		per unit cost	total cost/unit	units per year	Total per year:
LABOR:	Quantity	cost per hour		units per year	\$413,241.71
Mill Labor	8	\$24.00	278.4	2000	\$556,800.00
Mill Operator	1	\$28.50	\$41.33	2000	\$82,650.00
Mechanic	1	\$28.87	41.8615	2000	\$83,723.00
			0		\$0.00
ELECTRIC POWER	QNTY per Hr (Kw)	cost per KwHr		units per year	\$7,556.74
Vat Leach	4.45	\$0.07	0.32129	8400	\$2,698.84
Filter	3.73	\$0.07	0.269306	8400	\$2,262.17
Cementation Tank	2.98	\$0.07	0.215156	8400	\$1,807.31
Filter	1.3	\$0.07	0.09386	8400	\$788.42
Contingency Factor					\$0.00
CONSUMABLES	Quantity	Cost per unit		Units per year	\$1,995,000.00
Sulfuric Acid	1	\$ 135.00		7000	\$945,000.00
Sodium Carbonate	1	\$ 150.00		7000	\$1,050,000.00
Total:					\$ (2,416,000.00)

Table 5.7: Cashflow model for Increment A

		Cashflow	\$ (1,455,000.00)	\$ (1,953,879.25)	\$ (1,953,879.25)	\$ (1,953,879.25)	\$ (1,953,879.25)	\$ (1,953,879.25)	\$ (1,953,879.25)	\$ (1,953,879.25)	\$ (1,953,879.25)	\$ (1,953,879.25)	\$ (1,953,879.25)	\$ (1,953,879.25)
		Year	0	1	2	3	4	5	6	7	8	9	10	
		CAPEX	\$ (1,455,000.00)											
Zinc Price \$/Tonne	2745	OPEX	\$ -	\$ (2,416,000)	\$ (2,416,000)	\$ (2,416,000)	\$ (2,416,000)	\$ (2,416,000)	\$ (2,416,000)	\$ (2,416,000)	\$ (2,416,000)	\$ (2,416,000)	\$ (2,416,000)	\$ (2,416,000)
Value of A	1320	Value of Fraction A	\$ -	\$ 462,121	\$ 462,121	\$ 462,121	\$ 462,121	\$ 462,121	\$ 462,121	\$ 462,121	\$ 462,121	\$ 462,121	\$ 462,121	\$ 462,121
Value of E	-20	Value of Fraction E	\$ -	\$ (7,762)	\$ (7,762)	\$ (7,762)	\$ (7,762)	\$ (7,762)	\$ (7,762)	\$ (7,762)	\$ (7,762)	\$ (7,762)	\$ (7,762)	\$ (7,762)
Ga Grade	Fraction of Input Mass	Feed Processed (Tons)	0	7000	7000	7000	7000	7000	7000	7000	7000	7000	7000	7000
0%	0.05	Fraction A Recovered (Tons)	0	350	350	350	350	350	350	350	350	350	350	350
	0.055	Fraction E Recovered (Tons)	0	385	385	385	385	385	385	385	385	385	385	385
		Gallium Recovered (lb)	0	0	0	0	0	0	0	0	0	0	0	0
NPC	(\$13,591,549)	NPC/lb Ga	-											
NPV	(\$9,792,233)	IRR	-											

5.2.2 Increment B

Assuming that the process of Increment A exists, one could evaluate the additional economics of adding a process shown as Increment B in Figure 5.4.

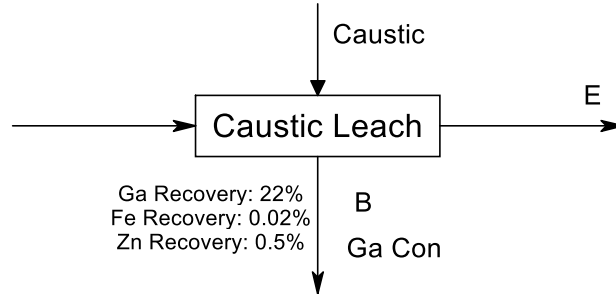


Figure 5.4: Incremental flowsheet B

The CAPEX for this additional separation is summarized in Table 5.8 and OPEX is summarized in Table 5.9. The sizing for the CAPEX is the same as that for the total flowsheet presented previously. The OPEX for this section includes a fraction of the labor cost from the original OPEX estimate. As in Increment A, this fraction of the labor is based on the number of unit operations in this interval versus the total number of unit operations. 1/7th of the labor cost is included in Increments B, C, and D. These are used to construct a cashflow model shown in Table 5.10.

Table 5.8: Capex for Increment B

CAPEX	
Caustic vat leach	\$ 23,100.00
Filter	\$ 73,345.72
Subtotal:	\$ 96,445.72
Delivery	\$ 2,893.37
Engineering	\$ 31,827.09
Installation	\$ 24,111.43
Electrical	\$ 24,111.43
Intrumentation:	\$ 9,644.57
Plumbing:	\$ 19,289.14
Subtotal 2	\$ 208,322.75
Operating Capital	\$ 62,500.00
Total with contingency	\$ 344,000.00

Table 5.9: OPEX for Increment B

Cost Item:		per unit cost	total cost/unit	units per year	Total per year:
LABOR:	Quantity	cost per hour		units per year	\$103,310.43
Mill Labor	8	\$24.00	278.4	2000	\$556,800.00
Mill Operator	1	\$28.50	\$41.33	2000	\$82,650.00
Mechanic	1	\$28.87	41.8615	2000	\$83,723.00
			0		\$0.00
ELECTRIC POWER	QNTY per Hr (Kw)	cost per KwHr		units per year	\$154.91
Caustic vat leach	1.49	\$0.07	0.107578	1440	\$154.91
Filter	1.3	\$0.07	0.09386		\$0.00
Contingency Factor					\$0.00
CONSUMABLES	Quantity	Cost per unit		Units per year	\$147,000.00
Sulfuric Acid	1	\$ 135.00		0	\$0.00
Sodium Carbonate	1	\$ 150.00		0	\$0.00
Sodium Hydroxide	1	\$ 300.00		490	\$147,000.00
Total:					\$ (250,000.00)

Table 5.10: Cashflow model for increment B

		Cashflow	\$ (344,000.00)	\$ 104,907.98	\$ 104,907.98	\$ 104,907.98	\$ 104,907.98	\$ 104,907.98	\$ 104,907.98	\$ 104,907.98	\$ 104,907.98	\$ 104,907.98	\$ 104,907.98	\$ 104,907.98
		Year	0	1	2	3	4	5	6	7	8	9	10	
		CAPEX	\$ (344,000.00)											
Zinc Price \$/Tonne	2745	OPEX	\$ -	\$ (250,000)	\$ (250,000)	\$ (250,000)	\$ (250,000)	\$ (250,000)	\$ (250,000)	\$ (250,000)	\$ (250,000)	\$ (250,000)	\$ (250,000)	\$ (250,000)
Value of B	35000	Value of Fraction B	\$ -	\$ 354,908	\$ 354,908	\$ 354,908	\$ 354,908	\$ 354,908	\$ 354,908	\$ 354,908	\$ 354,908	\$ 354,908	\$ 354,908	\$ 354,908
Ga Grade	Fraction of Input Mass	Feed Processed (Tons)	0	7000	7000	7000	7000	7000	7000	7000	7000	7000	7000	70000
46%	0.003	Fraction B Recovered (Tons)	0	22.092	22.092	22.092	22.092	22.092	22.092	22.092	22.092	22.092	22.092	220.92
		Gallium Recovered (lb)	0	20280.456	20280.456	20280.456	20280.456	20280.456	20280.456	20280.456	20280.456	20280.456	20280.456	202804.56
NPC	(\$1,582,265.93)	NPC/lb Ga												(\$7.80)
NPV	\$158,703.37	IRR	28%											

5.2.3 Increment C

CAPEX, OPEX, and cashflow are constructed for increment C as done for the increments above in Figure 5.5 and tables 5.11 through 5.13.

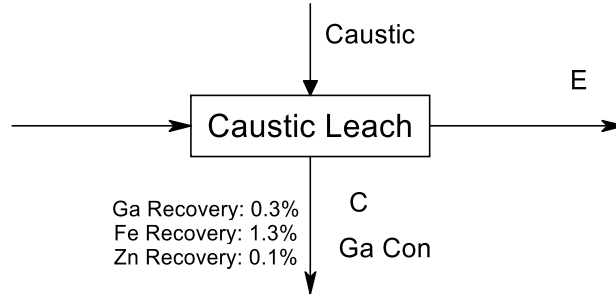


Figure 5.5: Incremental flowsheet C

Table 5.11: CAPEX model for Increment C

CAPEX	
Caustic vat leach	\$ 23,100.00
Filter	\$ 73,345.72
Subtotal:	\$ 96,445.72
Delivery	\$ 2,893.37
Engineering	\$ 31,827.09
Installation	\$ 24,111.43
Electrical	\$ 24,111.43
Intrumentation:	\$ 9,644.57
Plumbing:	\$ 19,289.14
Subtotal 2	\$ 208,322.75
Operating Capital	\$ 136,500.00
Total with contingency	\$ 418,000.00

Table 5.12: OPEX model for increment C

Cost Item:		per unit cost	total cost/unit	units per year	Total per year:
LABOR:	Quantity	cost per hour		units per year	\$103,310.43
Mill Labor	8	\$24.00	\$ 278.40	2000	\$556,800.00
Mill Operator	1	\$28.50	\$ 41.33	2000	\$82,650.00
Mechanic	1	\$28.87	\$ 41.86	2000	\$83,723.00
			0		\$0.00
ELECTRIC POWER	QNTY per Hr (Kw)	cost per KwHr		units per year	\$1,692.08
Caustic vat leach	1.49	\$0.07	0.107578	8400	\$903.66
Filter	1.3	\$0.07	0.09386	8400	\$788.42
Contingency Factor					\$0.00
CONSUMABLES	Quantity	Cost per unit		Units per year	\$441,000.00
Sulfuric Acid	1	\$ 135.00		0	\$0.00
Sodium Carbonate	1	\$ 150.00		0	\$0.00
Sodium Hydroxide	1	\$ 300.00		1470	\$441,000.00
Total:					\$ (546,000.00)

Table 5.13: Cashflow model for increment C

		Cashflow	\$ (418,000.00)	\$ (553,938.00)	\$ (553,938.00)	\$ (553,938.00)	\$ (553,938.00)	\$ (553,938.00)	\$ (553,938.00)	\$ (553,938.00)	\$ (553,938.00)	\$ (553,938.00)	\$ (553,938.00)	
		Year	0	1	2	3	4	5	6	7	8	9	10	
		CAPEX	\$ (418,000.00)											
Zinc Price \$/Tonne	2745	OPEX	\$ (546,000)	\$ (546,000)	\$ (546,000)	\$ (546,000)	\$ (546,000)	\$ (546,000)	\$ (546,000)	\$ (546,000)	\$ (546,000)	\$ (546,000)	\$ (546,000)	
Value of C	-300	Value of Fraction C	\$ -	\$ (7,938)	\$ (7,938)	\$ (7,938)	\$ (7,938)	\$ (7,938)	\$ (7,938)	\$ (7,938)	\$ (7,938)	\$ (7,938)	\$ (7,938)	
Ga Grade	Fraction of Input Mass	Feed Processed (Tons)	0	7000	7000	7000	7000	7000	7000	7000	7000	7000	7000	70000
0%	0.00378	Fraction C Recovered (Tons)	0	26.46	26.46	26.46	26.46	26.46	26.46	26.46	26.46	26.46	26.46	264.6
		Gallium Recovered (lb)	0	0	0	0	0	0	0	0	0	0	0	0
NPC	(\$3,429,939.67)	NPC/lb Ga												#DIV/0!
NPV	(\$2,780,944.92)	IRR	#NUM!											

5.2.4 Increment D

CAPEX (table 5.13), OPEX (table 5.14), and cashflow (table 5.15) are constructed for increment D as done for the increments above. Waste stream E that is the residue from the HCl leach in increment D is not included in this increment as it is already accounted for in Increment A. The difference in total mass of fraction E and composition of fraction E is not considered significant whether it is produced as a by-product of A, B, C, or D. There is little change in cashflow related to the reduction of mass in fraction E by the additional unit operations for increments B through D.

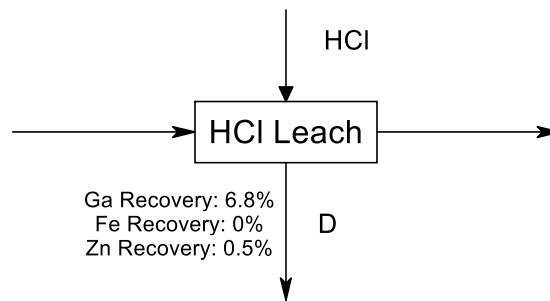


Figure 5.6: Incremental flowsheet D

Table 5.14: CAPEX model for Increment D

CAPEX	
HCL Leach	\$ 23,100.00
Filter	\$ 73,345.72
Subtotal:	\$ 96,445.72
Delivery	\$ 2,893.37
Engineering	\$ 31,827.09
Installation	\$ 24,111.43
Electrical	\$ 24,111.43
Intrumentation:	\$ 9,644.57
Plumbing:	\$ 19,289.14
Subtotal 2	\$ 208,322.75
Operating Capital	\$ 84,750.00
Total with contingency	\$ 366,000.00

Table 5.15: OPEX model for increment D

Cost Item:		per unit cost	total cost/unit	units per year	Total per year:
LABOR:	Quantity	cost per hour		units per year	\$103,310.43
Mill Labor	8	\$24.00	278.4	2000	\$556,800.00
Mill Operator	1	\$28.50	\$41.33	2000	\$82,650.00
Mechanic	1	\$28.87	41.8615	2000	\$83,723.00
				0	\$0.00
ELECTRIC POWER	QNTY per Hr (Kw)	cost per KwHr		units per year	\$788.42
HCL Leach	1.49	\$0.07	0.107578	8400	
Filter	1.3	\$0.07	0.09386	8400	\$788.42
Contingency Factor					\$0.00
CONSUMABLES	Quantity	Cost per unit		Units per year	\$235,200.00
Sulfuric Acid	1	\$ 135.00		0	\$0.00
Sodium Carbonate	1	\$ 150.00		0	\$0.00
Sodium Hydroxide	1	\$ 300.00		0	\$0.00
HCl	1	\$ 240.00		980	\$235,200.00
Total:					\$ (339,000.00)

Table 5.16: Cashflow model for Increment D

Cashflow			\$ (366,000.00)	\$ (236,590.00)	\$ (236,590.00)	\$ (236,590.00)	\$ (236,590.00)	\$ (236,590.00)	\$ (236,590.00)	\$ (236,590.00)	\$ (236,590.00)	\$ (236,590.00)	\$ (236,590.00)
Year			0	1	2	3	4	5	6	7	8	9	10
CAPEX			\$ (366,000.00)										
OPEX			\$ (339,000)	\$ (339,000)	\$ (339,000)	\$ (339,000)	\$ (339,000)	\$ (339,000)	\$ (339,000)	\$ (339,000)	\$ (339,000)	\$ (339,000)	\$ (339,000)
Zinc Price \$/Tonne	2745												
Value of D	35000	Value of Fraction D	\$ -	\$ 102,410.00	\$ 102,410.00	\$ 102,410.00	\$ 102,410.00	\$ 102,410.00	\$ 102,410.00	\$ 102,410.00	\$ 102,410.00	\$ 102,410.00	\$ 102,410.00
Value of E		Value of Fraction E											
Ga Grade	Fraction of Input Mass	Feed Processed (Tons)	0	7000	7000	7000	7000	7000	7000	7000	7000	7000	7000
25%	0.0017	Fraction D Recovered (Tons)	0	12	12	12	12	12	12	12	12	12	12
		Gallium Recovered (lb)	0	5852	5852	5852	5852	5852	5852	5852	5852	5852	5852
NPC	(\$2,226,371.14)	NPC/lb Ga											
NPV	(\$1,350,774.32)	IRR	#NUM!										(\$38.04)

5.2.5 Summary of Incremental Analysis

The results of the incremental analysis are summarized in Table 5.16. It is shown that the gallium recovery process in any of its variations is not investable in the base case. The expenditures related to recovery of the various process products are more expensive than the value of those products resulting in negative cashflow in most cases. These increments are Discussed as if the previous unit operations are already in existence, meaning that additional processing must provide sufficient cashflow to make the case for additional processing. This is found with Increment B as there is positive net present value associated with the gallium value recovery, however as Increment A is negative the case for increment B must also support accepting the negative value proposition associated with Increment A. Increments C and D lose money in the base case. Additional analysis will discuss the specific parameters that may change to affect these net present values most significantly.

Table 5.17: Summary of results from incremental economic analysis

Increment	CAPEX	OPEX, Year 1	Annual Cashflow, Year 1	NPV
A	(\$1,455,000)	(\$2,416,000)	(\$1,953,879)	(\$9,792,233)
B	(\$344,000)	(\$250,000)	\$104,908	\$158,703
C	(\$418,000)	(\$546,000)	(\$553,938)	(\$2,780,945)
D	(\$366,000)	(\$339,000)	(\$236,590)	(\$1,350,774)

5.3 Economic Decision Making

There are several economic decision-making methods that should all converge on the same economic conclusion when applied properly. methods are useful for summarizing the economic merit of a proposed project. Some of the methods used in this thesis is Net Present Value (or net present cost) assessments, breakeven analysis, and sensitivity analysis. As the net present values shown in section 5.1 for the total project and the section 5.2.5 for the various increments are negative for the base case it is interesting to consider the cases under which the process or some of these increments may have positive economics.

5.3.1 Sensitivity Analysis

Sensitivity analysis is completed to show the impact of changes to various parameters for the base case cost model. These are presented as changes to the net present value as a function of the change in a given parameter. The affect is determined for all 4 incremental analyses as well

as for the total flowsheet shown as figure 5.1. In some of the following charts the chart is simplified by only displaying the net present value response for those increments where the effect of the change in the parameter is noticeable.

5.3.1.1 Sensitivity to CAPEX

The capital expenditure is determined to the best of the authors' abilities to develop the cost model for the flowsheet and incremental analyses. It should be noted however that this early-stage cost estimate is considered inaccurate due to the many unknowns remaining in the process design as well as the scale at which test work is completed. Larger scale test work would lend itself to more accurate estimation of the capital expenditure and more detailed studies on various unit operations in the flowsheet would allow more accurate design of the process hardware. The sensitivity is interesting to show the influence these inaccuracies may have on the models discussed above as well as contributing to areas where the process economics may be benefited by additional research work.

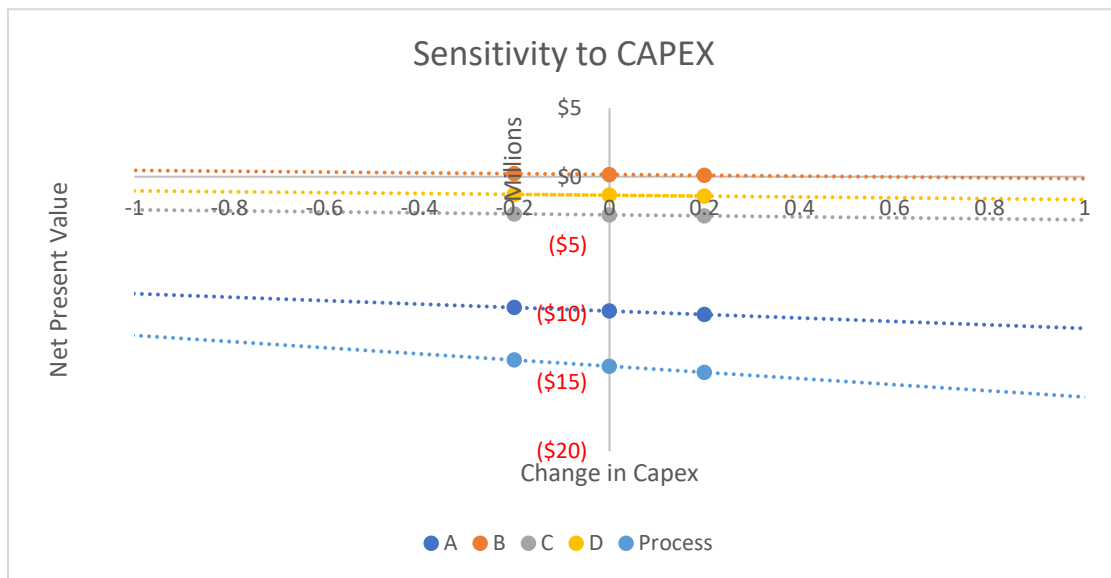


Figure 5.7: Sensitivity of the 5 increments and total process to changes or uncertainty in CAPEX

The sensitivity chart (Figure 5.7) shows that capex does not significantly affect the economics of the process. Increment A, and the total process are more sensitive to CAPEX changes than the lower CAPEX increments which would be expected considering their relative CAPEX costs. That said there is no reduction in CAPEX that would alone make the process, or any of the base case negative present value increments positive. It should be noted that increment

B (the only increment with a positive NPV in the base case) shifts to negative if the CAPEX is 53% higher than the estimate in the base case. Overall inaccuracies in the CAPEX and/or reduction in CAPEX by additional engineering will not alter the economic decision making for this process at this stage. If other economic conditions are changed the effect of CAPEX changes on the NPVs may be more significant and worthy of additional study.

5.3.1.2 Sensitivity to Sulfuric Acid

Sulfuric acid was identified originally as a significant contributor to the operating costs of a plant focused on co-product production. The sensitivity analysis has confirmed this initial assessment as the sulfuric acid consuming operations net present values are changed significantly by changes to the sulfuric acid costs. Figure 5.8 shows that both increment A and the process as a whole are largely dependent upon sulfuric acid costs. Increments B, C, and D do not use sulfuric acid and so are not included in the chart for this section.

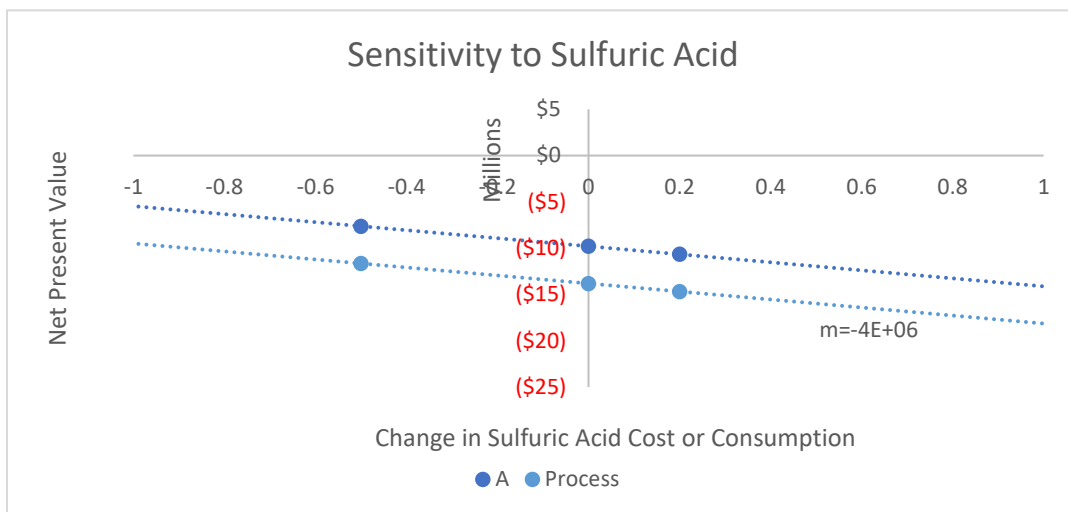


Figure 5.8: Sensitivity to Sulfuric acid costs

Though sulfuric acid costs do not make either of these models net present value positive over the range of costs considered realistic, the magnitude of the effect is considered worthy of additional technical research. It should be noted that the effect here could be achieved or observed with a range of technological developments or changes in market conditions. First, it should be noted that changes in sulfuric acid prices are quite possible in a magnitude that has significant effects on the process NPV. The spot price for sulfuric acid has fluctuated from \$120 per ton in 2017 to \$150 per ton in 2019 under normal circumstances. In the last seven months sulfuric acid spot price has increased from \$129 per ton to \$142 per ton. The base case used a

price of \$135 per ton but this price may well fluctuate by 20% positively or negatively based on market conditions. More extreme market fluctuations such as those seen in 2008 when sulfuric acid price reached about \$300 per ton indicate that 100% spikes in sulfuric price may be worthy of consideration even if they are uncommon. Technical changes would generally take the form of reduced acid consumption, in the net present value calculation these look similar to changes in commodity price, the x-axis should be interpreted as change in total sulfuric acid costs. Minor changes in sulfuric acid consumption may be possible with additional separations test work, the statistical analysis of leaching behavior showed that acid concentration cannot be reduced without reducing recovery but indicated that changes in slurry density may be possible to reduce the acid consumption per ton of CLP processed. This would probably result in small changes relative to the base case. Larger changes to sulfuric acid consumption are possible by the lixiviant regeneration process discussed technically in Chapters 7 & 8. The economics of this process are considered separately from the separations economics and are discussed in Chapter 9. For now, it is sufficient to indicate that sulfuric acid costs are a major contributor to the process economics.

5.3.1.3 Sensitivity to Soda Ash

Soda ash consumption by molar quantities is less than sulfuric acid consumption, however due to the higher molar mass of soda ash as well as the relatively higher price at the time of this writing the cost of soda ash is actually more affectual of the process economics than sulfuric acid. The interpretation of this chart should be similar to that for the sulfuric acid sensitivity discussed previously to represent either (or both) changes in commodity price or changes in reagent consumption. As for the section on sulfuric acid the increments A, B, and D are not considered here as they do not consume soda ash and so showed no sensitivity to this price change. The results of the sensitivity analysis are presented in figure 5.9.

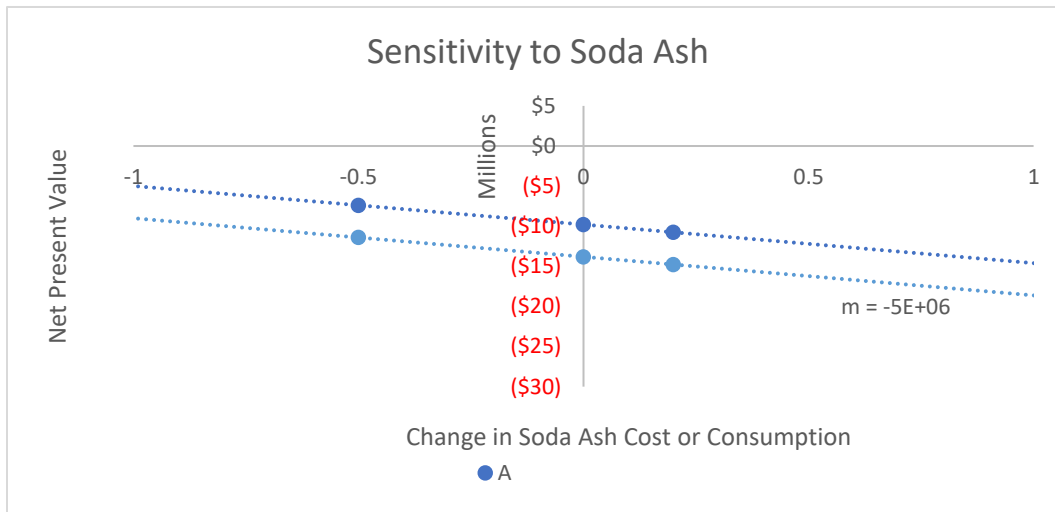


Figure 5.9: Sensitivity to soda ash costs

The producer price index for sodium (carbonate and sulfate considered together) has fluctuated less than sulfuric acid spot over recent years. The index has fluctuated between 210 and 157 since 2008 representing price fluctuations of 30% may be expected but 100% fluctuations as seen in the sulfuric acid price are considered less reasonable to discuss here. There are three major technical developments that may affect soda ash costs by reducing consumption. Firstly, and probably most significantly is the lixiviant regeneration process discussed in chapters 7-9 which may reduce new soda ash consumption by an amount approaching 100%. As soda ash is used in raising the pH of the sulfuric leach liquor any reduction in sulfuric acid consumption per ton of CLP processed would require less soda ash as well to neutralize the lower volume of sulfuric acid. Another technological development that may be influential to soda ash consumption is changing the pH range for precipitation to a lower range. Optimization of the precipitation conditions may improve the process economics significantly. The slope of the line for the full process is displayed in order to compare the effects of soda ash cost changes to sulfuric acid cost changes. The larger slope for the soda ash cost effects indicates that the process is more sensitive to changes in soda ash costs or consumption.

5.3.1.4 Sensitivity to Combined Reagent Costs

As there are significant combined effects on soda ash and sulfuric acid consumption from various technology improvements the combined effect on reagent costs must be considered. Though Increments B,C, and D do not include soda ash or sulfuric acid they do consume hydrochloric acid and caustic.

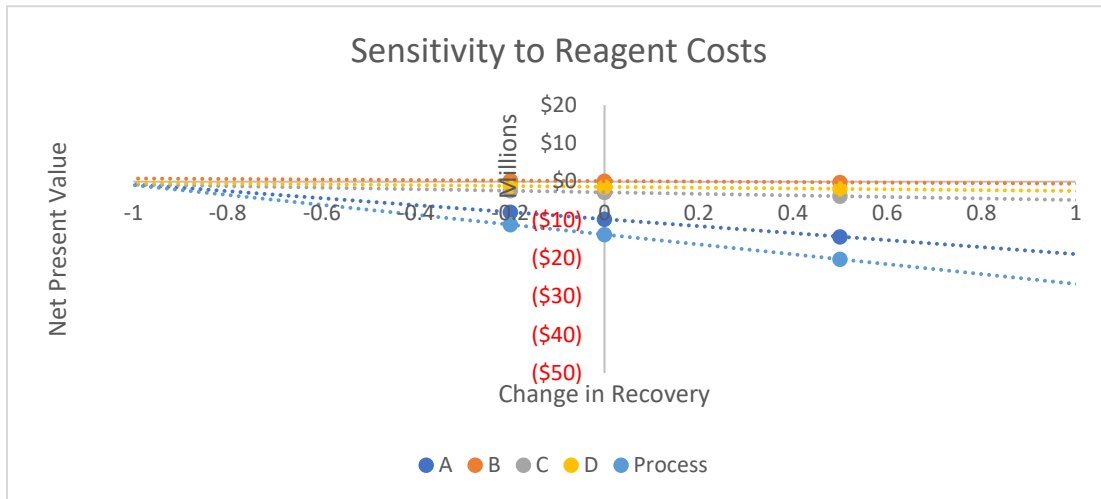


Figure 5.10: Sensitivity to total reagent costs

Increment B, C, and D are difficult to read from the chart (Figure 5.10) but are downward sloping representing a negative relationship with increased reagent costs. The Increment A and the total process are more noticeably affected by the reduction in reagent costs. Based on the trendline for the Increment A, a discussion of the necessary reduction in reagent costs in order to achieve positive NPV is possible. This is most interesting to consider for increment A as the addition of increment B is viable in the base case if a case for increment A is viable. An NPV of 0 is achieved mathematically by a 111% reduction in reagent costs. This is considered outside of the bounds of reality and so simply reducing reagent costs will not alone achieve a positive NPV. It is perhaps interesting to note the reduction at which cashflow for increment A becomes positive even if NPV is still negative. Positive cashflows from A require approximately 100% reduction in reagent costs. If this were possible through the reagent recovery process it would require significant additional CAPEX and so alone does not make this process investable under any circumstances. It may also be interesting to consider the reduction in reagent costs necessary to achieve a zero NPV for the combined case of increments A and B. Solving based on the trendline the reagent consumption costs must be reduced by ~109% to generate a combined NPV

of zero. This suggests that reducing reagent costs is not sufficient make this process economically viable.

5.3.1.5 Sensitivity to Materials Recovery

There are several technology alternatives discussed to improve recoveries. Of particular interest is improving the recovery of zinc and gallium. Most process changes that improve recovery of these value materials also increase recovery of components that negatively affect the process economics. Fractions A, B, and D are value components whereas fractions C and E are considered wastes in this work.

The unit operation most interesting to improved recovery is the leach operation. The current process shows a leach recovery of gallium on the order of 45% and of zinc of 21%. The sensitivity of every unit operation to recovery is not discussed here. The leach recovery would have the largest expected impact on total process economics of any single unit operation. It is also assumed for the purposes of this chart that the recovery of each of the major metal components increases proportionally. This meaning that the production of each value fraction and each waste fraction is increased simultaneously. The increment C has a negative relationship between NPV and leach recovery whereas all of the other fractions become more economically favorable with increased leach recovery. It should be understood that an increase in leach recovery of 100% is relative to the base case leach recovery and so represents a total leach recovery of 90%. One possibility for an alternative process that would improve leach recovery is discussed in section 4.3.3.3. The reduction of zinc ferrite to zinc and iron oxide to allow superior leach recoveries.

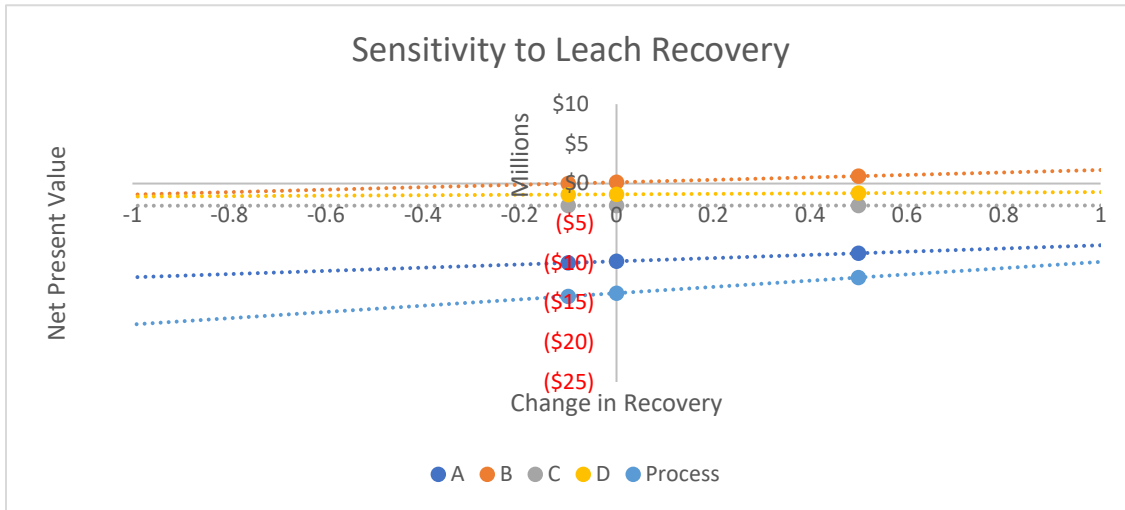


Figure 5.11: Sensitivity to leach recovery

5.3.1.6 Sensitivity to Zinc Value

The increments B, C, and D are taken out of this sensitivity analysis because the products of those increments, while containing zinc, are not priced based on zinc content. Similar to the charts representing sulfuric acid and soda ash simultaneously represent changes in consumption or changes in costs. It is the change in the cost to the model that is charted on the x-axis. In this case it is the change in revenue to the model that is charted on the x-axis, it could represent improved zinc recovery or increased zinc value by either a different pricing criterion than used in the base case or fluctuations in the zinc spot price.

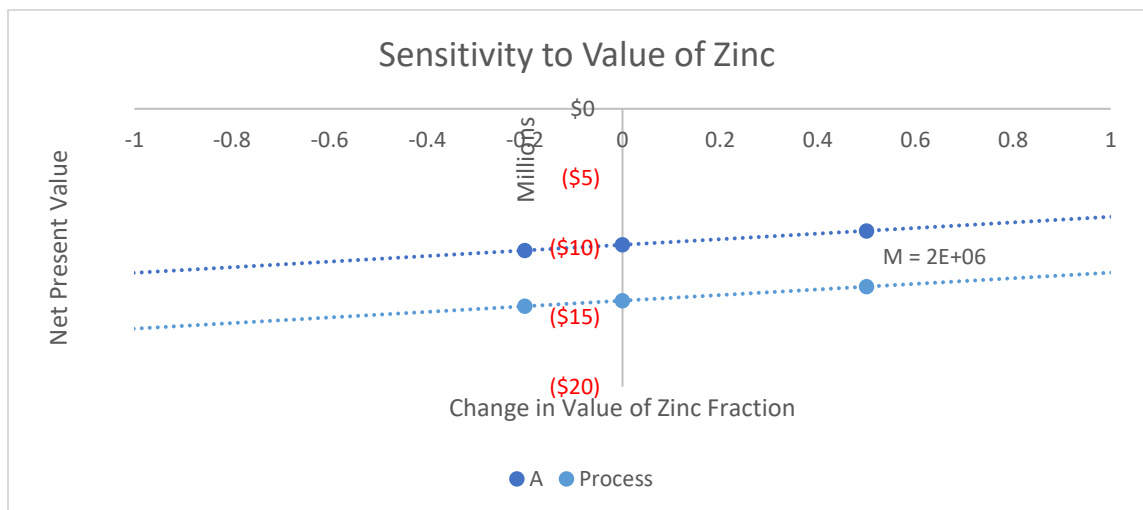


Figure 5.12: Sensitivity to Zinc fraction value

It can be seen in figure 5.12 that zinc value has significant impact on the economics of the process and on increment A. The slope of the sensitivity is provided so that the reader can compare the dependence on zinc value to the dependence on reagent costs. Zinc has fluctuated between \$0.80 per pound and \$1.60 per pound since April 2016. The value used for the base case is \$1.3675 per pound based on the 3-month moving average at the time of this writing. The zinc price has had more extreme moves such as the fall from \$2.05 per pound in 2007 to \$0.54 per pound in 2009 before rising to \$1.20 in 2010. Changes in the order of magnitude of 100% to the upside are quite possible in the zinc market, alternatively zinc price has historically shown downside volatility in the range of 30-50% regularly over the course of the past several years. Zinc recovery may be improved via various process modifications. Zinc recovery cannot be improved without affecting the mass balance of the other fractions recovered. It is unrealistic to expect improved recovery of zinc to the zinc fraction as 94% of the leached zinc is shown to report to that fraction without process modification.

5.3.1.7 Sensitivity to Gallium Value

The sensitivity to gallium value, similar to that for zinc value represents the sensitivity of the base case model to the change in value for gallium (figure 5.13). Gallium is the value commodity for fractions B and D and is not affectual of fractions A and C which are eliminated from this chart for clarity. Gallium leach recovery is also considered as part of the sensitivity to leach recovery chart (figure 5.11). The value of gallium is shown historically to fluctuate quite wildly including an increase on the order of 100% over the past 10 months. It should be considered very reasonable to consider cases for gallium price ranging +/- 60% from the current price.

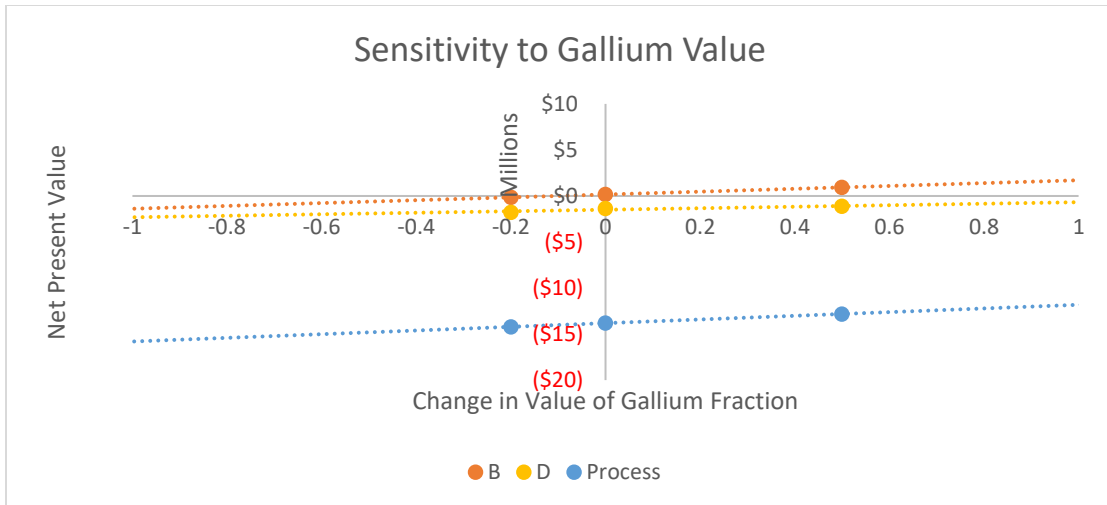


Figure 5.13: Sensitivity to gallium fraction value

5.3.1.8 Sensitivity to waste disposal costs

There are two waste products produced as part of the process identified as Fraction E and Fraction C. Fraction C is considered a hazardous waste and so there is significant cost associated with its disposal (~\$300 per ton). The sensitivity chart considers simply the effects of reduced disposal cost if this fraction could instead be considered as non-hazardous waste (\$20 per ton). As can be seen in figure 5.14. It should not be considered significant to the integrated process whether or not C is classified as a hazardous waste. It is effectual of Increment C's economics but this is not apparent from the scale on the graph.

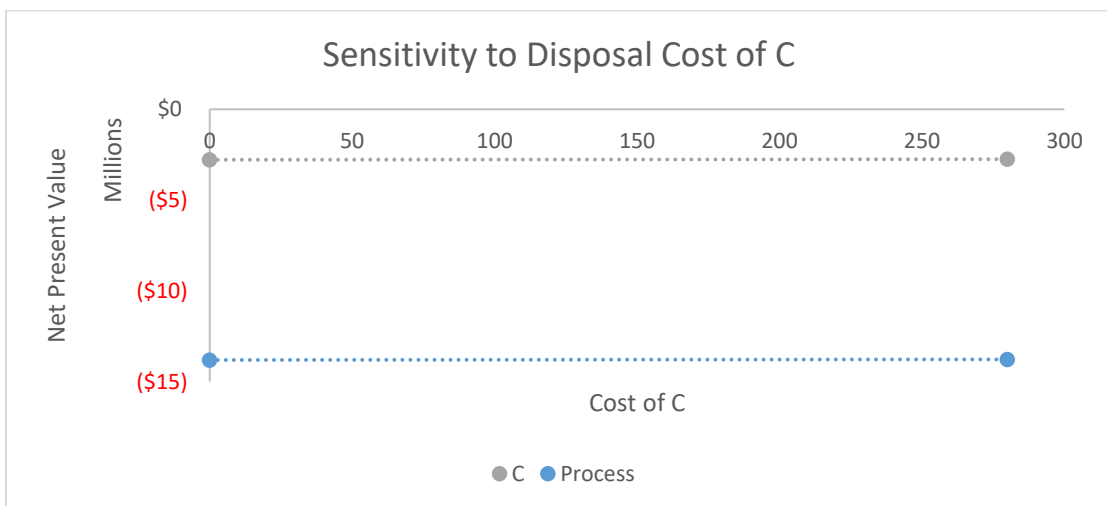


Figure 5.14: Sensitivity to disposal cost of fraction C

The other waste fraction is considered non-hazardous but has valuable component metals including ~20% copper by mass. If this material could achieve some value based on the copper content it could affect the NPV of the process. The base case is a \$20 disposal cost per ton. The challenge with realizing any copper (or iron value) for this product is the difficulty in separating the minerals shown via the XRD results for this fraction. (discussed in section 4.6.3.5) there is probably not enough material of this type in this model process to support additional operations to add value to this fraction but wastes like fraction E are common in the zinc industry and their utilization as a resource may be an interesting topic for future research. If a process is developed to separate copper from goethite, it may be interesting to reconsider this aspect of the process. The sensitivity of the process NPV to this possible change is considered and illustrated by figure 5.17.

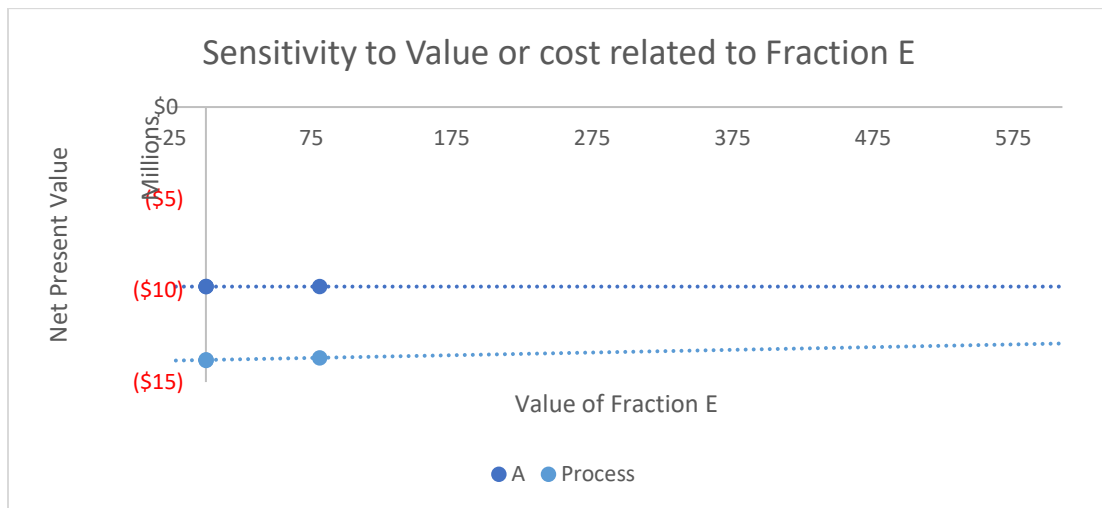


Figure 5.15: Sensitivity to value of fraction E

5.3.2 Process Alternatives

There are several process alternatives alluded to as part of the discussion of sensitivity analysis. Some of these alternatives would include additional CAPEX and possibly new OPEX items to deliver the process improvements discussed.

5.3.2.1 Zinc Ferrite Reduction to Improve Recovery

Zinc ferrite reduction to improve materials recovery may be an interesting addition to the plant process developed here. Initial results indicate that by roasting an additional 20% of the gallium in the CLP material may be liberated and recovered to the leach liquor. This represents a relative improvement of 50% over the non-roasted samples. The roasting also improved zinc

recovery and decreased iron recovery both of which are beneficial to plant economics. Based on the change in zinc recovery and the change in gallium recovery a value for this additional unit operation can be discussed. The value of the higher zinc recovery is discussed in section 5.3.1.6. It is estimated that the additional zinc recovery as observed in the reduction test work would contribute an additional \$3.5Million net present value to increment A, the additional gallium recovery based on the test results would contribute positive net present value to Increment B of \$1.5M. This suggests that the value of the unit operations could be on the order of \$5M to the process. This gives an assessment of the value added by that operation. It should be noted that the combined plant economics will not be made positive solely via the addition of this operation but it may contribute to a larger process that is ultimately economically viable.

5.3.2.2 Lixiviant Regeneration

Lixiviant regeneration economics is discussed on its own in chapters 7-9 including combined results for the model separations plant economics with the acid regeneration circuit. It could be considered an additional incremental improvement over the base case discussed herein and so this process should be developed such that it is economically viable prior to exploration of the additional investment related to the acid regeneration plant. There is also a higher level of precision for the cost estimates for this chapter than for the acid regeneration discussion. The precision of the economic models are limited largely by the level of technological development for the separate flowsheets.

5.3.3.3 Ferrite Leach-Precipitation

Discussed technically in section 4.6.4, a second sample of zinc rich material was obtained from industrial partners that produced a significantly larger precipitate. The ferrite sample contained gallium and indium but these materials did not report to the leach fraction. It may be interesting to consider the zinc recovery via sulfuric leaching and precipitation of major impurities particularly iron, copper, and cadmium. If processed similarly to the process described as increment A, a large fraction may be returned to the zinc process. Considering an adaptation of Increment, A to process this material the CAPEX is assumed to remain the same, the OPEX is considered equivalent (within the reasonably expected accuracy of this analysis).

The increment A for this feedstock is also non economical considering the zinc recovery from the ferrite waste material. If process variations existed which were economical or near-economical it could be interesting to consider the addition of this material as a second feedstock to allow a larger scale process plant.

Table 5.18: Cashflow model for Increment A considering the ferrite feed stock

		Cashflow	\$ (2,583,000.00)	\$ (2,907,030.95)	\$ (2,907,030.95)
		Year	0	1	10
		CAPEX	\$ (2,583,000.00)		
Zinc Price \$/Tonne	\$2,745	OPEX		\$ (3,554,000)	\$ (3,554,000)
Value of A per ton	\$1,320	Value of Fraction A	\$ -	\$ 646,969	\$ 646,969
Ga Grade	Fraction of Input Mass	Feed Processed (Tons)	0	7000	7000
0%	0.07	Fraction A Recovered (Tons)	0	490	490
NPV	(\$14,932,796)				

5.3.3 Breakeven Analysis

This research was initiated by the US Department of Energy’s Critical Materials Institute specifically to target the economic recovery of gallium from a zinc waste stream. It is interesting to consider the costs associated with a plant following the design developed in this work specifically as it pertains to recovery of gallium.

5.3.3.1 Gallium Breakeven

The first (and lowest cost to produce) gallium concentrate is the fraction B that could be produced by a process consisting of increments A and B in series (these increments are illustrated as figure 5.5 and 5.6) It is interesting to consider the price for the gallium concentrate that would be required to motivate investment in this process without regard for the other fractions produced. The net present cost is calculated by considering only the negative cashflows such as CAPEX, OPEX, and disposal costs (for fraction E in this case). This is normalized to the number of pounds of gallium produced. The estimated net present cost of increment A is \$13.6M, and for increment B is estimated at \$1.6M the combined NPC is \$15.2M. The flowsheet consisting of increments A and B together would recover a concentrate that includes 103 tons of gallium per year. The total cost per pound of gallium recovered from the CLP waste stream is estimated at \$74. Fraction D is the second gallium concentrate and is somewhat higher cost. Considering only the gallium revenue stream the price per pound of gallium recovered in this fraction is \$97 per pound, this is based on the net present costs of increment C and D combined. For the process as a whole the cost per pound is \$85. The value discussed for this product is supported at \$20-\$35 per pound of gallium, the market conditions under which this material

could realize a price such as to support a value of \$85 per pound would have to see the gallium price increase by about 200%.

5.3.3.2 Zinc Breakeven

The process could also be considered for its contributions to the zinc plant that produces the CLP material as a process waste. Reducing waste and recycling zinc to the process may be valuable under certain market conditions for zinc. The cost for increment A required to produce the zinc concentrate is \$13.6M. Based on expected zinc recovery of 528,000 pounds annually (as 75% zinc concentrate) the cost per pound of zinc production is \$2.6. The model uses a base price of \$0.66 per pound of zinc recovered. The price of zinc would have to increase by ~300% to make the increment A breakeven based just on zinc recovery. There are a range of combinations that may be imagined where the combined zinc, gallium price results in a breakeven price for this process.

CHAPTER 6 STATE OF THE ART OF REAGENT RECOVERY AND MANUFACTURE

6.1 Industrially relevant processes for sulfuric acid manufacture

Sulfuric acid is formed in nature by the oxidation and subsequent decomposition of sulfur and sulfur compounds. It is generated by bacterial digestion of coal brasses or on iron disulfide. It can be made atmospherically, as acid rain, by the oxidation of sulfur dioxide emitted as part of combustion reactions or is formed by chemical decomposition. The first manufacture of sulfuric acid was accomplished by Basil Valentine in the late 1400s. Valentine produced sulfuric acid by burning sulfur with saltpeter (potassium nitrate) in a glass retort with a small amount of water. He later calcined ferrous sulfate heptahydrate in the presence of silica. These processes were used until 1746 for the manufacture of sulfuric acid when Dr. Roebuck constructed a lead chamber in England for sulfuric acid manufacture. This is the first use of the “chamber process” which was the dominant method for the production of sulfuric acid until the mid-1800s. The procedure included burning sulfur and saltpeter in an eight to one ratio with intermittent air addition. The reaction produced sulfur trioxide which reacted with water to form sulfuric acid that condensed on the vessel walls and collected in pans. It was found that the saltpeter was not necessary for the reaction but rather served as a catalyst to the oxidation reaction. Various refinements for this process were developed through the nineteenth century. During World War I gypsum was burned with coal to produce sulfur dioxide for sulfuric acid production. The modern production of sulfuric acid is mostly from pyrite roasting.



First patented in 1831 in Britain, the patented process consisted of passing sulfur dioxide through a heated glass tube filled with fine platinum to convert the gas into sulfur trioxide. The trioxide of sulfur could be dissolved in chamber process acids to produce high purity acids. Commercialization was delayed until the later half of the 19th century as there was little demand for such concentrated acids. Refinement of the process allowed the contact process to continuously produce dilute acid which no longer required the chamber acid. Today no commercial chamber process plants are operating in the United States. [22]

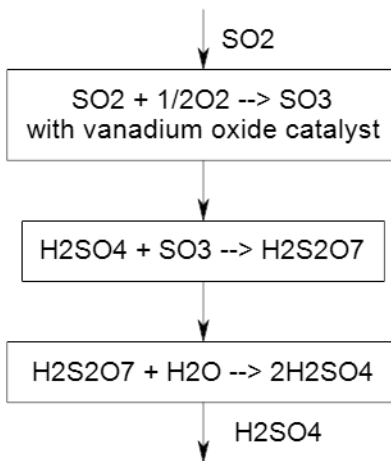


Figure 6.1: Flowsheet for the contact process for sulfuric acid manufacture

It is noted that the production of sulfur dioxide, its conversion to sulfur trioxide, and the dilution of dihydrogen sulfate are exothermic processes. This reduces the energy costs involved in sulfuric acid manufacture. The fundamental steps of the contact process are shown in figure 6.1.

Any number of processes can be used to produce sulfur dioxide and so it is convenient to treat the processes for sulfuric acid production as a separate discussion from those for sulfur dioxide production. [23]

The most recent developments in sulfuric acid manufacture are a shift away from pyrite roasting to acid produced as a byproduct of off gas capture. The main consumers of sulfuric acid are the agriculture industry specifically for fertilizer production, followed by petroleum refining especially for plastic and rubber manufacture, and finally mining and metals industry for leaching operations.

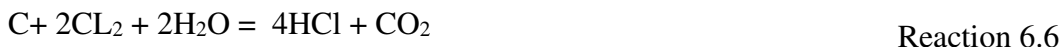
6.2 Muriatic acid

Muriatic acid also known as hydrochloric acid (HCl) is an inorganic acid primarily used a precursor to poly-vinyl chloride or PVC production. It is a strong acid that nearly completely dissociates in solution with water.



The Deacon process is used to convert chlorine into hydrochloric acid. A study of the equilibrium state of this reaction shows that chlorine is favored at lower temperatures while higher temperatures favor hydrogen chloride formation. The Deacon process for chlorine

production was historically carried out at a low temperature and catalyzed by cupric chloride. Above 500°C cupric chloride melts and is no longer useful as a catalyst. Between 600 and 700°C platinum chloride becomes a good catalyst, between 900 and 1000°C no catalyst is necessary.



Nauman and Mudford published an experimental investigation of the reaction between chlorine, steam, and carbon. Chlorine and steam were passed through a tube filled with carbon and heated to a specific temperature. Nagel in 1912 published a process where a mixture of chlorine and steam were passed over red-hot coke. He suggested that the reaction might be run continuously by charging the coke in regular intervals. Various other chemists including Gibbs showed the temperature and gas composition effects on this reaction. The reactions for the solvation of chlorine in water is strongly exothermic. At 1000°C the reaction is simplified to:



Adding chlorine gas to this mixture allows the following reaction to occur:

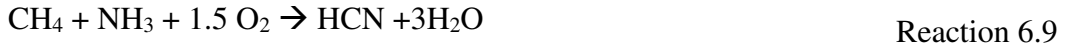


This reaction is generally carried out in a brick lined stack. The lower part of the stack is the reaction chamber while the upper part is used for storing and preheating coke. Chlorine and steam are fed from separate pipes at the bottom of the stack. The coke is charged from above in regular intervals. The gases leave the reaction chamber at between 800 and 950°C. The off gas is cooled and enters an absorption tower. A fan at the end of the absorption tower draws gases from the furnace through the cooling and absorption system. [24]

6.3 Cyanide

The common cyanogens have been used chiefly in extractive metallurgy of silver and gold, in electroplating, and for the surface hardening of metals. The original process for cyanide manufacture was the Landis and Castner processes, neither of which yielded hydrogen cyanide directly. Demand has grown since the 1930s with the development of acrylic polymeric compounds. The primary successful method is based on the work of Andrussow in 1930 which employed methane, ammonia, and air. Though cyanide is predominantly consumed in the chemical industry for acrylics it is often used in mining and extraction to recover precious metals from ore. The production of cyanide in the modern age is based on this process. [25] The

adrussow process produced hydrogen cyanide from ammonia and methane in the presence of oxygen and a catalyst.



The reaction above is exothermic with a negative enthalpy change of 481kj per mole of HCN produced. The heat evolution pushes other reactions including:



These side reactions are minimized by limiting exposure to the catalyst for these species. The original developmental flowsheet for this process from Adrussow's work is shown in figure 6.2. [26]

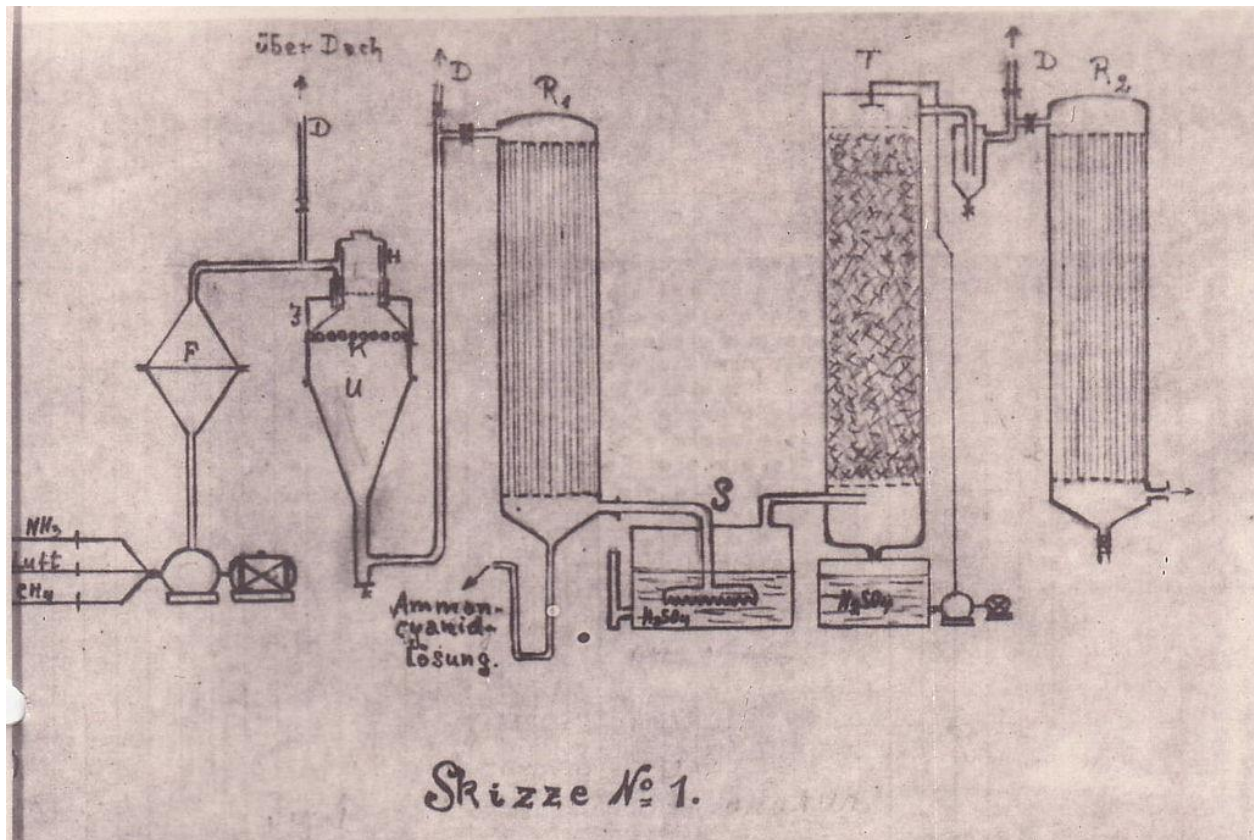


Figure 6.2: An original flowsheet from Adrussow's work for the cyanide production process

6.4 Soda ash

Soda ash (or sodium carbonate) is generally manufactured by the Solvay process developed by Ernest Solvay in the 1860s. The process starts with salt brine and limestone (calcium carbonate) both of which are readily available.

The primary reaction for this process is:

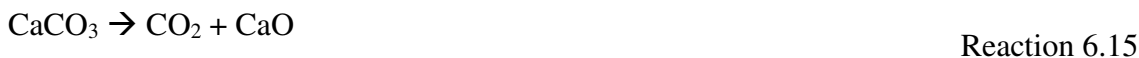


Soda ash is used in a range of applications including glass making as one of the main components of soda lime glass, for water treatment particularly to precipitate out Mg^{2+} and Ca^{2+} carbonates, for making soaps and detergents as an alternative to caustic, for paper making, as a common alkali for industrial processes as an alternative to caustic, for production of sodium bicarbonate for fire suppression, and for removing sulfur dioxide from gaseous emissions from power plants or industrial sites.

It is really inappropriate to consider the process as a single reaction except for mass balances. The reactions that occur include several intermediate components. The reaction can be simplified to four interacting chemical reactions. In the first step carbon dioxide is flowed through an aqueous sodium chloride, ammonia solution.



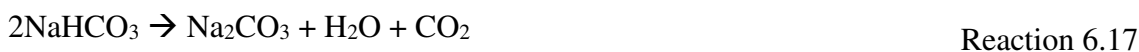
Industrially this is accomplished by flowing brine solution through the ammonia tower and carbonation tower in figure 6.3. Note that the ammonia serves as a buffer solution, without excess ammonia a hydrochloric acid product would form that would force a backward reaction. The limestone (calcium carbonate addition) is partially converted to quicklime via the reaction:



The ammonium chloride solution from reaction 6.15 is filtered to remove the sodium bicarbonate precipitate and then reacted with the quicklime from reaction 16. The resulting reaction is as follows:



The ammonia produced from this reaction is recycled into the initial reaction 6.16. The precipitate from that reaction is converted to soda ash by calcination between 160 and 230 C.



The carbon dioxide from this step is recovered and used in reaction 6.18. Due to the various recycling of intermediate products the only inputs for the Solvay process are salt,

limestone, and energy. And the only major products are soda ash and calcium chloride which is used to de-ice roads. [28]

6.5 Economic considerations of reagent regeneration

The costs for a metallurgical operation are usually significantly impacted by the cost of the reagents consumed and by associated disposal of waste from those reagents. The costs of various common metallurgical reagents are shown in figures 6.3-6.5. The volatility of the reagent market is of note. Extreme price shocks add to the uncertainty of economic success for a mining operation.

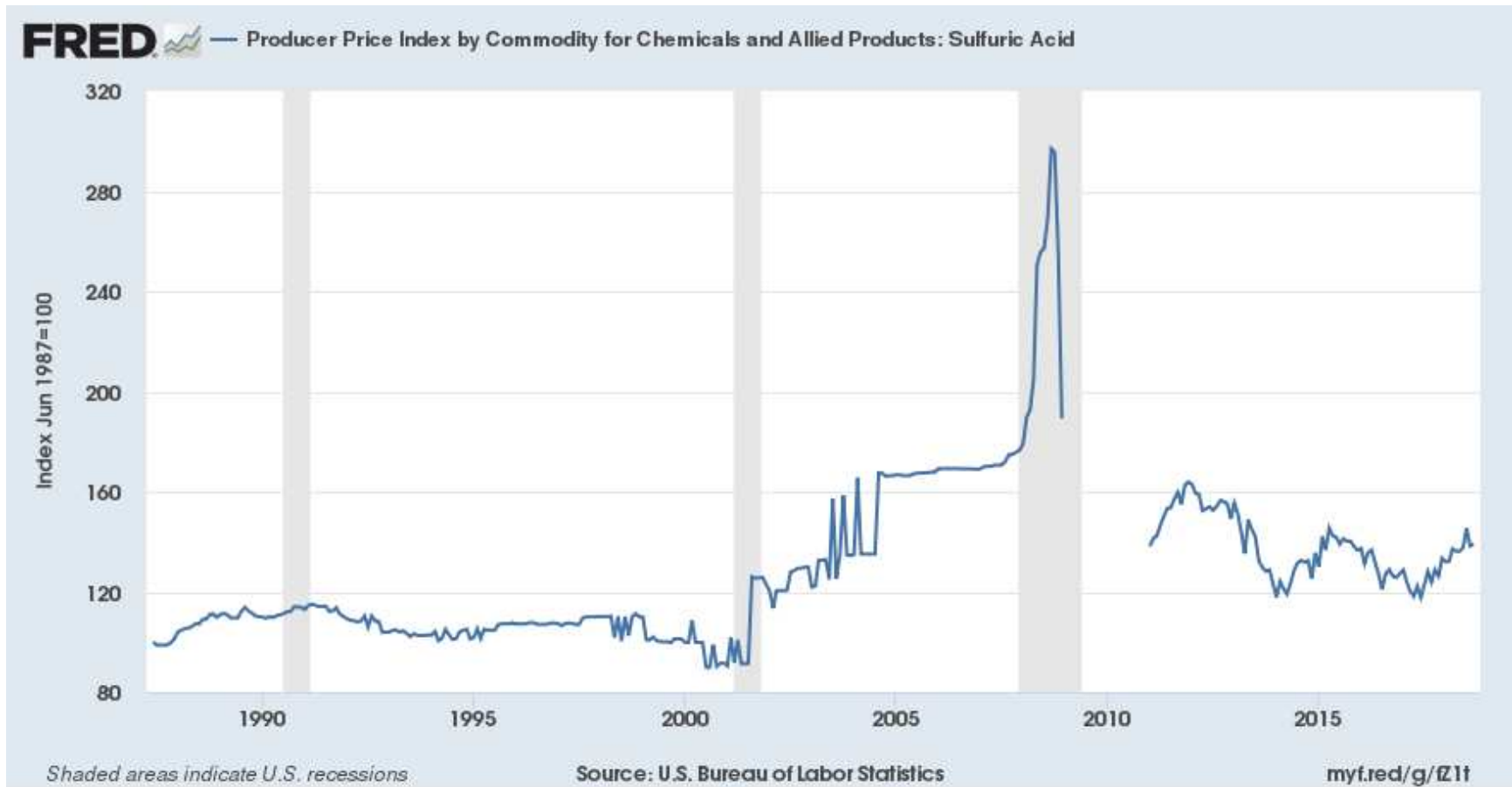


Figure 6.3: Sulfuric acid price index since the 1980s [29]

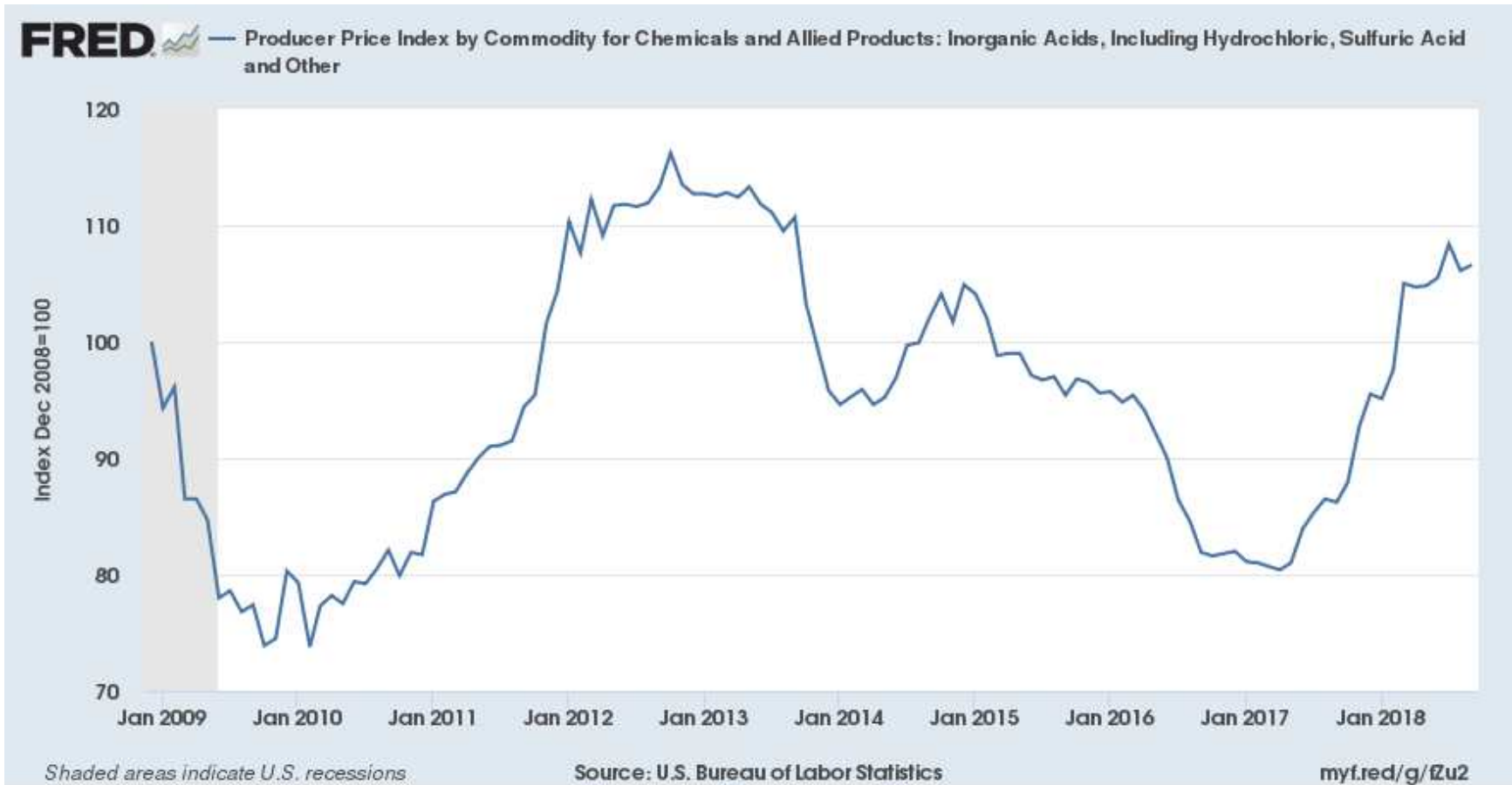


Figure 6.4: Price index for a range of inorganic acids including muriatic acid and sulfuric acid discussed in the paper [30]

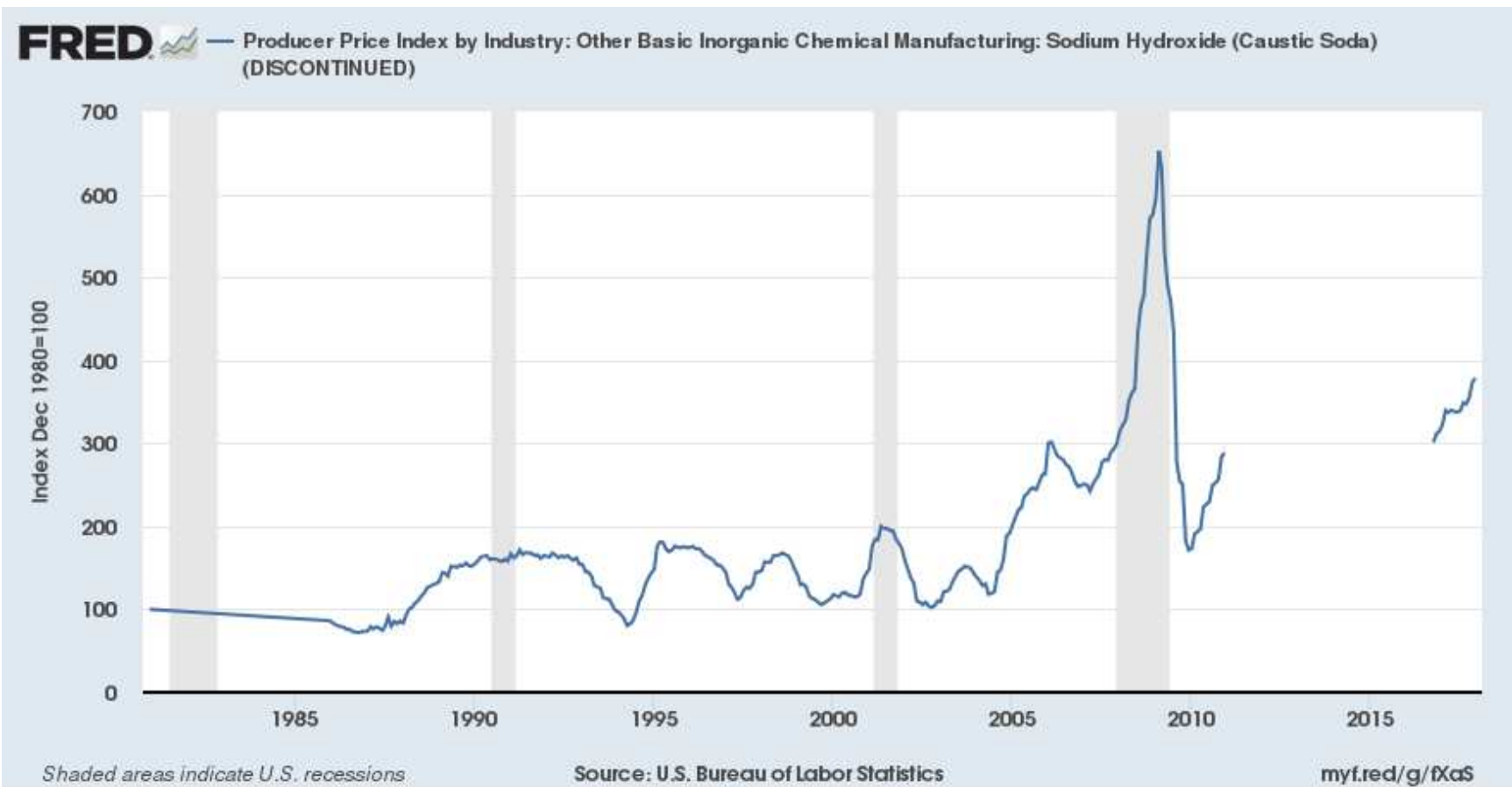


Figure 6.5: Price index for soda ash [31]

The price shocks depicted in the historic economic charts support the potential benefit of reagent regeneration. These benefits are not limited to establishing a neutral state cost recovery and immunity to price shocks. Political climate can drastically change and affect disposal costs for reagent contaminated wastes. The social license to begin mining operations can be limited by reagent consumption and wastewater contamination. Soda ash, one of the subjects of this paper is a common substitute for caustic due to its low cost, however regeneration is still of interest for maintaining profitability and desensitizing plant economics to market effects. [32]

6.6 Sulfuric acid regeneration in the petroleum industry

In general, in its common uses, sulfuric acid is diluted in the process for which it is used. The dilute sulfuric acid is either utilized for processes that require dilute sulfuric acid or re-concentrated for reuse. The method of re-concentration can be a range of vacuum distillation, thin film distillation, or submerged combustion distillation process. The petroleum industry is the second largest consumer of sulfuric acid in the United States, sulfuric acid is used as a catalyst for synthetic rubber or plastics manufacture. This consumption represents about 10% of sulfuric acid consumption. The acid is not really consumed during these uses but contamination with water, hydrocarbons, and other chemicals will reduce its effectiveness as a catalyst. It is important to note that contamination is limited by “bleeding” spent sulfuric acid from the catalyst circuit, and regenerating this acid to form a fresh 98% pure sulfuric acid for reuse. The process for regenerating the spent acid is as follows:

1. Decomposing H_2SO_4 (l) to SO_2 , O_2 , and H_2O in a furnace.
2. Cooling the furnace off gas in a heat recovery system
3. Cleaning ash and soot particles from the cooled off gas
4. Condensing H_2O from the off gas
5. Dehydrating the cleaned gas by contact with sulfuric acid
6. Oxidizing the SO_2 to SO_3
7. Making H_2SO_4 by the contact process.

This is the primary sulfur material flow, The process is illustrated in figure 6.6.

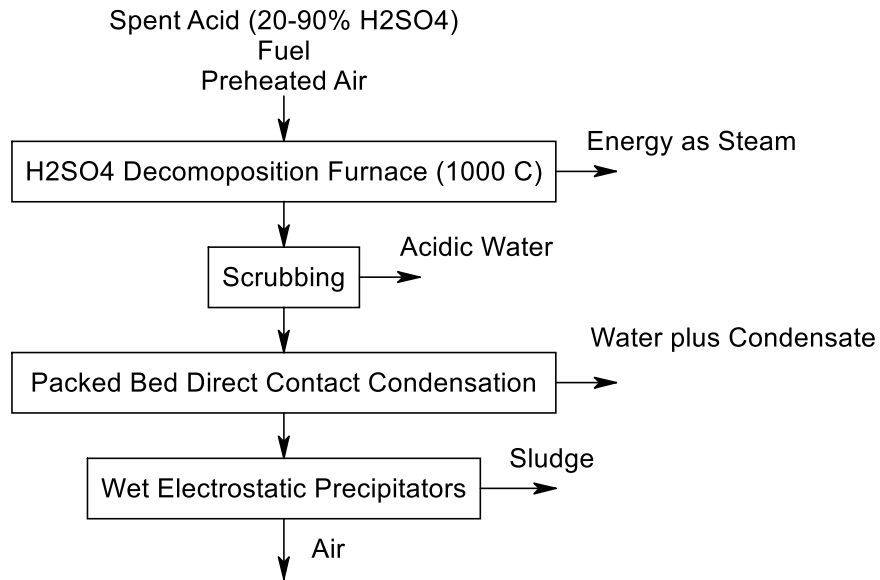


Figure 6.6: Flow diagram of the sulfuric acid regeneration process used in the petroleum industry

All of these steps can be operated continuously. The furnace from step (a) is operated at 1000 Celsius to decompose H_2SO_4 . Acids that are highly contaminated with water are generally vacuum distilled prior to feeding into the furnace to limit the amount of water that must be heated per ton of new sulfuric acid recovered, this minimizes fuel consumption and increases the sulfur dioxide concentration in the off gas. [35]

Handling of spent sulfuric acid is a major concern, stainless steel pumps, pipes, or railcars must be used to move sulfuric acid around a plant. The sulfuric acid can continue to react with hydrocarbons during transport and storage. Spent acid is decomposed in the furnace in an oxidizing atmosphere. The decomposition reaction is:

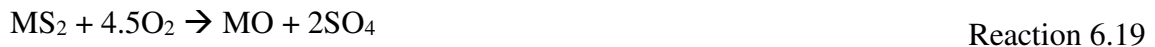


This is an endothermic reaction, heat is primarily provided by burning hydrocarbon fuels, H_2S containing waste gas, and molten sulfur. Burning of sulfur bearing wastes is generally preferred as they generate additional SO_2/SO_3 for conversion to sulfuric acid than do hydrocarbon fuels. The feed air is generally oxygen enriched to increase SO_2 concentration in the product gas, the O_2 from reaction 6.18 also contributes to the oxidizing atmosphere. The acid is generally contaminated with hydrocarbons and those contaminants are a significant contributor to the energy balance.

There are multiple patents on variations and alternatives to this process including combustion of the acid species with fuel gases and aqueous processes that utilize an electrolytic cell, precipitation, and distillation to purify the remaining acids. Unfortunately, in metallurgical leaching reactions the spent leach liquors are no longer mostly H₂SO₄ but rather contain significant amounts of metal sulfates and various salts. There are a few patents and papers on the subject of handling salts to regenerate sulfuric acid. Patent 3,549,320 on the regeneration of acid is for a process where ammonium hydrogen sulfate is decomposed to produce sulfur dioxide which can be oxidized and dissolved in water to form sulfuric acid.

6.7 Sulfur Dioxide Sequestration by the Contact Process

Sulfur dioxide is produced in a range of metallurgical operations as an off-gas. There exist restrictions on the sulfur dioxide output of metallurgical plants. Off-gas treatment by the contact process contributes positively to plant economics. For instance, in roasting operations such as for Chalcopyrite (a copper-iron sulfide ore) the following reactions and reaction products are expected.



Where M is a given metal cation in this case copper or iron. The equilibrium between sulfur dioxide and sulfur gas is governed by reaction 6.19. while further oxidation of the sulfur ion can result in sulfur trioxide formation as in reaction 6.20.

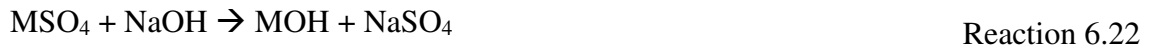


Sulfur-oxygen compounds are common for pyrometallurgical operations involving sulfide ores but are also quite common in hydrometallurgical leaching operations. In these applications, sulfur sequestration as sulfuric acid is preferable due to the potential revenue (or internal cost savings) of producing a valuable reagent. Indeed, many smelters include acid plants in their capital investment in order to capture additional value from their off gas.

Regeneration of reagents is not unique to pyrometallurgical applications for sulfuric acid, as the same can be said about hydrometallurgical processes. Hydrometallurgical leaching utilizing sulfuric acid is common. Sulfuric acid leaching of a metal cation proceeds according to the following reaction:



The separation of cations is then performed either by solvent extraction or ion-exchange dependent on factors relating to the ore and its behavior. Often metal hydroxides are precipitated at neutral or slightly basic pH upon neutralization of the hydronium ions with caustic. This is often very reagent consumptive as excess sulfuric acid is consumed in the leaching of both the desired metals as well as gangue metals as well as to adjust pH to acidic enough conditions to drive leaching. Then excess caustic or soda ash is required to neutralize that acid. The result is a sodium sulfate or bisulfate compound as well as metal hydroxide.

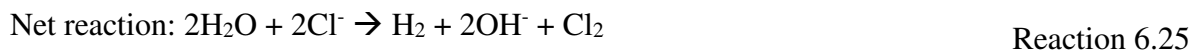
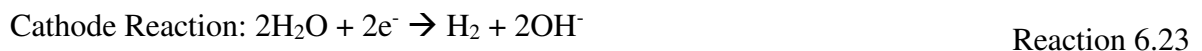


The sodium sulfate ionic compound is of interest as a potential source from which to regenerate sulfuric acid either by the contact process or by roasting to liberate the sulfate ion from the sodium. There is current investment to develop regeneration technology for sulfuric acid in hydrometallurgical leaching applications. [32]

6.8 Chlor-Alkali regeneration at Mountain Pass Operation

The Mountain Pass mine in the southern part of the Clark Mountain Range in California was once the supplier for much of the world's rare earth consumption. The mine and associated mineral processing facility have been shut down for a variety of reasons, however one successful aspect of the process was a reagent regeneration plant that allowed conservation of reagents. The reagents used at Mountain Pass included muriatic (hydrochloric) acid. This was neutralized with a caustic solution of sodium hydroxide. The neutralization was necessary to precipitate ions from the pregnant solution. The resulting solution contained sodium chloride salt and water. The chlor-alkali plant required energy input to liberate chlorine and hydrogen from the water on 2 sides of a semi-permeable membrane. The Chlorine is oxidized at the anode and nucleates diatomic chlorine gas. At the cathode hydroxide is reduced and diatomic hydrogen evolves. [31, 32]

The products of this process are hydrogen and chlorine gases that can be used to produce muriatic acid according to reaction 6.8 above. It is necessary to provide power to the cell in order to oxidize Cl^- and make the Cl_2 product.



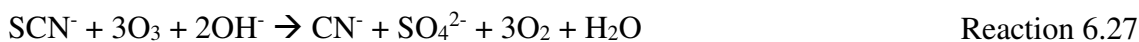
Though the liberation reaction is endothermic and requires significant energy to progress according to reaction 6.25 there is significant energy generated in the subsequent steps. These steps represent chances to recover heat energy. [35] Ultimately the mixing of the two off gases from the chlor-alkali cell Cl_2 and H_2 are reacted as follows:



6.9 Cyanide Regeneration from Thiocyanate

Cyanide consumption is often one of the main contributors to the operating cost of a cyanidation plant. Most of the cyanide consumption is actually wasted. For instance, only three to four grams of cyanide per ton of ore are actually consumed to leach the gold contained in an ore. In practice consumption ranges from 300 to 2000 grams per ton. The extra cyanide forms hydrogen cyanide, oxidizes to cyanate, or forms thiocyanate complexes with copper, iron, and zinc. It is documented in literature that thiocyanate formation can account for up to 50% of the total cyanide consumption. Thiocyanate in the process plant effluents vary depending on ore type and operational parameters, however the range is between 40mg/l and 600mg/l. Merrill-Crowe operation effluents can have thiocyanate concentrations up to 2000mg/l. Thiocyanate is considered non-toxic and is not regulated in effluents by the EPA. Exposure to UV light can cause decomposition of thiocyanate to cyanide, sunlight can produce enough cyanide to be toxic to aquatic life. Because of this there is significant social and political motivation to impose regulations on thiocyanate in mine and mill effluents.

The state of the art in the 1990s for cyanide removal from solution was the oxidation of cyanide with hydrogen peroxide or sulfur dioxide. Neither of these oxidants is strongly enough oxidizing to decompose thiocyanate. More powerful reagents such as ozone or chlorine are required. Chlorine can produce toxic gases itself and so its use is limited, ozone is widely applied in water treatment and continues to replace chlorine as a bleaching agent. The reaction of thiocyanate with ozone in basic aqueous solution is as follows:



According to these equations, regeneration of cyanide from thiocyanate would be possible if the subsequent oxidation of the cyanide could be stopped. The regeneration of cyanide would certainly be more advantageous than destruction of thiocyanate.

Soto et. al showed the range over which thiocyanate can be oxidized by ozone, to be from pH 2 to pH 12 yielding cyanide (figure 6.10). If copper concentration is lower than 10mg/l and pH is kept acidic it is expected that cyanide regeneration of up to 90% is possible. It consumes about 1 kg of ozone per kg of thiocyanate. High metals content can be reduced and precipitated with hydrogen peroxide prior to ozone oxidation of the thiocyanate solution. [36]

6.10 Carbon Sequestration by the Solvay Process

Carbon dioxide emissions are a concern for societal and political stakeholders of mining impacts. Suggested carbon taxes or emission standards are extremely restrictive to potential future mining operations. It is suggested that the Solvay process could take advantage of carbon dioxide off gas as a precursor to soda ash. Soda ash is co-produced with calcium chloride in the Solvay process traditionally sodium chloride (brine) and calcium carbonate (lime). The suggestion to replace lime with carbon dioxide would remove the lime kiln from the process. Brine would still be necessary to produce soda ash to contribute the sodium constituent.

The chief incentive to adopt this sort of process would be regulation to severely limit the carbon dioxide output of a process facility. However, the advantage of generating a valuable product from the otherwise costly treatment process would soften the blow of such regulation. [27]

6.11 Limitations of Reagent Regeneration

It should be mentioned that reagent regeneration always has losses and no conversion process is one hundred percent efficient. However, these reagent processing unit operations generally have better mass accountability than metallurgical operations. There is usually still a requirement for some virgin reagent even in plants with robust reagent regeneration systems.

Reagent costs are a primary driver of hydrometallurgical plant economics and success. The implementation of reagent regeneration technologies benefits these plants by allowing reduced reagent consumption and price stability of reagents consumed. There are also real and perceived environmental benefits that can greatly contribute to the social license required to open and operate a plant in local communities. These environmental benefits take 2 main forms. Waste disposal often requires significant processing beyond that which is necessary to recover value from the metallurgical plant. Regeneration of reagents allows some cost minimization if treatment is required by legislation. It is expected that reagent regeneration will become more

common in metallurgical plant design and operation in the future as communities become more concerned about the environmental impact of mining and metallurgical operations.

Reagent regeneration is not limited to treating aqueous phase effluents, the current developments of techniques for sequestration of gaseous waste products as useable reagents can also minimize environmental impact and improve economic outlook.

It is expected that the current trajectory of mining will lead to processing lower grade ores and more complex ores. Lower ore grades particularly can increase reagent consumption for production. Lixiviant regeneration will therefore become more important to minimize additional costs.

6.12 Reduction of sodium sulfate to sodium sulfide

The thermodynamics and energetics of the reduction process to manufacture sodium sulfide from sodium sulfate is discussed in the thermodynamics section, Chapter 7. The interest in this presently widely used industrial process is as a possible process route to recover the sulfur from the leach process in a form that can be readily oxidized to produce sulfur dioxide and then sulfuric acid. The most common reaction for this process is shown as reaction 6.30.



This reaction is generally accomplished at high temperatures above about 884°C using carbonaceous materials. The temperature is such that sodium sulfate is in the liquid phase which lends itself to favorable kinetics over a solid-gas reaction. Commercial operations generally operate between 900°C and 1000°C. The challenges to this process are rapid furnace lining degradation, “objectionable odors” and energy consumption due to the high temperature. Academic work has studied reduction to sodium sulfide at lower temperatures using various charcoals, hydrogen, and carbon monoxide as reducing agents. One example is the work by John and Alfred White. [35] They studied various other reductants to determine conditions under which sodium sulfide reduction could be accomplished at lower temperatures. They identify low melting point mixtures of sodium sulfate and sodium sulfide. Their work showed that hydrogen reduction is rapid in the solid-gas state but slows for conditions under which the salt is liquid. Carbon monoxide was not as favorable kinetically as hydrogen, and solid carbon bearing materials were slow until the salt became liquid. Several different solid carbonaceous materials were studied in this work with a range of kinetics probably related to activity, surface condition, or the mixture of the liquid salt and reducing material. [36]

Cameron et al [39] studied the kinetics of the sulfate reduction with carbon. They modeled the kinetics for sulfate reduction with graphite and sodium sulfide oxidation.

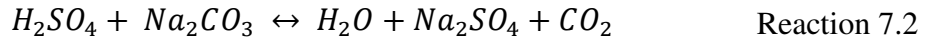
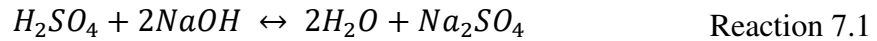
6.13 Summary of literature review

Due to the modern concern over the potential environmental impact of mining and its effluents, recent research has intended to develop technologies to address the concerns of the sustainable development movement. One example of this is the development of technologies for the recycling of reagents used in common metallurgical operations. This paper overviewed the recycling of various reagents in mining and other industries as a demonstration of those reagents that can be recycled and reused. The recycling of sulfuric acid, muriatic acid, and cyanide is discussed. The paper also discussed the sequestration of gaseous metallurgical by-products of sodium dioxide and carbon dioxide. Technologies such as these can contribute positively to plant economics particularly in a sustainable development driven world.

CHAPTER 7 THERMODYNAMIC CONSIDERATIONS FOR LIXIVIANT
REGENERATION

7.1 Sodium sulfate formation in the separations process

The species expected upon neutralization of sulfuric acid for separation by either solvent extraction or by the sequential precipitation process are sodium sulfate when the sulfuric has been neutralized with either caustic or more commonly soda ash. The chemical reactions for these reactions are as follows:



The leach liquor after whole or partial neutralization contains some number of remaining metals, sodium sulfate. Evaporation of the process water yields solid sodium sulfate salt along with some metal sulfates (mostly zinc). It is possible that the neutralization reaction is incomplete and would contain some amount of sodium bisulfate. These sulfur containing compounds are of interest to be processed such as to make reagents consumed previously in the separations process in order to reduce reagent consumption and the associated costs of reagent consumption.

7.2 Sodium sulfate reduction to sodium sulfide

The process must be considered in light of the processes used in industry to produce sulfuric acid from sodium sulfate via sodium sulfide. Comparison of these process economics and energy balance will be discussed more thoroughly in Chapter 8, together with the economics of this process. This chapter will focus on the driving force for these reactions at various conditions. The sodium sulfate to sulfur dioxide process used in the chemical industry is a two-step process, the first step is carbothermic reduction shown in reaction 7.3.



This reaction is generally accomplished at high temperatures above 884°C using carbonaceous materials. The temperature is such that sodium sulfate is in the liquid phase which lends itself to favorable kinetics over a solid-gas reaction. Commercial operations generally operate between 900°C and 1000°C. The challenges to this process are rapid furnace lining degradation, “objectionable odors” and energy consumption due to the high temperature. Academic work has studied reduction to sodium sulfide at lower temperatures using various

charcoals, hydrogen, and carbon monoxide as reducing agents. The process is endothermic as shown in figure 7.1.

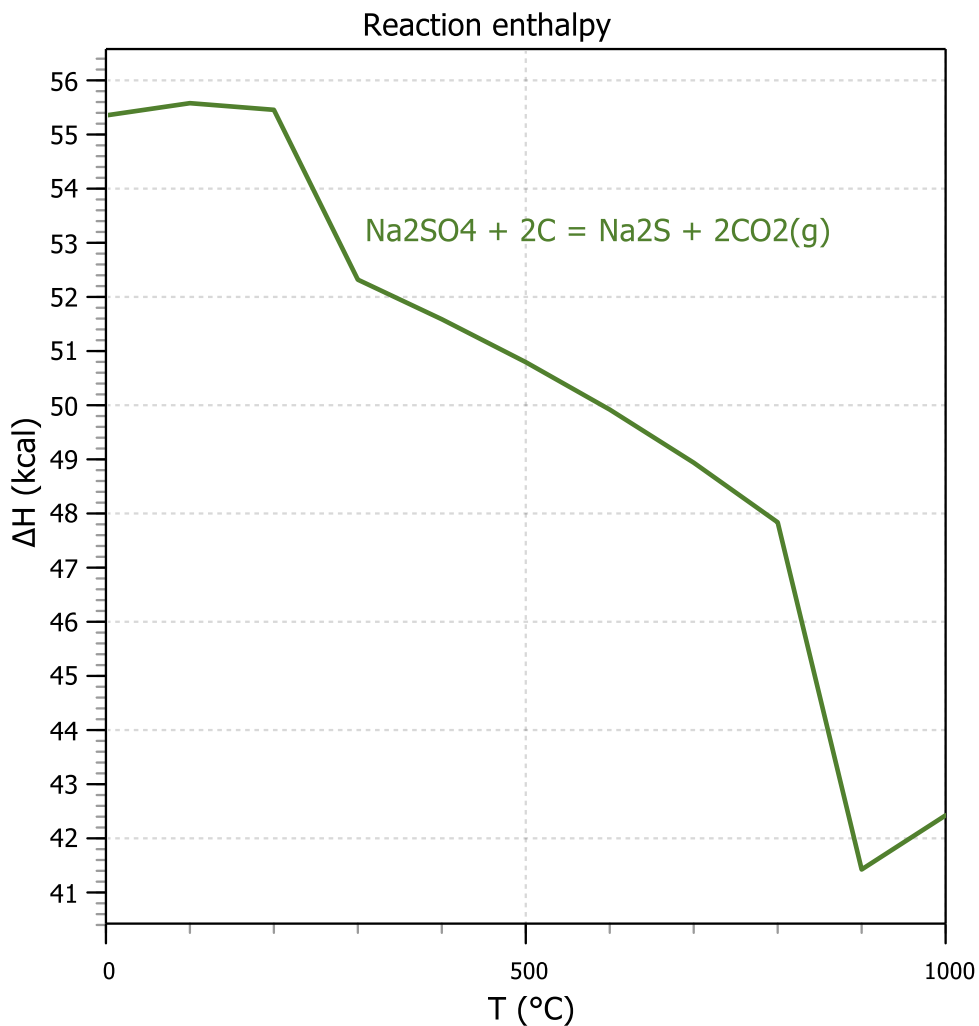
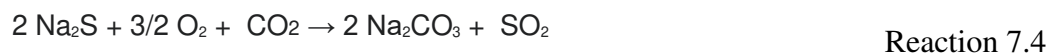


Figure 7.1: Enthalpy for sodium sulfide intermediary process

The second operation is to burn the sodium sulfide in the presence of carbon dioxide and oxygen to form soda ash and sulfur dioxide as shown in reaction 7.4.



The sulfur dioxide from this process can be oxidized to sulfur trioxide and reacted with water as per the contact process to produce sulfuric acid. These reactions are discussed in detail in section 6.1 on the contact process for manufacture of weak sulfuric acid. Generally speaking, SO₂ can be oxidized in an exothermic process to form SO₃ which is then dissolved in water to form H₂SO₄ (also exothermic).

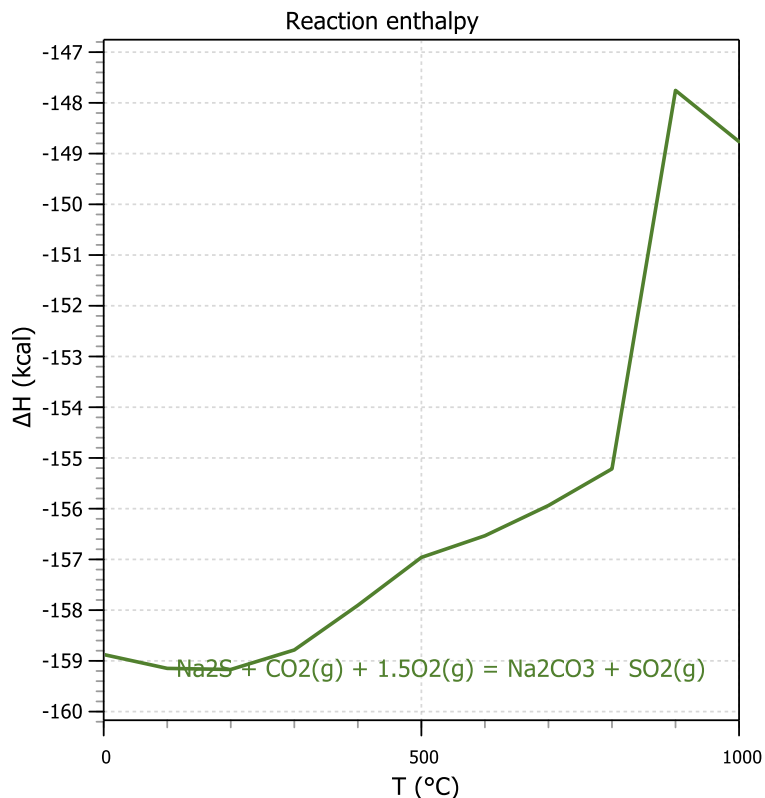
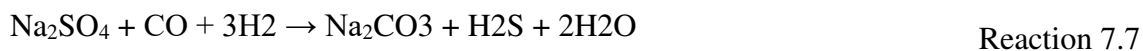
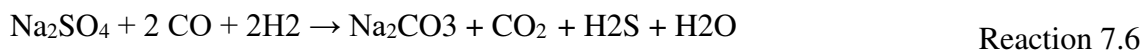
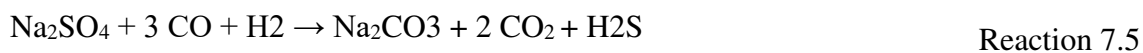


Figure 7.2: Enthalpy for sodium sulfide oxidation

7.3 Proposed alternative reaction Na₂SO₄ to Na₂CO₃

The proposed reaction studied in this work is an alternative to this process to accomplish this conversion at lower temperature with more favorable energetics, and a single step process. There are a variety of stoichiometries that are possible and are explored in this work. Those are shown in reactions 7.5 through 7.7



The free energy for these reactions is shown in figure 7.3. It can be observed that reaction 7.5 has the most driving force.

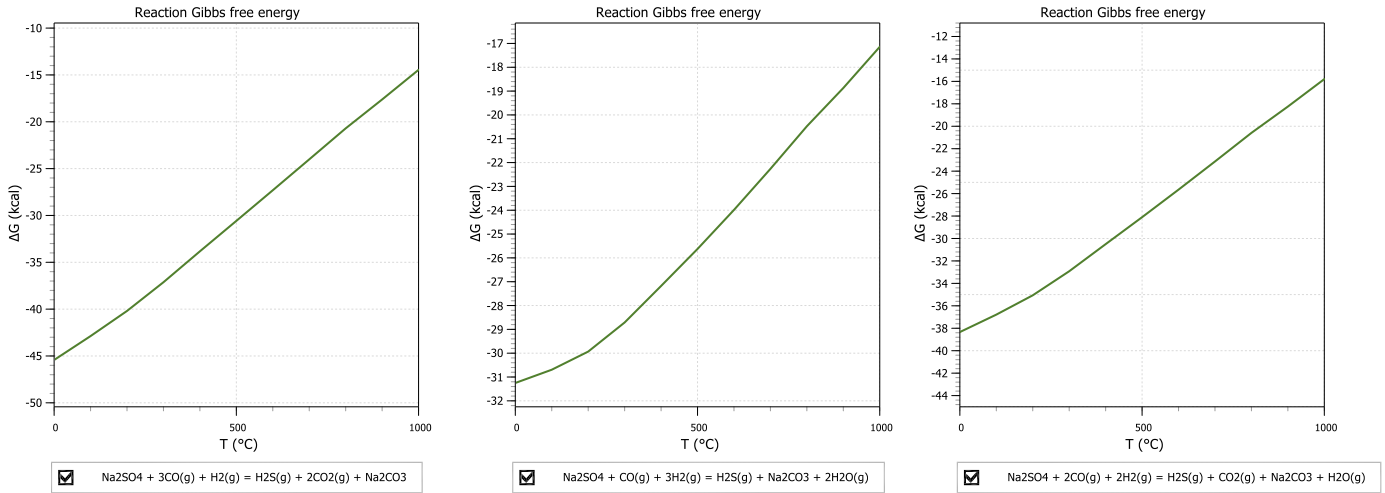
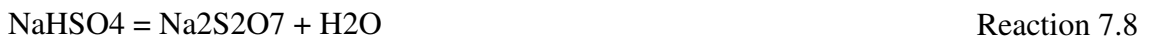


Figure 7.3: Free energy for several reactions for the conversion of sodium sulfate directly to carbonate.

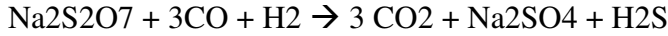
It is desirable to perform the reaction at the highest possible temperature particularly if the desirable equilibrium can be achieved at a temperature where the salt is liquid. Higher energy conditions will improve reaction kinetics. The liquid phase for pure sodium sulfate starts at 884C. the liquidus is depressed with the addition of sodium carbonate. A phase diagram for this system is developed in the work of Khlapova and Kovaleva [40]. Mixtures of sodium sulfate and sodium carbonate have lower melting points than the pure salts, the solution of sodium carbonate and sodium sulfate will be liquid down to just over 800°C.

The equilibrium is shifted significantly toward sodium sulfide evolution at and above this liquidus temperature. The addition of oxygen to the furnace atmosphere will raise the temperature at which sodium sulfide becomes favorable over sodium carbonate. It is also possible that sodium bisulfate is present in the neutralization product. If bisulfate is present in the furnace feed it would decompose according to reaction 7.8 at approximately 250°C.

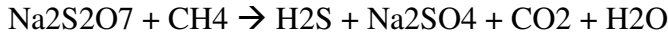


At higher temperatures then, there may be Na₂S₂O₇ in the process feed, if this is the case the sulfur can be reduced in order to form sodium sulfate with the evolution of H₂S and either carbon dioxide or water. Three stoichiometries for this reaction are shown in reaction 7.9 through 7.11 with the energetics for these reactions shown in figure 7.4.





Reaction 7.10



Reaction 7.11

Sodium pyrosulfate may also contribute to melting point depression

of the sodium sulfate-sodium carbonate solution significantly allowing better kinetics at lower temperatures. The melting point of sodium pyrosulfate is 400°C.

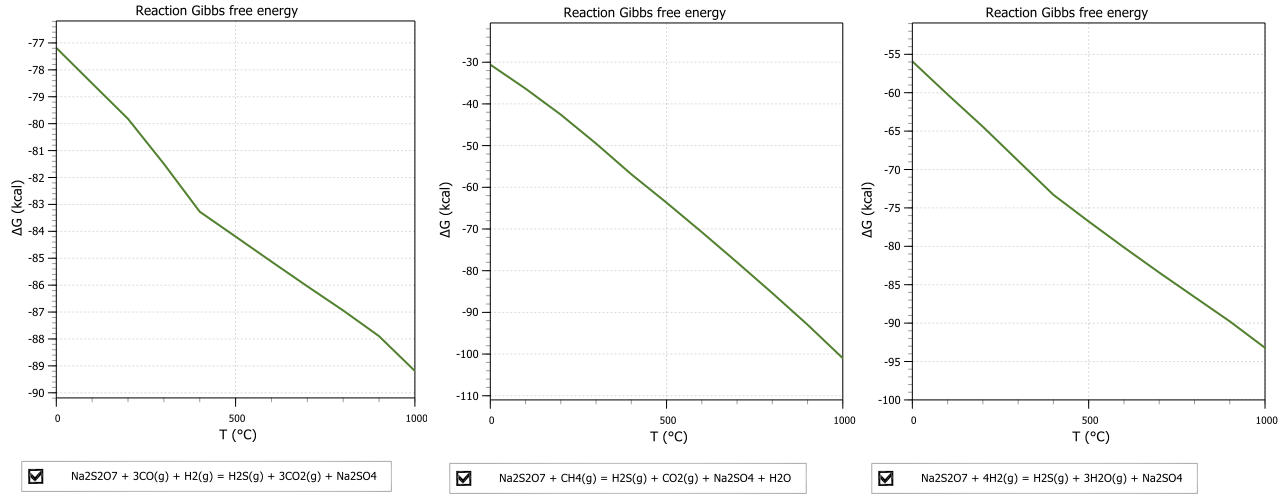


Figure 7.4: Free energy for several reactions for reduction of sodium pyrosulfate to sodium sulfate

The reaction is exothermic except at very high temperatures with methane as a reductant.

The free energies for these reactions are shown in figure 7.5.

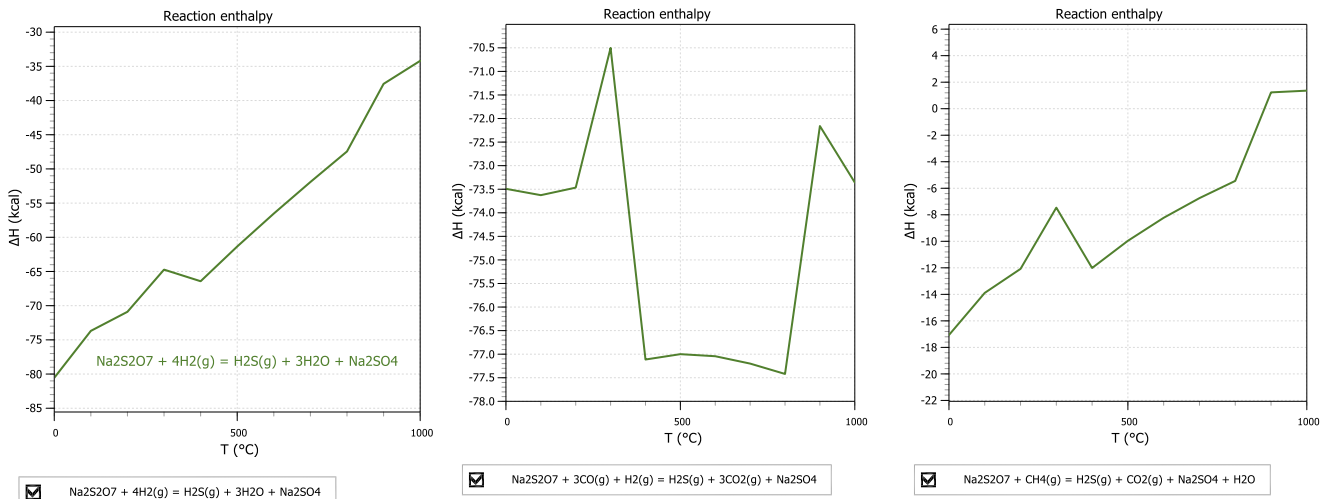


Figure 7.4: Enthalpy for several reactions for reduction of sodium pyrosulfate to sodium sulfate

Sodium pyrosulfate is not a stable phase under the furnace conditions with a reducing atmosphere and high temperatures, the sodium pyrosulfate is favorable to be converted to sodium sulfate.

The direct reduction to sodium carbonate is more favorable at lower temperatures and sodium sulfide is more favorable at higher temperatures. This can be seen in the equilibrium composition charts. Based on these HSC models it is observed that the sodium carbonate phase is stabilized at higher temperatures by changing the atmosphere to be less strongly reducing via starving the reaction of reducing gases to some degree. This is done experimentally via adding air rather than nitrogen and so the equilibriums are presented with some amount of oxygen in addition to the reducing gas. The temperatures for various interesting points of the equilibrium are shown in table 7.1 for several gas mixtures. The goal of the process is to avoid the formation of Na₂S so the temperature at which sulfide begins to form (and the equilibrium yield is less than 100% Na₂CO₃) is an interesting consideration for the design of this system. It is hoped that sufficiently fast kinetics may be achieved at a temperature below which sodium sulfide is the majority phase.

Table 7.1: Temperature for sulfide evolution, and sodium carbonate equilibrium amount for various furnace atmospheres

Feed Gas Ratio			Temperature for Na ₂ S evolution	Temperature for Na ₂ S>Na ₂ CO ₃ @ Equilibrium	Temperature for Na ₂ CO ₃ <0.5 at Equilibrium
Parts CO	Parts H ₂	Parts O ₂			
3	1	0	325	650	650
2	2	0	425	675	675
2	2	0.25	425	685	650
2	2	0.5	475	700	625
2	2	1	525	725	425

These temperatures understood in combination with the liquidus of the sodium sulfate, sodium carbonate, sodium pyrosulfate mixed salt may indicate temperatures at which the reaction kinetics may be improved. Full size copies of the various equilibrium diagrams produced by HSC that are used to construct this table are provided in Appendix II.

7.4 Reaction Energetics

The enthalpy for these reactions is important for the energy balance the direct reduction to sodium carbonate reaction is exothermic at lower temperatures, below 600°C, at temperatures above 600°C the reaction becomes endothermic. The energy balance considers this reaction enthalpy as well as the enthalpy intervals for the materials involved in the reaction. The enthalpy for the reaction is shown in table 7.2 as part of the energy balance for the reaction system.

The second step of oxidizing the remaining reactant gases and dihydrogen sulfide to form sulfur dioxide and then sulfur trioxide. This step also includes the oxidation of remaining reactant gases carbon monoxide or hydrogen. All three of these reactions are exothermic. The enthalpy for the H₂S combustion to SO₃ is shown in table 7.3 as part of the energy balance. The recovery energy from the oxidation reactions may provide the energy for the primary reaction or to preheat feed materials.

Table 7.2: Energy balance for sodium sulfate to sodium carbonate conversion reaction

INPUT SPECIES (2) Formula	Temper. K	Pressure bar	Amount kmol	Amount kg	Amount Nm ³	Heat Content kWh	Total H kWh
CO(g)	298.150		737.837	20666.888	16537.583	0.00	-22655.96
H ₂ (g)	298.150		245.070	494.032	5492.901	0.00	0.00
Na ₂ SO ₄	298.150		204.165	29000.000	10.821	0.00	-78711.19
OUTPUT SPECIES (2) Formula	Temper. K	Pressure bar	Amount kmol	Amount kg	Amount Nm ³	Heat Content kWh	Total H kWh
CO(g)	1223.000		123.000	3445.242	2756.873	997.97	-2778.86
H ₂ (g)	1223.000		40.500	81.643	907.751	309.29	309.29
CO ₂ (g)	1223.000		408.000	17955.876	9144.749	5190.44	-39406.81
H ₂ S(g)	1223.000		204.165	6958.123	4576.073	2193.51	1030.81
Na ₂ CO ₃	1223.000		204.165	21639.130	8.546	10178.68	-53950.00
BALANCE:			kmol	kg	Nm ³	kWh	kWh
			-207.242	-80.906	-4647.314	18869.895	6571.593
MATERIAL BALANCE							
ELEMENT	Input	Output	Balance	Input	Output	Balance	
	kmol	kmol	kmol	kg	kg	kg	
C	737.837	735.165	-2.672	8861.939	8829.846	-32.093	
H	490.140	489.330	-0.810	494.032	493.215	-0.816	
Na	408.330	408.330	0.000	9387.402	9387.412	0.011	
O	1554.496	1551.495	-3.001	24871.004	24822.989	-48.015	
S	204.165	204.165	0.000	6546.543	6546.551	0.007	
Temperature of products = 991.7 K (when Heat Balance = 0)							

Table 7.3: Energy balance for oxidation of off gases

INPUT SPECIES (1) Formula	Temper. K	Pressure bar	Amount kmol	Amount kg	Amount Nm ³	Heat Content kWh	Total H kWh
CO(g)	1223.000		123.000	3445.242	2756.873	997.97	-2778.86
H2(g)	1223.000		40.500	81.643	907.751	309.29	309.29
CO2(g)	1223.000		408.000	17955.876	9144.749	5190.44	-39406.81
H2S(g)	1223.000		204.000	6952.500	4572.374	2191.74	1029.98
O2(g)	298.000		601.000	19231.279	13470.574	-0.73	-0.73
N2(g)	298.000		2003.000	56110.840	44894.441	-2.43	-2.43
OUTPUT SPECIES (1) Formula	Temper. K	Pressure bar	Amount kmol	Amount kg	Amount Nm ³	Heat Content kWh	Total H kWh
CO2(g)	1900.000		531.426	23387.793	11911.170	12612.31	-45476.26
O2(g)	1900.000		110.795	3545.307	2483.315	1706.15	1706.15
N2(g)	1900.000		2003.000	56110.840	44894.441	29237.52	29237.52
H2O(g)	1900.000		244.700	4408.339	5484.608	4621.34	-11816.11
SO3(g)	1900.000		204.000	16332.893	4572.374	6704.73	-15721.93
BALANCE:			kmol	kg	Nm ³	kWh	kWh
			-285.579	7.792	-6400.853	46195.772	-1221.079
MATERIAL BALANCE							
ELEMENT	Input	Output	Balance	Input	Output	Balance	
	kmol	kmol	kmol	kg	kg	kg	
C	531.000	531.426	0.426	6377.682	6382.798	5.117	
H	489.000	489.400	0.400	492.883	493.286	0.403	
N	4006.000	4006.000	0.000	56110.840	56110.840	0.000	
O	2141.000	2141.142	0.142	34254.715	34256.987	2.272	
S	204.000	204.000	0.000	6541.260	6541.260	0.000	
Temperature of products = 1932.0 K (when Heat Balance = 0)							

7.5 Process Alternatives

7.5.1 Aqueous Reduction of Sodium Sulfate

It was suggested that the reaction would be more useful if it were possible to accomplish the conversion in aqueous solution such that the salt did not have to be precipitated and water could be recovered to the flowsheet more easily. The Reaction with carbon monoxide and hydrogen is shown to be favorable over a useful temperature range in Figure 7.7. There are several stoichiometries by which this reaction may occur according to reactions 7.5, 7.6, and 7.7 above the equilibrium compositions for the aqueous version of these reactions, shown in Figure 7.8, suggest that either reaction may occur at a useful temperature range.

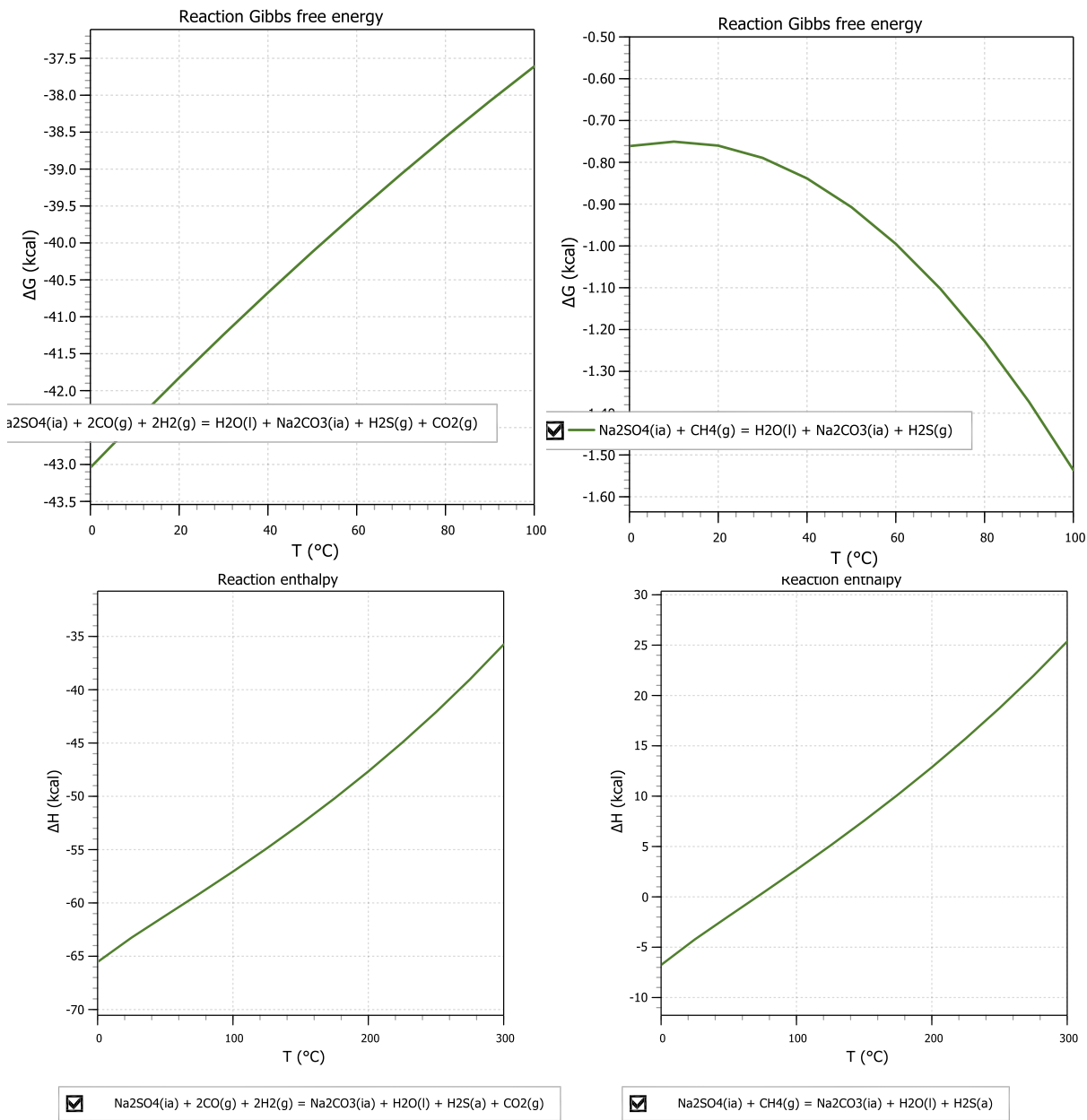


Figure 7.5: Entropy and Enthalpy for aqueous reaction with carbon monoxide/hydrogen and methane

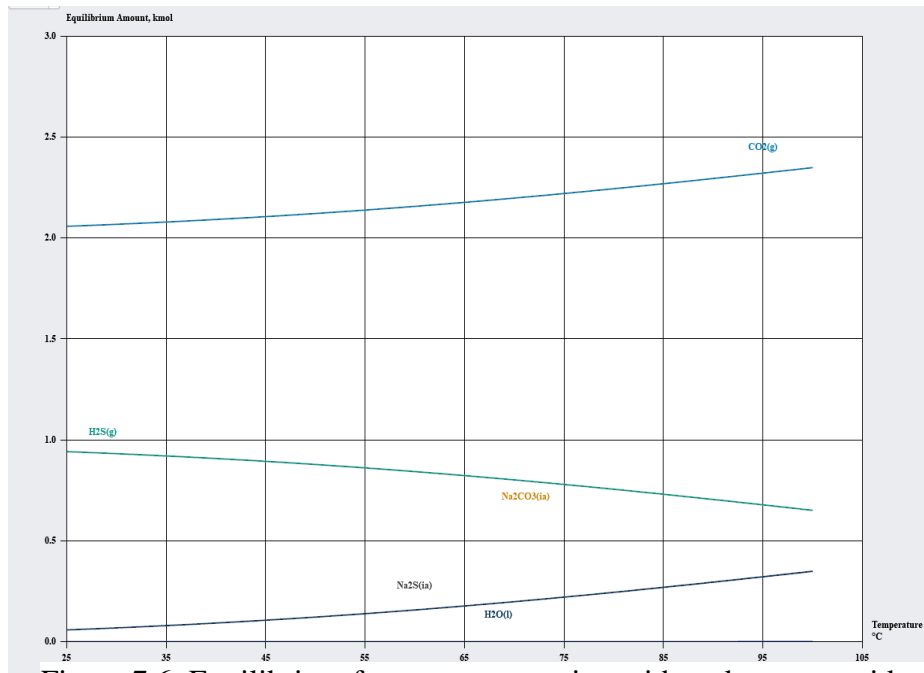


Figure 7.6: Equilibrium for aqueous reaction with carbon monoxide and hydrogen.

7.5.2 Methane Reduction

Methane was considered as a potential reducing gas in place of CO and H₂. This was explored as methane (as natural gas) is a relatively cheap reactant (relative to CO and H₂) that requires low energy investment (again relative to CO and H₂). The methane reaction is shown in reaction 7.12.

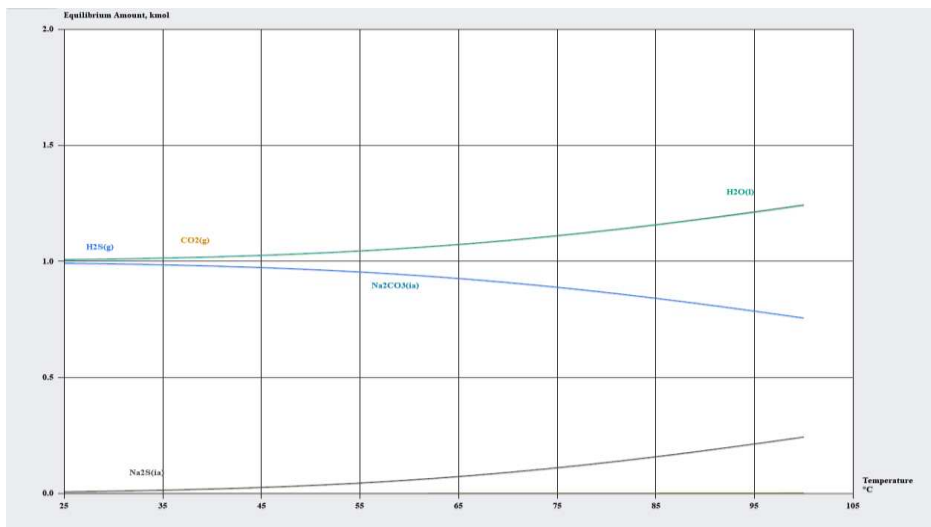


Figure 7.7: Equilibrium for aqueous reaction with methane



Reaction 7.12

The thermodynamics for this reaction from HSC show that it is not favorable in the aqueous case discussed above (figure 7.9). It is favorable for the solid furnace reaction that is the primary avenue of research. The free energy for this reaction is shown in Table 7.4 as a function of temperature. It is not favorable at room temperature but at high temperature there is a driving force for this reaction to progress.

The relative equilibrium amount of various phases is interesting as at high temperatures sodium sulfide becomes the stable phase as in the carbon monoxide and hydrogen reaction. The

Table 7.4: Thermodynamics for conversion directly to sodium carbonate with methane.

Na₂SO₄ + CH₄(g) = H₂S(g) + H₂O(g) + Na₂CO₃					
T	deltaH	deltaS	deltaG	K	Log(K)
C	kcal	cal/K	kcal		
0	16.501	46.881	3.696	1.10E-03	-2.957
100	16.82	47.882	-1.047	4.11E+00	0.613
200	16.971	48.258	-5.862	5.10E+02	2.708
300	14.452	43.361	-10.401	9.25E+03	3.966
400	14.764	43.855	-14.757	6.19E+04	4.791
500	15.023	44.237	-19.179	2.64E+05	5.422
600	14.629	43.758	-23.578	7.98E+05	5.902
700	14.259	43.357	-27.933	1.88E+06	6.274
800	13.857	42.964	-32.25	3.70E+06	6.568
900	14.852	43.996	-36.762	7.07E+06	6.849
1000	14.763	43.924	-41.159	1.16E+07	7.066

sulfide phase starts at temperatures above 325C and the equilibrium amount crosses over the sodium carbonate amount at 625C. Above this temperature the equilibrium conditions would have a higher sodium sulfide composition than sodium carbonate. This is shown in figure 7.10.

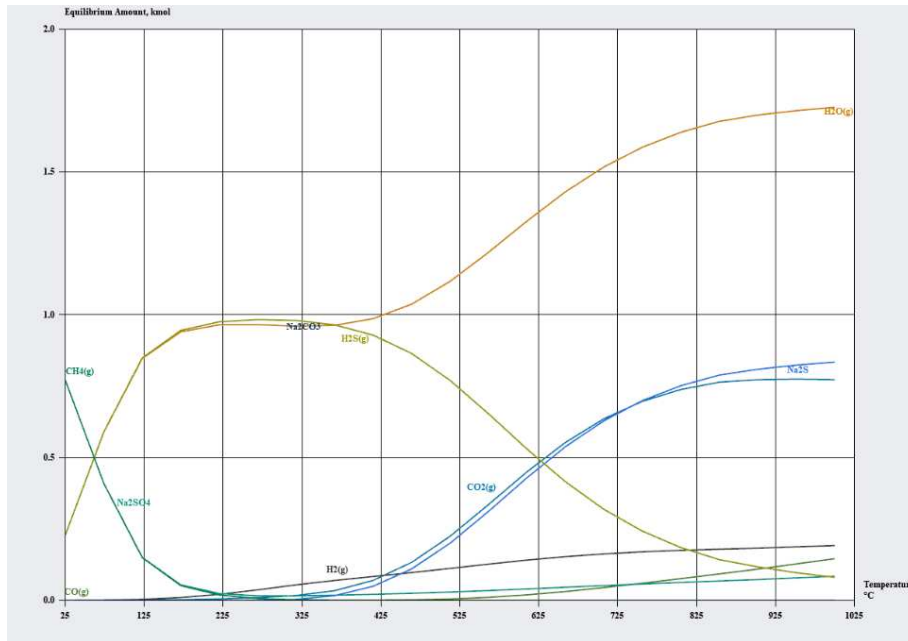


Figure 7.8: Equilibrium for the methane reaction

7.6 Summary of Thermodynamics

The thermodynamics shows favorability over a range of temperatures, Initial test work of the furnace type reaction tried to accomplish this reaction at a low temperature range. The furnace was designed to accommodate tests up to 350°C. Initial results showed very low conversion rates. It was expected that the reaction was limited by kinetic factors and that higher energies would enable faster reaction rates. For this reason, the test apparatus was redesigned to enable tests at up to 1000°C. The evaluation of the thermodynamic data shows a driving force that is limited by solid-gas kinetics over a broad range of conditions. It is hoped that kinetics may be improved by performing the reduction under conditions where the salt would be in the liquid phase rather than the solid phase.

CHAPTER 8 ACID REGENERATION RESULTS AND DISCUSSION

8.1 Initial Test work

The first test was designed using a live pH measurement of a caustic scrubber to determine reaction progress. No change from sodium sulfate to sodium carbonate was observed during this test and so the results are omitted. This test was a total of 10 minutes at a reaction temperature of 350°C. As no reaction was observed additional tests were designed with the goal of proving the feasibility of the reaction after which kinetics could be considered. These tests are summarized by Table 8.1.

Table 8.1: Results of initial furnace tests

Test	Temperature	Time at Temperature (min)	Feed Gases	Conversion (%)
17-A	300	10	CH ₄	0
17-B	300	30	CH ₄	0
17-C	250	30	CH ₄	0
17-D	450	600	CH ₄	3.5
23-A	450	480	CO + H ₂	5.3
23-B	450	480	CO + H ₂	3.7
29-A	450	720	CO + H ₂	11.6

The initial results show several tests with no conversion observed, these represent the shortest tests in this research effort, subsequent tests were over several hours. the test titled 17-E showed a lower conversion mathematically than 17-D, a shorter test, this is probably due to loss of material (mostly due to the CH₄ feed stream) over the period of

8.2 Aqueous Reaction Alternative

These initial tests showed the possibility of conversion but forced a redesign of the furnace to try higher temperatures where kinetics would be more favorable. The system was also designed to allow aqueous tests as seen in figure 8.1.

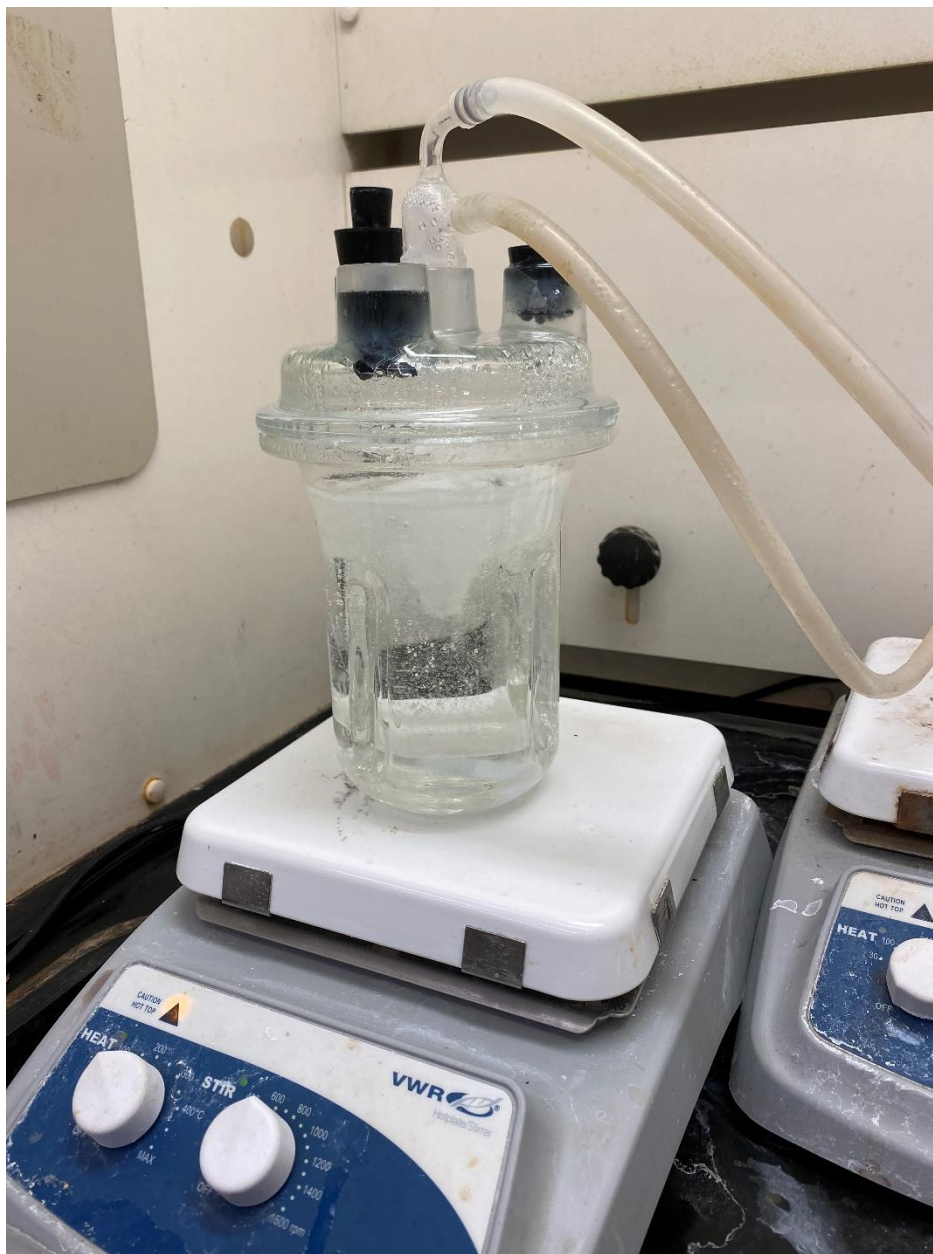


Figure 8.1: Reactor for aqueous lixiviant regeneration test work

The results of the aqueous tests were disappointing with only one test showing any conversion (1.4%) at a temperature of 100°C for 8 hours with carbon monoxide and hydrogen as feed gases. This is considered outside of the realm of practicality as A) maintaining the solution

above the boiling temperature for this time is costly in terms of energy and money, and B) the conversion was still very low. Additional tests via an autoclave may be interesting however they are difficult to design as most autoclaves are not made to handle such reducing environments. Titanium is very strong and corrosion resistant under oxidizing conditions even at high temperatures and pressures, but breaks down quickly when the atmosphere becomes too reducing. The project budget would not support an autoclave designed for this work and so the idea is not explored.

8.3 Higher temperature test work

The tube furnace was redesigned including a new furnace, new ceramic tube, and new plumbing for reactant gases. The first tests with this furnace were conducted at temperatures around 800°C. Ash was observed on the products of these tests and so an additional filtering step was added to the analytical technique. This is discussed in detail in section 3.9.

8.3.1 Ashing and the boudouard reaction

The Boudouard reaction named for Octave Leopold Boudouard is the reduction-oxidation reaction representing the equilibrium between carbon monoxide and carbon dioxide as shown in Reaction 8.1.



Ash was observed on several higher temperature samples particularly near the temperature for this reaction to progress to the right. CO₂ is the stable phase at lower temperatures, at sufficiently high temperatures CO₂ breaks down to CO. At the furnace temperature of 800°C the reaction is shifted strongly toward the evolution of CO but the reaction may reverse rapidly at temperatures just below this. If the furnace has certain colder spots (does not reach equilibrium on heating, or the thermocouple is biased) it is possible that CO could break down to CO₂ and carbon soot, this soot interferes with the copper chloride wet chemical

analysis but is correctable in most cases via water leaching the salt and filtering the soot. It is expected that this would interfere with the reaction as the additional solid layer decreases solid-gas contact and solid-solid kinetics are slow.

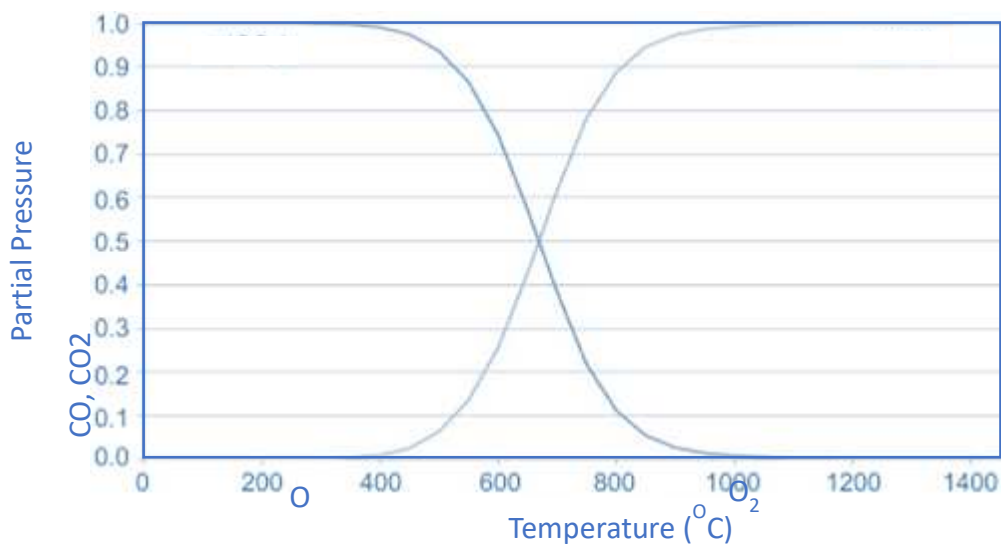


Figure 8.2: Graph of the equilibrium condition of the boudouard reaction from 0 to 1600°C

Higher temperature tests also observed the evolution of sodium sulfide in certain amounts. The color of the precipitate was readily observable and so some of the samples were analyzed further by XRD to determine the phases present in the salt. Several tests were conducted that showed little or no sodium carbonate direct conversion and instead showed reduction to sodium sulfide. These test results were compared with the thermodynamic models to develop conditions under which direct conversion could take place.

Three tests were selected for XRD based on observations of the samples and copper chloride precipitation behavior. These tests were designed such that two parallel samples were available; one that could be used for precipitation, and another that may be used for XRD analysis. The XRD analysis presents quantified phases but should be understood in terms of its inaccuracies.

Identification of phases was completed via XRD to complement wet chemical analysis with copper chloride. It should be noted that the phase quantification at this level is not accurate and should be considered only as an aide in indicating the major phases. Trusting the identification of any minor phases (typically less than 10 or 15%) is not supported by the

analytical technique. Additionally, using the phase quantification for calculations of conversion percent would be inherently inaccurate. The spectra and their phases as well as estimated phase compositions are included as it may help identify major phases. (greater than 35%).

8.3.2 87-1

The sample labeled 87-1 appeared as a mixture of black and yellow solids. The conditions for this test were 72 hours at 800°C with a gaseous feed of carbon monoxide, hydrogen, and nitrogen. Carbon monoxide and hydrogen are fed in a 3 to 1 ratio according to one of the stoichiometries discussed in the thermodynamic section. This sample was expected to yield sodium sulfide but the black phase was somewhat unexpected. Via XRD the major phases were identified as sodium sulfate, and burkeite with the possibility of sodium sulfide and/or nitrate as minor phases. The major phases represent a partial conversion has occurred at these conditions. This is in the solid state for the entirety of the reaction, a discussion that will be relevant below.

8.3.3 87-2

This sample was tested with a mixture of hydrogen and carbon monoxide as feed gases (again a 1 to 3 ratio) and analyzed via XRD. This sample was reacted at 800°C for 8 hours. The XRD indicated that sodium sulfide was the major phase constituting about half of the product sample. Sodium carbonate made up a minority of the product on the order of 40% according to the qualitative XRD results. This result can be understood in the context of the 115-test series discussed below. This test shows that above the liquidus for sodium sulfate the products are as expected by the thermodynamics and the kinetics for breakdown of sodium sulfate are somewhat rapid compared to the solid-state tests discussed above.

8.3.4 87-3

This sample was tested at a higher temperature at 950°C with the hydrogen, carbon monoxide, nitrogen feed similar to 87-1. This sample as expected showed the evolution of sodium sulfide as a major phase. Some natrite/sodium carbonate were indicated by the XRD. Sodium thiosulfate remained representing a partial conversion to either sodium carbonate or sodium sulfide. The sample was apparently liquid at the operating temperature. Natrite was estimated by the XRD on the order of 40%, Thiosulfate on the order of 25%, sodium sulfide on the order of 15% and sodium sulfate on the order of 15%. These are not quantitative measures of the composition but rather indicate that a partial conversion did occur and indicate that sodium

sulfide has started to evolve significantly under these conditions. Because of the interference in the wet-chemical method between sodium sulfide and sodium carbonate a precise composition is difficult to determine.

8.4 Separation of sodium carbonate from sodium sulfate

Based on the early results with relatively low conversions a method for separating product soda ash from unreacted sodium sulfate was explored. The method takes advantage of different solubilities of these materials in non-polar solvents. Sodium carbonate is soluble in methanol, whereas sodium sulfate has very limited solubility in methanol. The possibilities for this separation are shown in Figure 8.3.

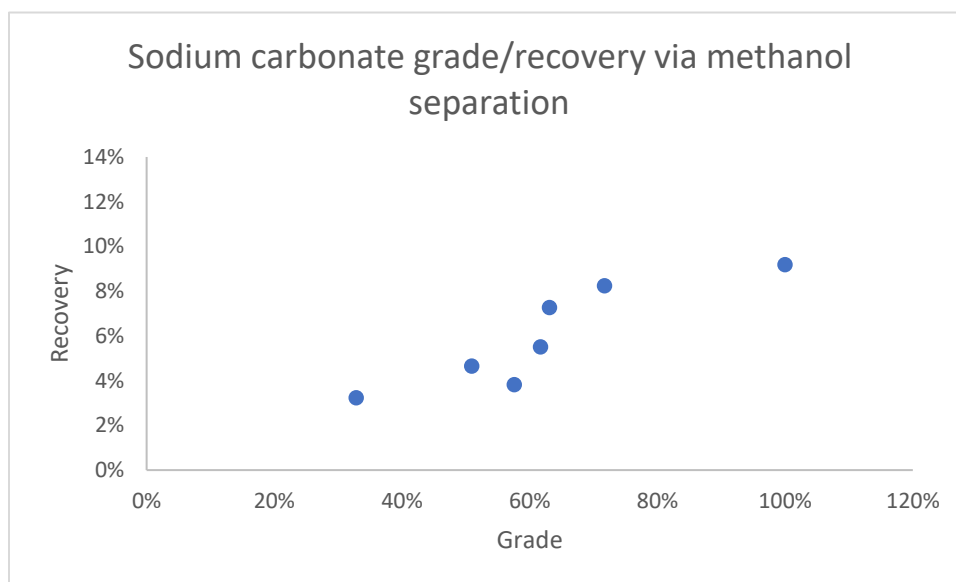


Figure 8.3: Grade and recovery for sodium carbonate separation with single stage methanol leaching.

With additional test work this problem turned out to be a minor concern as conversion progress was sufficiently complete for sodium carbonate to be used directly from the furnace reaction based on final test work. The separation of carbonate from sulfate is therefore not included in the final flowsheet or the economics considerations.

8.5 Experiments near the sodium sulfate-sodium pyrosulfate liquidus

As mentioned in the thermodynamic section sodium bisulfate is expected in the case of partial neutralization of the sulfuric acid leach liquor, this bisulfate thermally decomposes at higher temperatures to form sodium pyrosulfate. The sodium pyrosulfate was expected to depress the liquidus of the sulfate mixture. By adjusting the atmospheric composition of the

reactor, the phase stability can be manipulated such that sodium carbonate is the stable phase while the sulfate mixture is in the liquid state. There are several tests conducted at high temperatures just below the formation of sodium sulfide is expected to be significant. It should be noted that for the process some sodium sulfide production is probably more desirable than incomplete reaction as the sulfide can be oxidized under a carbon dioxide rich atmosphere to form sodium carbonate. This would eliminate the need for a salt separation unit operation.

8.5.1 113-A

Sample 113-A has the gas ratio 3 parts CO, 1-part H₂, at a flow rate of 60ml/min with 15-20 ml/min of nitrogen. The furnace was heated to a temperature of 500°C and held for 8 hours. Under these conditions the stable sodium containing phase is sodium carbonate. The reaction at this temperature is between the gaseous phase and a solid sodium sulfate phase. The expected result of the test is a kinetically limited partial conversion of sodium sulfate to sodium carbonate as per the thermodynamics and considering the expectedly slow reaction rate for solid-gas reactions at this temperature. A small section of the XRD scan result and the peak matching is shown in figure 8.5 for the product of this test. The XRD matched strongly two different sodium sulfate phases, and no other phases could reasonably be considered. It is sufficient for this analysis to say that no significant reaction progress could be identified. Significance in this respect refers to occurring at a level noticeable by the XRD scan technique. Very minor (insignificant) chemical reaction progress may have occurred (on the order of 1-5% as seen in earlier exploratory studies) but it is not identifiable with this instrument used in this manner. The minimum phase amount for reliable detection with this methodology is on the order of 5%. As the sodium sulfate is unstable at this temperature the test is considered kinetically limited.

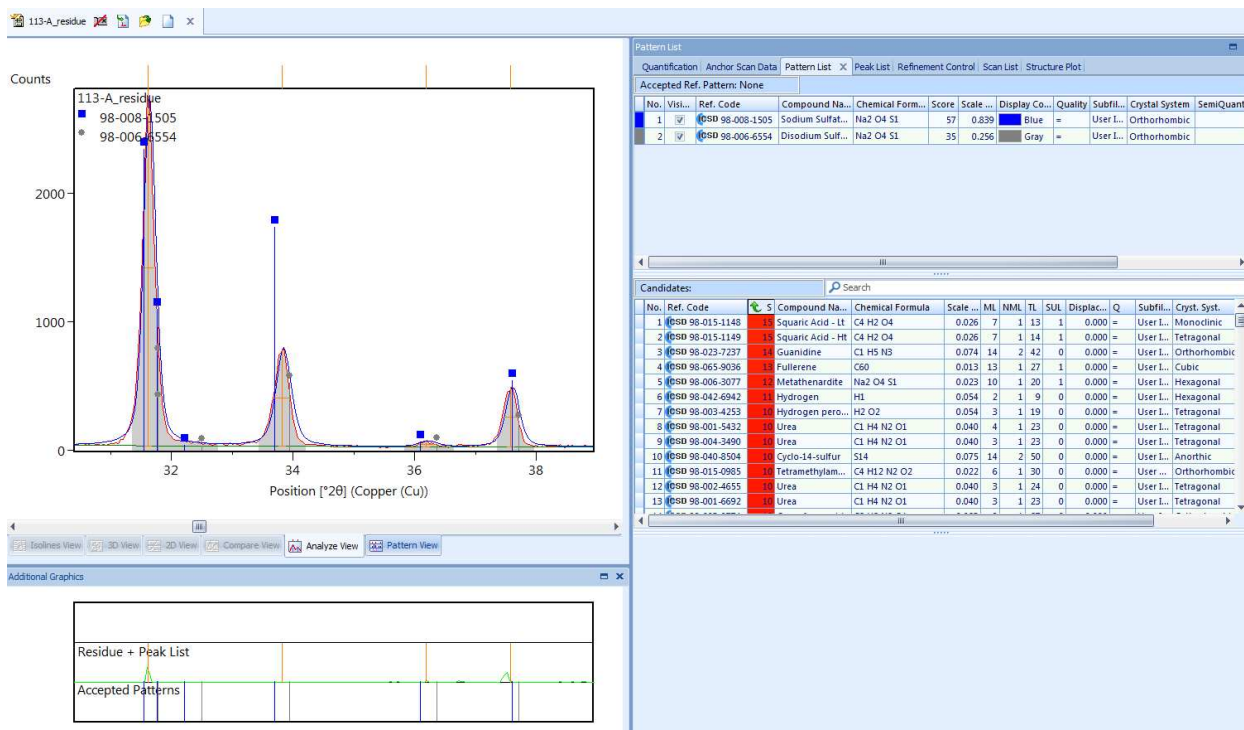


Figure 8.4: XRD result for the product of test 113-A

The relative phase amounts are not very important for the analysis of sodium sulfate to sodium carbonate conversion and so are not included here. It is sufficient to say that any sodium carbonate that may be present is sufficiently minor so as to be insignificant.

8.5.2 113-B

Test 113-B had a different atmospheric composition and a higher temperature (600°C) than test 113-A. In the 1 to 1 CO to H2 ratio the sodium carbonate phase remains stable at higher



Figure 8.5: XRD result for the product of test 113-B

temperature than in the 3 to 1 atmospheric condition in test 113-A. The temperature is selected based on the thermodynamic equilibrium charts. Figure 1 in appendix II can be referenced to understand the expected equilibrium solid phase composition under these conditions. The XRD result for the solid product is shown in figure 8.5.

The phases identified using the matching software and manual matching matches best to the two phases listed. In this case neither phase independently accounts for all of the measured peaks, but together the significant peaks are accounted for. The phases represent sodium sulfate with no progress toward sodium carbonate as expected by the equilibrium. Some carbonate may be present but it is not a significant phase in the XRD result.

8.5.3 113-E

Test 113-E was designed at a temperature and with an atmosphere where sodium carbonate and sodium sulfide are the stable sulfur containing phases. This test used an atmosphere of 1 to 1 carbon monoxide to hydrogen. The expected equilibrium composition can be seen referencing figure 2 in Appendix I. The XRD results show a single phase of sodium sulfate and no significant conversion to sodium carbonate. The XRD result is shown in figure 8.6.

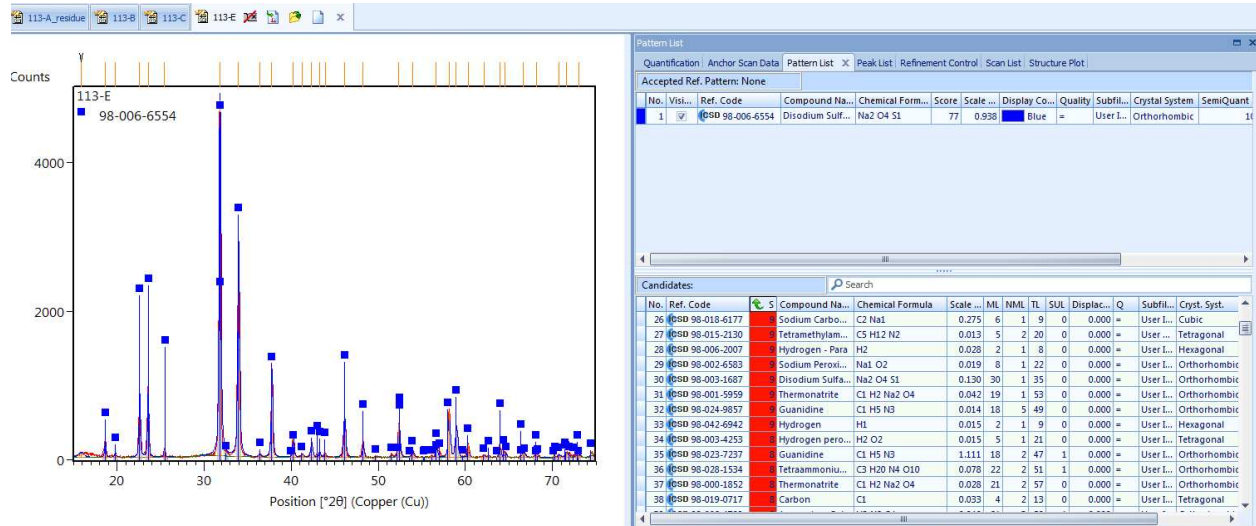


Figure 8.6: XRD result for the product of test 113-E

8.5.4 115-A

115-A was a test designed for a 700°C holdiNang temperature for 8 hours with carbon monoxide and hydrogen fed in a 1:1 ratio. Oxygen was fed (as air) in a ½ ratio. Due to a

programming error in the furnace controller the test did not hold temperature stable at 700°C and instead heated to 800°C over the course of the 8-hour holding period. An XRD analysis was completed and the results are included in spite of this programming error. The feed to the reactor in this test was a mixture of 2.0g sodium sulfate and 3.08g sodium bisulfate hydrate. As the sample is heated in the furnace the hydrates are expected to be driven off near 100°C resulting in a mixture of 2.67g sodium bisulfate and 2.0g sodium sulfate. As discussed in the thermodynamic section bisulfate thermally decomposes at temperatures on the order of 250°C. Upon this reaction it is expected that ~0.2g of water would be evolved and approximately 2.47g of sodium pyrosulfate would remain in the system. The remaining salt mixture would have a depressed liquidus from the pure sodium sulfate phase. The design is that the sample is reacted at a temperature where sodium sulfide is not the majority stable phase and sodium carbonate can be formed directly by the reactions discussed in chapter 7 from the liquid salt phase. It is expected that the kinetics will be superior to the solid-state reaction due to this liquid phase formation. The XRD results are shown in figure 8.7.

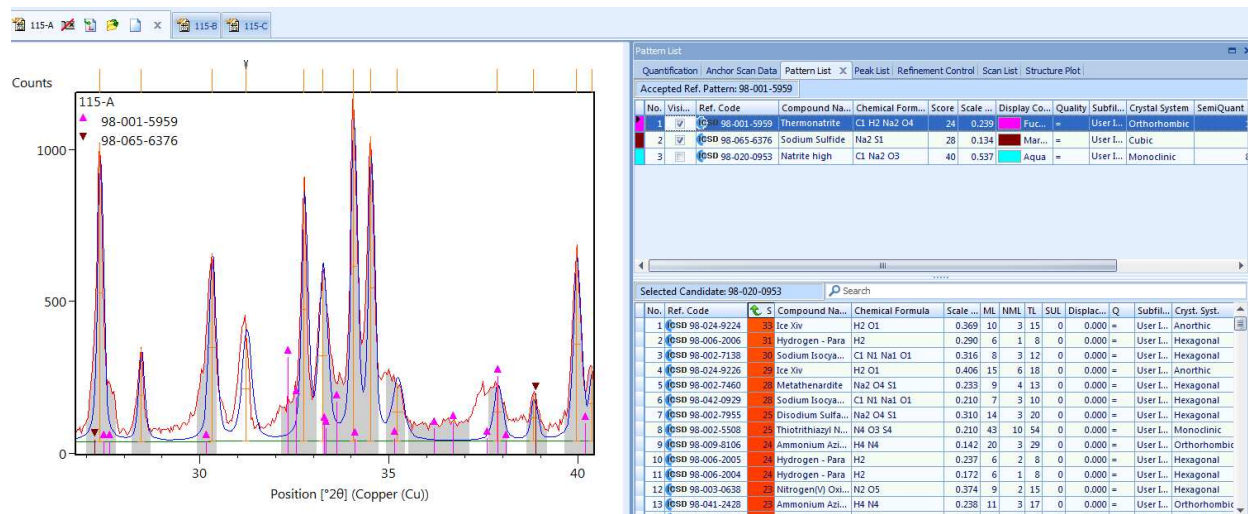


Figure 8.7: XRD result for the product of test 115-A

The results of the XRD analysis show three phases. Natrite is a sodium carbonate structure and is well supported by the XRD results. It is the strongest match to the measured spectrum and all of the primary peaks are present in the measured spectrum. Thermonatrite is a hydrated sodium carbonate structure. The existence of this phase is somewhat surprising considering the process temperature but is well supported by the XRD result. It is possible that this hydration occurred after removal from the furnace somehow. The analysis strongly

supported the presence of sodium sulfide especially with the matching of the peaks at 38.9 degrees. The authors believe that the presence of minor sodium sulfide is highly probable in this sample.

The phase composition is estimated from the XRD result. As mentioned previously in this work the composition generated this way is semi-quantitative at best or could even be considered qualitative. The majority phase is natrite representing that most of the sodium sulfate

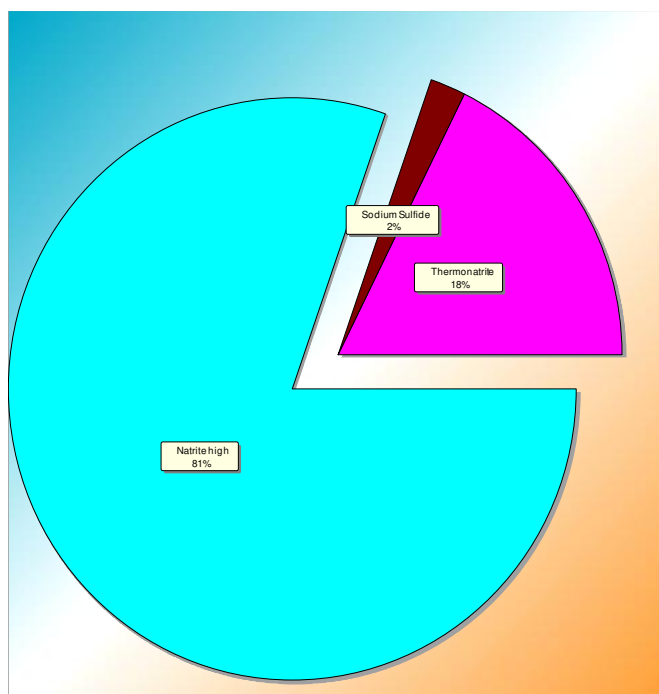


Figure 8.8: estimated relative phase amounts from the XRD for the product of test 115-A

phase was successfully converted to sodium carbonate under these furnace conditions. It could be estimated that at least a large majority of the sodium sulfate feed is successfully converted to sodium carbonate in this test.

8.5.5 115-B

115-B was designed similarly to A but is operated at a lower temperature (700°C). The feed was again a mixture of sodium sulfate and sodium bisulfate mixed as 2.20g sodium sulfate and 2.8g sodium bisulfate hydrate. The bisulfate is difficult to mass as it is hydrated and tends to form difficult to separate clumps. The gaseous feed was again CO, H₂, and O₂ in a 1:1:0.5 ratio with nitrogen as part of the air feed. The XRD results for the solid product are shown in figure 8.10. The primary phases identified by the XRD are burkeite and sodium sulfate. Sodium sulfate is of course the feed material and presence in the product represents unreacted material. Burkeite

is a double salt with a stoichiometry of $\text{Na}_6(\text{CO}_3)(\text{SO}_4)_2$. It represents a partial conversion of sodium sulfate to sodium carbonate. The sample in this test was at a lower temperature than the test 115-A, based on the appearance of the material it did not form significant liquid at the operating temperature which probably led to the lower kinetics compared to 115-A.

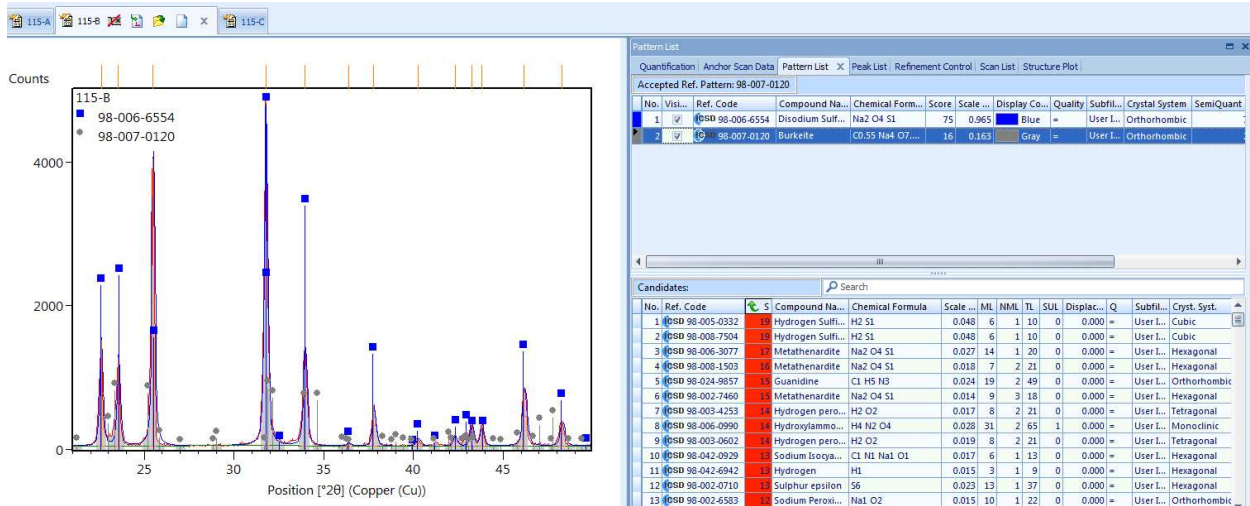


Figure 8.9: XRD result for the product of test 115-B

The estimated phase composition is included it is noticeable that burkeite is on the order of ¼ of the furnace product representing a conversion to sodium carbonate on the order of magnitude of 10%. This cannot be easily confirmed via the copper chloride wet chem method as the double salt does not react with copper chloride as sodium carbonate does. The reaction results can be interpreted to understand that at the furnace conditions the conversion was lower than the sample 115-A and therefore kinetics were slower under these conditions. The difference in conditions between these two tests was the temperature and particularly the temperature relative to the liquidus. It should be understood that the conversion of 10% is from sodium sulfate, the reaction progress was from a mixture of sodium sulfate and bisulfate and so the reaction progress for the combined reaction of reducing sodium pyrosulfate to sodium sulfate (bisulfate's high temperature phase) and converting sodium sulfate to sodium carbonate is significantly above 10%.

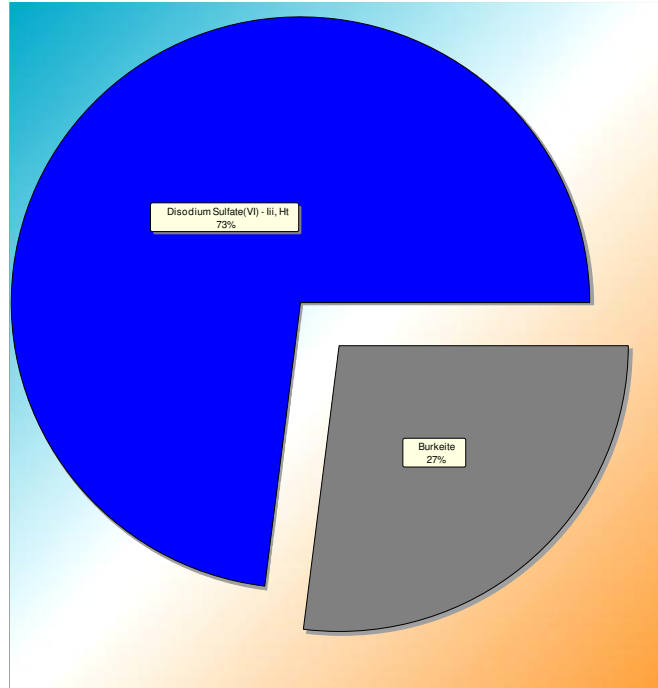


Figure 8.10: Estimated relative phase amounts based on the XRD result for 115-B.

8.5.6 115-C

115-C was designed for comparison to the test 115-A. It used the same composition and flow rate of reactant gases including CO, H₂, and O₂ in a 1:1:0.5 ratio. The feed in this sample was just sodium sulfate and had no sodium bisulfate or any other salt species. This is expected to result in a higher liquidus and lower conversion rate than in tests 115-A and 115-B with the depressed liquidus. The phases identified in this furnace product are again burkeite and sodium

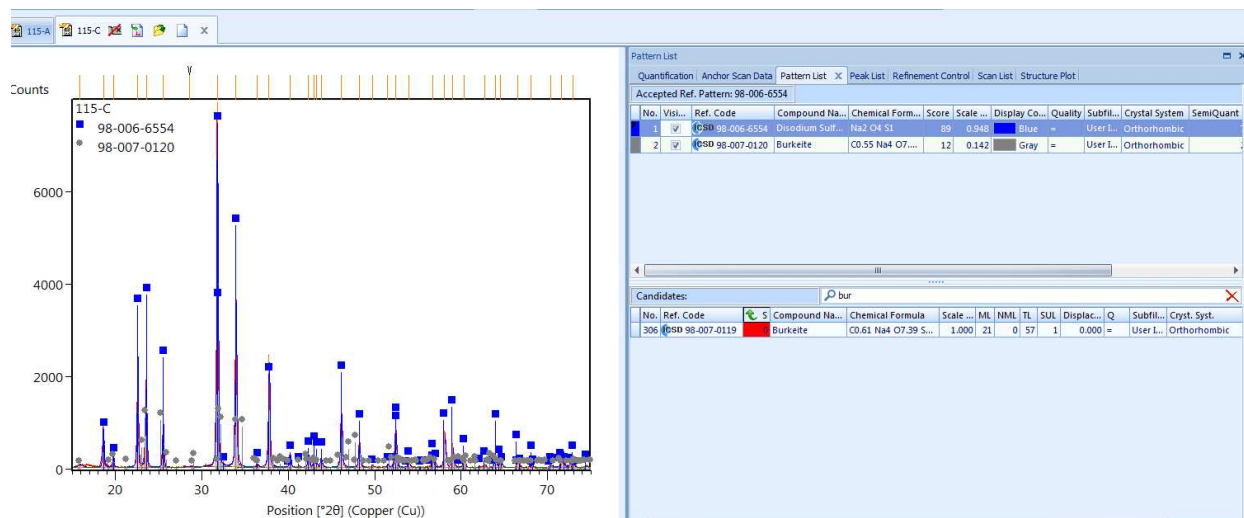


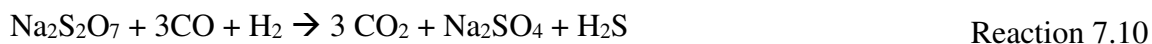
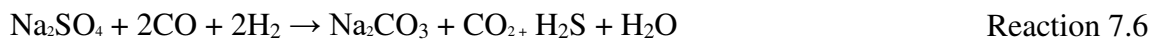
Figure 8.11: XRD result for the product of test 115-C

sulfate. The sodium sulfate phase matches the feed material, burkeite as discussed for test 115-B represents the partial conversion of sulfate to carbonate (stoichiometrically). The phase amounts are similar to those shown for 115-B with the software estimating 24% burkeite and 76% sodium sulfate. The difference between this estimate and the estimate for 115-B is negligible considering the accuracy expected.

8.6 Summary of Acid Regeneration Results

The test work near the sodium sulfate mixed salt liquidus revealed some operating parameters under which sodium sulfate could indeed be directly reduced to sodium carbonate. The test 115-A apparently exceeded the liquidus as the material had apparently melted and solidified in the shape of the crucible. At this reaction above the liquidus the reactions desired progressed sufficiently rapidly that the reaction may be interesting for an acid regeneration process. The solid-state reaction is severely limited kinetically and, though carbonate is the stable phase, the reaction does not progress rapidly enough to develop a useful process based on the solid state reaction.

Focusing on the process development for a process near the liquidus. There are three main reactions that must be controlled for this reaction to progress as designed. The three reactions are presented here for the reader's reference.



The first is the conversion of sodium sulfate to sodium carbonate presented as reaction 7.6 in section 7.3. This reaction is favorable at conditions similar to those in test 115-A at a temperature above 115-C with a gas composition of 2:2:0.5 CO:H₂: O₂, with oxygen fed as air. The second reaction is that of sodium sulfate being reduced to sodium sulfide via reaction 7.3 in section 7.2. It is the goal of the process designed here to mitigate the driving force for that reaction. This is accomplished by changing the atmosphere to be slightly less reducing via addition of air to the process. The third reaction is the reduction of sodium pyrosulfate to form sodium sulfate under the furnace conditions. The presence of pyrosulfate is important to control of the liquidus and therefore this reaction rate relative to the reaction rate for sodium sulfate conversion to sodium carbonate must be slow. If the reaction rate for reaction 7.10 exceeds that for reaction 7.6 the liquidus of the system will increase to a temperature above which reaction

7.3 is favored over reaction 7.6. However, if reaction 7.10 has a lower reaction rate than reaction 7.3 the liquidus will decrease as the reaction progresses and the process discussed or direct conversion of sodium sulfate to carbonate may have a sufficiently fast reaction rate to be a useful alternative to a process intentionally forming sodium sulfide.

CHAPTER 9 ACID REGENERATION ECONOMICS

The success of the novel process for acid regeneration is dependent upon the economic considerations for the process. The case of a plant utilizing the acid regeneration technology is compared to the case of a plant that does not recover their acid. The comparison of net present costs between these two cases includes the cost of capital and operating expenses related to the two conceptual plants. The inputs except for the differences are the same in each case and so the interval net present cost represents the increased or decreased cost between the two conceptual plants. The net present cost per unit of sulfuric acid recovered can thereby be directly compared to the expected price of sulfuric acid purchased from the broader market. This very abstract early-stage analysis does not consider uncertainty in the cost of process inputs. Sensitivity analysis based on reasonable expectations of changes in price are conducted but there is an investment advantage to more well understood prices for process inputs even if there is not significant savings projected.

The cost of capital items is of course relative to the total throughput. The estimates included here are based on a plant that consumes 7000 tons of sulfuric acid on an annual basis this is designed to match the plant designed in Chapter 5 to recover gallium from the CLP waste product. A larger plant would be expected to show better economics per ton as costs do not scale linearly with plant size. Considering a base case of increment A or increments A and B from Chapter 5, The optional addition of the acid regeneration process would result in increased capital expenditure (representing more negative cash flows in the early periods) and decreased operating expenditure representing lower operating costs later in the plant life. For the purposes of this analysis the acid regeneration economics are considered separately from any discussion of the gallium recovery plant. The cost savings to the recovery process are represented as positive cashflows for the model considering just the reagent recovery plant.

9.1 Engineering mass and energy balance

The economics discussion is based on the designed flowsheet and the mass and energy balance discussed as part of the engineering work. The flowsheet modeled by the economics in this section is shown in figure 9.1. The primary unit operations are: Acid regeneration, Oxidation of off gases, Scrubbing of off gases, and sulfate/carbonate separation.

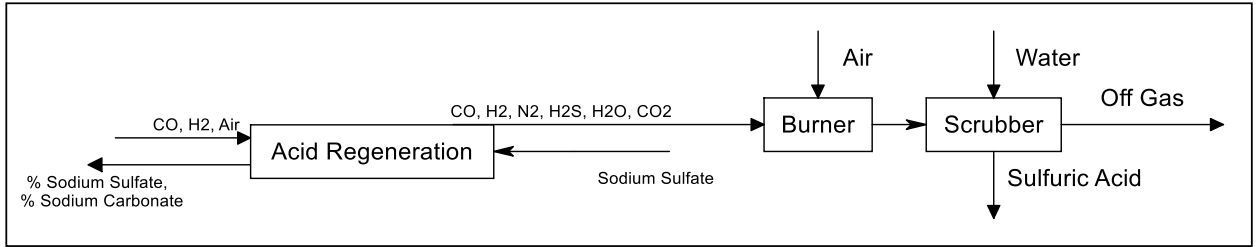


Figure 9.1: Flowsheet for lixiviant regeneration process

9.1.1 Acid Regeneration Unit Operation

The acid regeneration unit operation as shown in figure 9.2 is the novel process developed in the engineering section of this report.

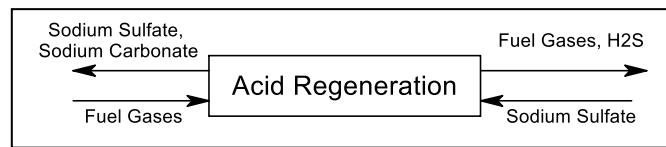


Figure 9.2: Segment of flowsheet relating to the high temperature salt reaction for acid regeneration

The Process is designed to handle a feed of 10150 tons of sodium sulfate per day which is the expected waste stream for an acid regeneration plant treating the neutralization product of a 7000 ton per day CLP leach-precipitate plant. This material is reacted at 800°C based on the results presented in Chapter 8. This reaction is designed with a feed with a 20% excess of both CO and CO₂ to the stoichiometric quantities. This mass balance is shown in Table 9.1 from the HSC software program,

Table 9.1: Mass and energy balance for acid regeneration unit operation

INPUT SPECIES (2) Formula	Temper. K	Pressure bar	Amount kmol	Amount kg	Amount Nm ³	Heat Content kWh	Total H kWh
CO(g)	298.150		737.837	20666.888	16537.583	0.00	-22655.96
H2(g)	298.150		245.070	494.032	5492.901	0.00	0.00
Na2SO4	298.150		204.165	29000.000	10.821	0.00	-78711.19
OUTPUT SPECIES (2) Formula	Temper. K	Pressure bar	Amount kmol	Amount kg	Amount Nm ³	Heat Content kWh	Total H kWh
CO(g)	1223.000		123.000	3445.242	2756.873	997.97	-2778.86
H2(g)	1223.000		40.500	81.643	907.751	309.29	309.29
CO2(g)	1223.000		408.000	17955.876	9144.749	5190.44	-39406.81
H2S(g)	1223.000		204.165	6958.123	4576.073	2193.51	1030.81
Na2CO3	1223.000		204.165	21639.130	8.546	10178.68	-53950.00
BALANCE:			kmol	kg	Nm³	kWh	kWh
			-207.242	-80.906	-4647.314	18869.895	6571.593
MATERIAL BALANCE							
ELEMENT	Input	Output	Balance	Input	Output	Balance	
	kmol	kmol	kmol	kg	kg	kg	
C	737.837	735.165	-2.672	8861.939	8829.846	-32.093	
H	490.140	489.330	-0.810	494.032	493.215	-0.816	
Na	408.330	408.330	0.000	9387.402	9387.412	0.011	
O	1554.496	1551.495	-3.001	24871.004	24822.989	-48.015	
S	204.165	204.165	0.000	6546.543	6546.551	0.007	
Temperature of products = 991.7 K (when Heat Balance = 0)							

The designed feed is then 20.66 Tons of CO and 0.49 Tons of H2. The Capital cost of this unit operation is based on values from costmine for a rotary kiln that handles 3-6 tons per hour of solid feed material. This number is scaled via the 6/10ths rule to estimate the cost of a smaller kiln for this plant.

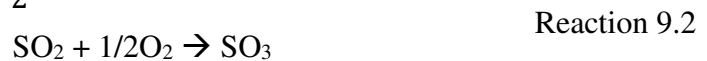
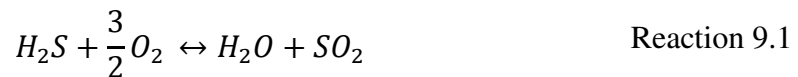
9.2 Oxidation of Off Gases

The off gases including excess fuel and product gases to include CO2 and H2S are burned to convert the H2S to SO2 and water. This process would require blown air feed to provide oxygen for the combustion reaction. The sizing of this capital line item is based on the expected off gas volume and composition from the rotary kiln mentioned earlier. The capital price for this unit operation is based on the price of a burner from costmine. Industry contact was attempted but did not yield useful data.

Table 9.2: Mass and energy balance for off gas oxidation unit operation

INPUT SPECIES (1) Formula	Temper. K	Pressure bar	Amount kmol	Amount kg	Amount Nm ³	Heat Content kWh	Total H kWh
CO(g)	1223.000		123.000	3445.242	2756.873	997.97	-2778.86
H2(g)	1223.000		40.500	81.643	907.751	309.29	309.29
CO2(g)	1223.000		408.000	17955.876	9144.749	5190.44	-39406.81
H2S(g)	1223.000		204.000	6952.500	4572.374	2191.74	1029.98
O2(g)	298.000		601.000	19231.279	13470.574	-0.73	-0.73
N2(g)	298.000		2003.000	56110.840	44894.441	-2.43	-2.43
OUTPUT SPECIES (1) Formula	Temper. K	Pressure bar	Amount kmol	Amount kg	Amount Nm ³	Heat Content kWh	Total H kWh
CO2(g)	1900.000		531.426	23387.793	11911.170	12612.31	-45476.26
O2(g)	1900.000		110.795	3545.307	2483.315	1706.15	1706.15
N2(g)	1900.000		2003.000	56110.840	44894.441	29237.52	29237.52
H2O(g)	1900.000		244.700	4408.339	5484.608	4621.34	-11816.11
SO3(g)	1900.000		204.000	16332.893	4572.374	6704.73	-15721.93
BALANCE:			kmol	kg	Nm³	kWh	kWh
			-285.579	7.792	-6400.853	46195.772	-1221.079
MATERIAL BALANCE							
ELEMENT	Input	Output	Balance	Input	Output	Balance	
	kmol	kmol	kmol	kg	kg	kg	
C	531.000	531.426	0.426	6377.682	6382.798	5.117	
H	489.000	489.400	0.400	492.883	493.286	0.403	
N	4006.000	4006.000	0.000	56110.840	56110.840	0.000	
O	2141.000	2141.142	0.142	34254.715	34256.987	2.272	
S	204.000	204.000	0.000	6541.260	6541.260	0.000	
Temperature of products = 1932.0 K (when Heat Balance = 0)							

The primary reaction of interest for the sake of acid regeneration for this unit operation is the oxidation of H₂S to SO₂ and then to SO₃ as shown in reaction 9.1 and 9.2.



Additionally, the unreacted reactant gases from the sodium sulfate reduction are oxidized. The energy balance for this reaction is quite interesting as it may be used to contribute the energy to the previous unit operation.

9.2.1 Scrubbing of Off Gases

The off gas is scrubbed to capture SO₃ as sulfuric acid. The sizing of this equipment is based on the mass balance for the oxidation unit operation. The process feed for this unit operation is water. The price for this unit is based on a spray scrubber from cost mine.

The sizing of this unit and the oxidation burner are somewhat imprecise as they are very dependent upon conversion percentage from the acid regeneration unit operation. Sizing was based on 100% conversion which was not observed in the research.

The main reaction of interest in this unit operation is the dissolution of sulfur trioxide produced from the oxidation operation in water to form sulfuric acid H₂SO₄ according to Reaction 9.3



9.2.2 Sulfate/Carbonate Separation

The sulfate/carbonate separation is fed from the solid phase fraction of the rotary kiln, in the case of incomplete reaction it may be interesting to separate the reacted sodium carbonate and recycle the sodium sulfide/sodium sulfate back into the kiln feed. It is sized to handle the expected process output of the rotary kiln of sodium carbonate, sodium sulfide, sodium sulfate, and sodium peroxide.

9.3 Estimation of CAPEX

The estimated prices of various capital items are presented in table 9.3. The first subtotal represents the sum of the prices for these items. Subsequent prices for Delivery, Engineering, Installation, Electrical, and Instrumentation are based on capital cost estimation factors. These factors generally represent a range and the number selected is based on prior experience and quality of information. In this work the values for factors were selected at the top of the range published by Villbrandt and Dryden. [15] This is decided based firstly on the small size of the plant, the factors are generally shifted toward the lower end of the range for larger projects that have economies of scale and secondly due to uncertainty at this early stage of process development. The second subtotal represents the sum of all equipment in addition to these coefficients calculated costs. The total represents these along with operating capital (3 months of operating expenditures) and a contingency also calculated as a fraction of the initial cost. The total estimated Capex is \$1.7million to the order of precision at which this estimate may be sensible. This is the number used for the base case cashflow model.

Table 9.3: Capex estimate for acid regeneration plant

CAPEX		
Cost Item	Size	Price Per
Rotary Kiln Furnace	1.3 ton/hr	\$ 372,740.00
Burner		\$ 214,000.00
scrubber	1700	\$ 55,100.00
Mixer		\$ 40,400.00
Subtotal		\$ 641,840.00
Delivery		\$ 19,255.20
Engineering		\$ 211,807.20
Installation		\$ 160,460.00
Electrical		\$ 160,460.00
Intrumentation		\$ 64,184.00
Subtotal 2		\$ 1,258,006.40
Operating Capital		\$ 45,562.76
Total with Contingency		\$ 1,744,000.00

9.4 Estimation of OPEX

OPEX is calculated similarly to that for the separations process and is summarized in Table 9.4.

Table 9.4: OPEX model for acid regeneration plant

Cost Item:		per unit cost	total cost/unit	units per year	Total per year:
LABOR:	Quantity	cost per hour		units per year	\$291,450.00
Mill Labor	3	\$24.00	104.4	2000	\$208,800.00
Mill Operator	1	\$28.50	\$41.33	2000	\$82,650.00
ELECTRIC POWER	QNTY per Hr (Kw)	cost per KwHr		units per year	\$2,256.11
Rotary Kiln	3.72	\$0.07	0.268584	8400	\$2,256.11
CONSUMABLES	Quantity	Cost per unit		Units per year	\$182,250.91
Carbon Monoxide	1	\$ 0.30		567005	\$170,101.50
Hydrogen	1	\$ 0.065		186914	\$12,149.41
Methanol	1	\$ 519.00		0	\$0.00
Contingency Factor					\$0.00
Total:					\$ (476,000.00)

9.5 Cashflow Model

5Cashflow is projected using the estimated CAPEX, OPEX, and an estimation of the value of the products. The value of these products is considered as positive cashflow. The cashflow model is presented as Table 9.5. The revenues used for the sale of sulfuric acid and soda ash are more accurately considered cost savings for an operating plant. They are based on the spot price for sulfuric and soda ash, this is the price used in the OPEX models and so the savings offered here are indicative of reduced operating expenditure for the process plant

designed in this work. This model is designed for a base case where conversion is at or approaching 100%. This is not shown in the accompanying experimental work but is an interesting case for considering future research toward this goal. The sensitivity analysis will be used to scale the revenues to represent conversions closer to those shown in the experimental work. Unlike some process where recoveries can easily be changed and those changes can be carried through the process the mass and energy balance become complicated as conversion is changed. For example, the excess energy produced in the off-gas oxidation unit operation increases as the conversion percent is reduced, the use of this energy would be important for the process economics. The equipment also changes nonlinearly with conversion as the kiln reaction has lower total mols of gas on the forward side than the left side as can be seen in reaction 9.1. For this reason, the sensitivity analysis must be done carefully to have any real meaning.

Table 9.5: Cashflow model for acid

Cashflow	\$ (1,926,251.04)	\$ 1,741,468.96	\$ 1,741,468.96	\$ 1,741,468.96	\$ 1,741,468.96	\$ 1,741,468.96	\$ 1,741,468.96	\$ 1,741,468.96	\$ 1,741,468.96	\$ 1,741,468.96	\$ 1,741,468.96
Year	0	1	2	3	4	5	6	7	8	9	10
CAPEX	\$ (1,744,000.00)										
OPEX	\$ (182,251.04)	\$ (182,251.04)	\$ (182,251.04)	\$ (182,251.04)	\$ (182,251.04)	\$ (182,251.04)	\$ (182,251.04)	\$ (182,251.04)	\$ (182,251.04)	\$ (182,251.04)	\$ (182,251.04)
Value of H2SO4	\$ -	\$ 873,720.00	\$ 873,720.00	\$ 873,720.00	\$ 873,720.00	\$ 873,720.00	\$ 873,720.00	\$ 873,720.00	\$ 873,720.00	\$ 873,720.00	\$ 873,720.00
Value of Na2CO3	\$ -	\$ 1,050,000.00	\$ 1,050,000.00	\$ 1,050,000.00	\$ 1,050,000.00	\$ 1,050,000.00	\$ 1,050,000.00	\$ 1,050,000.00	\$ 1,050,000.00	\$ 1,050,000.00	\$ 1,050,000.00
Tons H2SO4 Recovered		6472	6472	6472	6472	6472	6472	6472	6472	6472	6472
Tons Na2CO3 Recovered		7000	7000	7000	7000	7000	7000	7000	7000	7000	7000
NPV	\$5,925,024.97	IRR	90%								

9.6 Combination of acid regeneration and Separations Economics

The acid regeneration process may be applicable at any operation where acid consumption is a major driver of costs. As the focus of this research is on gallium recovery it is useful to consider whether acid regeneration may be applied to the process developed such that that process becomes investable. The combination is especially interesting considering the increments that contributed the most to reagent consumption. Increment A, Increment B, and the acid regeneration process as a third increment to the process design is considered and presented in table 9.6.

Table 9.6: Summary of separations increments from Chapter 5 and acid regeneration considered as an incremental investment to the separations plant model

Process	CAPEX	OPEX, Year 0	Annual Cashflow, Year 1	NPV
A	\$ (1,455,000)	\$ (2,416,000)	\$ (1,961,579)	\$ (9,825,837)
A+Acid Regen	\$ (3,034,000)	\$ (1,940,000)	\$ 438,141	\$ (312,237)
A+ B	\$ (1,799,000)	\$ (2,666,000)	\$ (1,856,671)	\$ (9,667,133)
A+B+Acid Regen	\$ (3,378,000)	\$ (2,190,000)	\$ 543,049	\$ (153,534)

The combination shows the changing of the economics that is possible via the acid regeneration process. This validates the analysis in the sensitivity to reagent consumption in sections 5.10 through 5.12 for the increments presented here that show that acid regeneration can make significant contributions to the process economics. This specific process for this specific feed stock as currently designed is still net present value negative and so additional engineering and perhaps better market conditions are necessary to support the development of this project, however acid regeneration may contribute to a variety of otherwise borderline projects that are hampered by lixiviant costs.

9.7 Comparison to sodium sulfide process

The viability of this recycling process is compared thermodynamically (Chapter 7) & technically (section 8) to a process that produces sodium carbonate via sodium sulfide as is done in the chemical industry, this comparison should also include considerations of the energy balance and economics. An energy balance for the sodium sulfide process is shown in Tables 9.7 and 9.8.

Table 9.7: Energy balance for sodium sulfate reduction to sodium sulfide.

INPUT SPECIES (1) Formula	Temper. K		Amount kmol	Amount kg	Amount Nm ³	Heat Content MJ	Total kWh
Na ₂ SO ₄	298.150		204.225	29008.606	10.824	0.000	-21872.457
C	298.150		408.451	4905.779	2.171	0.000	0.000
OUTPUT SPECIES (1) Formula	Temper. K	P r e s s	Amount kmol	Amount kg	Amount Nm ³	Heat Content MJ	Total H kWh
Na ₂ S	1200.000		29.000	2263.292	1.219	691.003	-633.800
CO ₂ (g)	1200.000		58.000	2552.551	1299.989	716.928	-1562.035
BALANCE:			0.000	0.000	9140.347	9904.061	6401.755

Table 9.8: Energy balance for sodium sulfide oxidation to form sodium carbonate.

INPUT SPECIES (2) Formula	Temper. K		Amount kmol	Amount kg	Amount Nm ³	Heat Content kWh	Total H kWh
Na ₂ S	1200.000		29.000	2263.293	1.219	691.003	-2281.499
CO ₂ (g)	1200.000		14.500	638.138	324.997	179.232	-1405.720
O ₂ (g)	298.150		21.750	695.974	487.496	0.000	0.000
OUTPUT SPECIES (2) Formula	Temper. K		Amount kmol	Amount kg	Amount Nm ³	Heat Content kWh	Total H kWh
Na ₂ CO ₃	298.150		29.000	3073.665	1.214	0.000	-9108.963
SO ₂ (g)	298.150		14.500	928.925	324.997	0.000	-1195.497
Balance:			-21.750	405.187	-487.501	-870.234	-6617.243

This process can be accomplished with carbon monoxide and/or hydrogen similar to the direct process but it is generally accomplished using solid carbon mixed with the salt phase (that is liquid at the reaction temperature). The mass and energy balance do not reflect process kinetics

but do demonstrate the energy and material costs of the reaction fairly well. For this comparison the CAPEX is considered to be roughly the same as the novel reaction to directly form sodium carbonate from sodium sulfate and so simple comparison of the operating costs are more informative. The wear of the furnace lining, labor, and materials handling costs are considered equal in both cases and so are also left out of the comparison. It is possible that the novel process improves the furnace lining wear life but this cannot be concluded without significant additional study.

The important components of the cost structure for the purposes of this comparison are the energy and materials costs summarized in the mass balance. The sodium sulfide process consumes carbon mostly from charcoals as part of the process.

9.8 Summary

The acid regeneration economics are considered mostly related to the theoretical process that is shown to be favorable via thermodynamic analysis. The kinetics are an important consideration in discussing the energy expenditure for the direct conversion process and its advantages or disadvantages relative to the sodium sulfide intermediary process. The stoichiometric energy balance suggests that there is more excess enthalpy for the direct reduction case than for the sodium sulfide process. This may indicate reduced fuel consumption, of course if this reaction requires drastically longer reaction times the improvement may be moot. It is also hoped that furnace wear may be reduced at lower temperatures and possibly in the absence of a liquid salt phase. Empirical tests are early stage and so are not suitable for contributing directly to the economic model to the same degree as the separations test. It is important to note from the test results that the direct conversion was shown with the test 115-A discussed in section 8.5.4 showing mostly sodium carbonate present in the product are achieved at a temperature lower than that used for the sodium sulfide process industrially. The novel reactions are potentially useful for reducing the reagent costs for metallurgical operations as the project value shows significant improvement toward positive economics. The costs related to regenerating sulfuric acid in this manner are lower than the costs of purchasing sulfuric acid for the plant.

CHAPTER 10 CONCLUSIONS

10.1 Conclusions

- Gallium recovery from zinc smelter waste streams is technically feasible by a leach-precipitation process but faces significant economic challenges under typical market conditions for the metals and the reagents at the time of this writing. Additional technical work to improve the process should focus on reducing reagent consumption and improving leach recovery as those are the primary influencers of the modeled process economics.
- The economic modelling suggests that for current market conditions or market conditions that may reasonably be expected in the near future the leach-precipitation process is not economically viable.
- Gallium recovery by solvent extraction is still interesting especially with regard to the novel extractants. The primary economic challenges of the leach-precipitation flowsheet namely reagent costs in the form of leach sulfuric acid and soda ash for pH adjustment, and poor leach recovery are expected to impact a solvent extraction-based separations process similarly to the leach-precipitation flowsheet. The novel extractants are particularly interesting if additional testing can reveal a pH domain where selective absorption of the primary metals in the leach liquor is possible.
- The novel lixiviant regeneration process is shown to allow direct conversion of sodium sulfate to sodium carbonate without the formation of intermediate sodium sulfide that must be oxidized to form sulfur dioxide for the contact process. The direct conversion can be accomplished at lower temperatures to minimize wear of the furnace and reduce energy requirements for processing sulfates to form sulfuric acid for leaching processes. The possibilities for this reaction are determined via thermodynamic model and confirmed with experimental results. Process parameters around which this process may be designed are briefly discussed and direction for future development of this process can be evaluated from the results presented.
- The initial mass and energy balance for the lixiviant regeneration process suggest that it may be used to reduce costs associated with a leach process significantly. It was not sufficiently economically positive to shift the process economics for the leach-precipitation process but this speaks more toward the negative economics of that process

than the usefulness of the acid regeneration reaction. Its usefulness is almost certainly highly dependent upon scale of the leach operation but could be an interesting consideration for future extractive projects as reduction in reagent consumption becomes increasingly socially and economically important.

10.2 Suggestions for future research

Five primary directions for future research exist that are considered interesting by the authors. The future work directions are informed simultaneously by the technical results and the economic modelling of the process.

Firstly, the separation of gallium (as well as germanium and indium) from similar gallium containing waste products via preferential chlorination or bromidation and volatilization may be a possibility for efficient separations of these materials. This concept could be compared to the economic discussion presented for the leach-precipitate process to determine viability relative to the solvent extraction and cementation processes.

Secondly, the continuation of solvent extraction work may be interesting particularly referring to the novel extractants provided by ORNL. Of the three extractants TODGA showed rapid absorption of zinc, gallium, and iron, development of an absorption isotherm may indicate a pH domain over which a separation may be achieved. The other two novel extractants showed a preference for iron absorption suggesting that there is a pH domain over which they can be selective between iron and gallium. One could envision a system based on a combination of the leach-precipitation process to remove zinc and then utilization of solvent extraction to create a zinc concentrate with higher grade than is possible via caustic leach.

Thirdly, The development of the lixiviant regeneration process must focus on understanding the relative rates of reaction between reactions 7.3, 7.6, and to allow design of a reactor and further refinement of the process development. The operation is largely dependent upon the effects of the relative phase amounts on the liquidus for this salt mixture. Carbon dioxide in the gas phase may be useful to influence the relative favorability of these reactions as they have different stoichiometries for carbon dioxide formation. Further study of the effect of carbon dioxide could expand the operating window for the direct conversion process.

Fourthly, additional research toward catalysis of the acid regeneration reaction may improve process viability. The study here did not include lengthy discussion of kinetics related to the acid regeneration process and only discussed energetics of the system. The kinetics related to

the process may be improved with an appropriate catalyst which is out of the scope of this initial exploratory research. Indeed, yields sufficient to positively affect economics in reasonable reaction times may only be possible via catalysis.

Fifthly, a study of the possibilities for separation of iron in the form of goethite and copper would contribute both to the value of this process, and add value to the zinc industry as a whole. Significant copper value is lost as material similar to that constituting fraction E is disposed of as waste, whether hazardous or non-hazardous. The challenges with minor co-product recovery are made apparent in the economic model as the revenue generated by the gallium concentrates are simply insufficient considering the other metals that consume inputs but do not contribute value. This is the case in this system where significant cost is input to leach several metals including iron, copper, and manganese which do not correspondingly contribute to the revenue of the process. These metals represent a reagent and cost sink with little returned value from the reagent consumption. The market conditions under which gallium and zinc could support the initial leaching and pH adjustment unit operations are considered extreme. Additional revenue from other metals may contribute to viable economics under realistic market conditions. The copper value of Fraction E represents on the order of \$1.5M of potential revenue over the 10-year plant life discussed in the economics section. Additional revenue from base metals recovery may be necessary to economically recover the critical materials in the system.

REFERENCES

- [1] "Gallium - Critical Metal - Market Report," *Roskill*, 22-Mar-2021. [Online]. Available: <https://roskill.com/market-report/gallium/>. [Accessed: 12-May-2021].
- [2] Ott, B., Taylor, P., and Spiller, E. (2018). Experimental Methods of Flowsheet Development for Hard Drive Recycling by Preferential Degradation and Physical Separation. M.S. Colorado School of Mines.
- [3] S. A. Wood and I. M. Samson, "The aqueous geochemistry of gallium, germanium, indium and scandium," *Ore Geology Reviews*, vol. 28, no. 1, pp. 57–102, 2006.
- [4] F. Lu, T. Xiao, J. Lin, Z. Ning, Q. Long, L. Xiao, F. Huang, W. Wang, Q. Xiao, X. Lan, and H. Chen, "Resources and extraction of gallium: A review," *Hydrometallurgy*, vol. 174, pp. 105–115, 2017.
- [5] Z. Zhao, Y. Yang, Y. Xiao, and Y. Fan, "Recovery of gallium from Bayer liquor: A review," *Hydrometallurgy*, vol. 125-126, pp. 115–124, 2012.
- [6] R. A. Abdulvaliyev, A. Akcil, S. V. Gladyshev, E. A. Tastanov, K. O. Beisembekova, N. K. Akhmediyeva, and H. Deveci, "Gallium and vanadium extraction from red mud of Turkish alumina refinery plant: Hydrogarnet process," *Hydrometallurgy*, vol. 157, pp. 72–77, 2015.
- [7] Y. Qu, B. Lian, B. Mo, and C. Liu, "Bioleaching of heavy metals from red mud using *Aspergillus niger*," *Hydrometallurgy*, vol. 136, pp. 71–77, 2013.
- [8] S. V. Gladyshev, A. Akcil, R. A. Abdulvaliyev, E. A. Tastanov, K. O. Beisembekova, S. S. Temirova, and H. Deveci, "Recovery of vanadium and gallium from solid waste by-products of Bayer process," *Minerals Engineering*, vol. 74, pp. 91–98, 2015.
- [9] T. Kinoshita, Y. Ishigaki, N. Shibata, K. Yamaguchi, S. Akita, S. Kitagawa, H. Kondou, and S. Nii, "Selective recovery of gallium with continuous counter-current foam separation and its application to leaching solution of zinc refinery residues," *Separation and Purification Technology*, vol. 78, no. 2, pp. 181–188, 2011.
- [10] F. Liu, Z. Liu, Y. Li, Z. Liu, Q. Li, and L. Zeng, "Extraction of gallium and germanium from zinc refinery residues by pressure acid leaching," *Hydrometallurgy*, vol. 164, pp. 313–320, 2016.
- [11] T. S. Fayram and C. G. Anderson, "The Development and Implementation of Industrial Hydrometallurgical Gallium and Germanium Recovery," *Electrometallurgy and Environmental Hydrometallurgy*, pp. 1461–1486, 2013.
- [12] B. Gupta, N. Mudhar, Z. Begum, and I. Singh, "Extraction and recovery of Ga(III) from waste material using Cyanex-923," *Hydrometallurgy*, vol. 87, no. 1-2, pp. 18–26, 2007.

- [13] B. Y. Mishra, M. D. Rokade, and P. M. Dhadke, "Liquid-liquid extraction and separation of gallium(III) with Cyanex 921," *Indian Journal of Chemistry*, vol. 39A, pp. 1114–1116, Oct. 2000.
- [14] G. V. K. Puvvada, "Liquid–liquid extraction of gallium from Bayer process liquor using Kelex-100 in the presence of surfactants," *Hydrometallurgy*, vol. 52, no. 1, pp. 9–19, 1999.
- [15] G. V. K. Puvvada, K. Chandrasekhar, and P. Ramachandrarao, "Solvent extraction of gallium from an Indian Bayer process liquor using Kelex-100," *Minerals Engineering*, vol. 9, no. 10, pp. 1049–1058, 1996.
- [16] T. Kekesi, "Gallium extraction from synthetic Bayer liquors using Kelex-100-kerosene, the effect of loading and stripping conditions on selectivity," *Hydrometallurgy*, vol. 88, no. 1-4, pp. 170–179, 2007.
- [17] K. Xu, T. Deng, J. Liu, and W. Peng, "Study on the recovery of gallium from phosphorus flue dust by leaching with spent sulfuric acid solution and precipitation," *Hydrometallurgy*, vol. 86, no. 3-4, pp. 172–177, 2007.
- [18] S. Lower, "Acid/Base Titration," in *Chemistry*, LibreTexts, 2021.
- [19] "Strategic Metals: Kitco," *Kitco Metals Inc.* [Online]. Available: <https://www.kitco.com/strategic-metals/>. [Accessed: 12-May-2021].
- [20] U.S. Bureau of Labor Statistics, Import Price Index (End Use): Zinc [IR14260], retrieved from FRED, Federal Reserve Bank of St. Louis; <https://fred.stlouisfed.org/series/IR14260>, August 14, 2021.
- [21] "Managing Hazardous Waste," *dtsc.ca.gov*, 2021. [Online]. Available: <https://dtsc.ca.gov/disposal-fee/>. [Accessed: Apr-2021].
- [22] Fairlie, A. (1936). *Sulphuric acid manufacture*. {S.l.: s.n.}.
- [23] King, M., Davenport, W. and Moats, M. (2013). *Sulfuric acid manufacture*. Burlington, Mass.: Elsevier.
- [24] Hirschkind, W. (1925). Manufacture of Hydrochloric Acid from Chlorine. *Industrial & Engineering Chemistry*, 17(10), pp.1071-1073.
- [25] Botz, M., Dimitriadis, D., Polglase, T., Phillips, W. and Jenny, R. (2001). Processes for the regeneration of cyanide from thiocyanate. *Mining, Metallurgy & Exploration*, 18(3), pp.126-132.
- [26] Bodke, A., Olschki, D. and Schmidt, L. (2000). Hydrogen addition to the Andrussov process for HCN synthesis. *Applied Catalysis A: General*, 201(1), pp.13-22.

- [27] Glanville, J. and Rau, E. (1973). Soda ash-manufacture - An example of what?. *Journal of Chemical Education*, 50(1), p.64.
- [28] Steinhauser, G. (2008). Cleaner production in the Solvay Process: general strategies and recent developments. *Journal of Cleaner Production*, 16(7), pp.833-841.
- [29] U.S. Bureau of Labor Statistics, Producer Price Index by Commodity: Chemicals and Allied Products: Sulfuric Acid [WPU0613020T1], retrieved from FRED, Federal Reserve Bank of St. Louis; <https://fred.stlouisfed.org/series/WPU0613020T1>, August 14, 2021.
- [30] Fred.stlouisfed.org. (2018). *Producer Price Index by Commodity for Chemicals and Allied Products: Inorganic Acids, Including Hydrochloric, Sulfuric Acid and Other*. [online] Available at: <https://fred.stlouisfed.org/series/WPU0613020T1> [Accessed 26 Nov. 2018].
- [31] U.S. Bureau of Labor Statistics, Producer Price Index by Industry: Other Basic Inorganic Chemical Manufacturing: Sodium Hydroxide (Caustic Soda) (DISCONTINUED) [PCU32518032518014], retrieved from FRED, Federal Reserve Bank of St. Louis; <https://fred.stlouisfed.org/series/PCU32518032518014>, August 14, 2021.
- [32] Sullivan, T. (2012). *Sulphuric acid handbook*. [Place of publication not identified]: Rarebooksclub Com.
- [33] Lakshmanan, S. and Murugesan, T. (2013). The chlor-alkali process: Work in Progress. *Clean Technologies and Environmental Policy*, 16(2), pp.225-234.
- [34] Van Weert, G. and Peek, E. (1992). Reagent recovery in chloride hydrometallurgy —some missing links. *Hydrometallurgy*, 29(1-3), pp.513-526.
- [35] Mazrou, S., Kerdjoudj, H., Che´rif, A., Elmidaoui, A. and Mole´nat, J. (1998). Regeneration of hydrochloric acid and sodium hydroxide with bipolar membrane electro dialysis from pure sodium chloride. *New Journal of Chemistry*, 22(4), pp.355-361.
- [36] Soto, H., Nava, F., Leal, J. and Jara, J. (1995). Regeneration of cyanide by ozone oxidation of thiocyanate in cyanidation tailings. *Minerals Engineering*, 8(3), pp.273-281.
- [37] J. F. White and A. H. White, “Manufacture of Sodium Sulfide: Reduction of Sodium sulfate to Sodium Sulfide at Temperatures below 800deg; C.,” *Industrial & Engineering Chemistry*, vol. 28, no. 2, pp. 244–246, 1936.
- [38] J. Li and A. R.P. van Heiningen, “Kinetics of sodium sulfate reduction in the solid state by carbon monoxide,” *Chemical Engineering Science*, vol. 43, no. 8, pp. 2079–2085, 1988.
- [39] J. H. Cameron and T. M. Grace, “Kinetic study of sulfate reduction with carbon,” *Industrial & Engineering Chemistry Fundamentals*, vol. 22, no. 4, pp. 486–494, 1983.

[40] A. N. Khlapova and E. S. Kovaleva, "The hexagonal burkeite solid solution (??-phase) in the $\text{Na}_2\text{SO}_4\text{-Na}_2\text{CO}_3$ system," *Journal of Structural Chemistry*, vol. 4, no. 4, pp. 517–523, 1964.

[41] F. C. Vilbrandt and C. E. Dryden, *Chemical Engineering Plant Design*. New York: McGraw-Hill, 1959.

APPENDIX A

Table A.1: Equilibrium chart for feed gas ratio of 3CO:1H₂

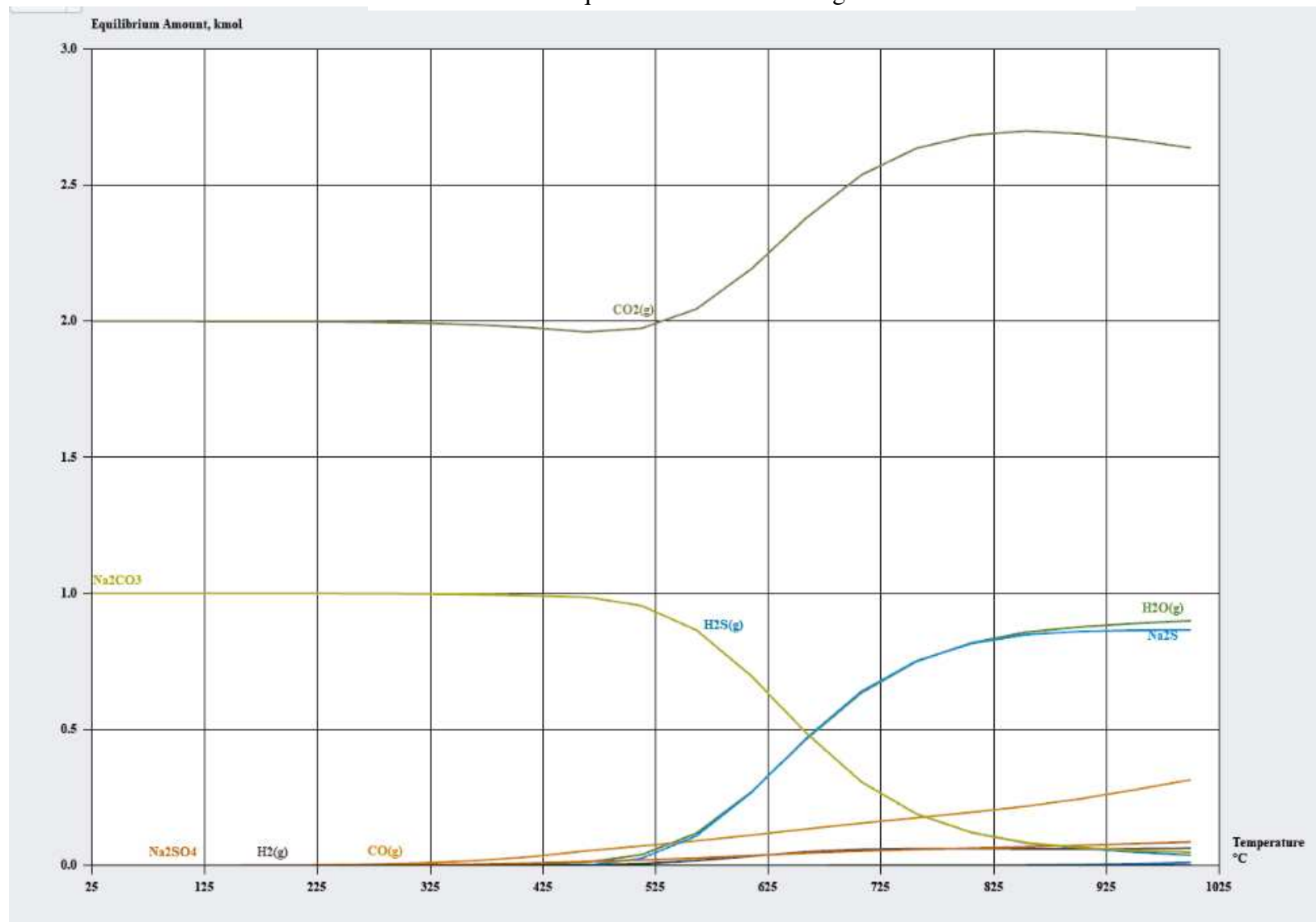


Table A.2: Equilibrium chart for feed gas ratio of 1CO:1H₂

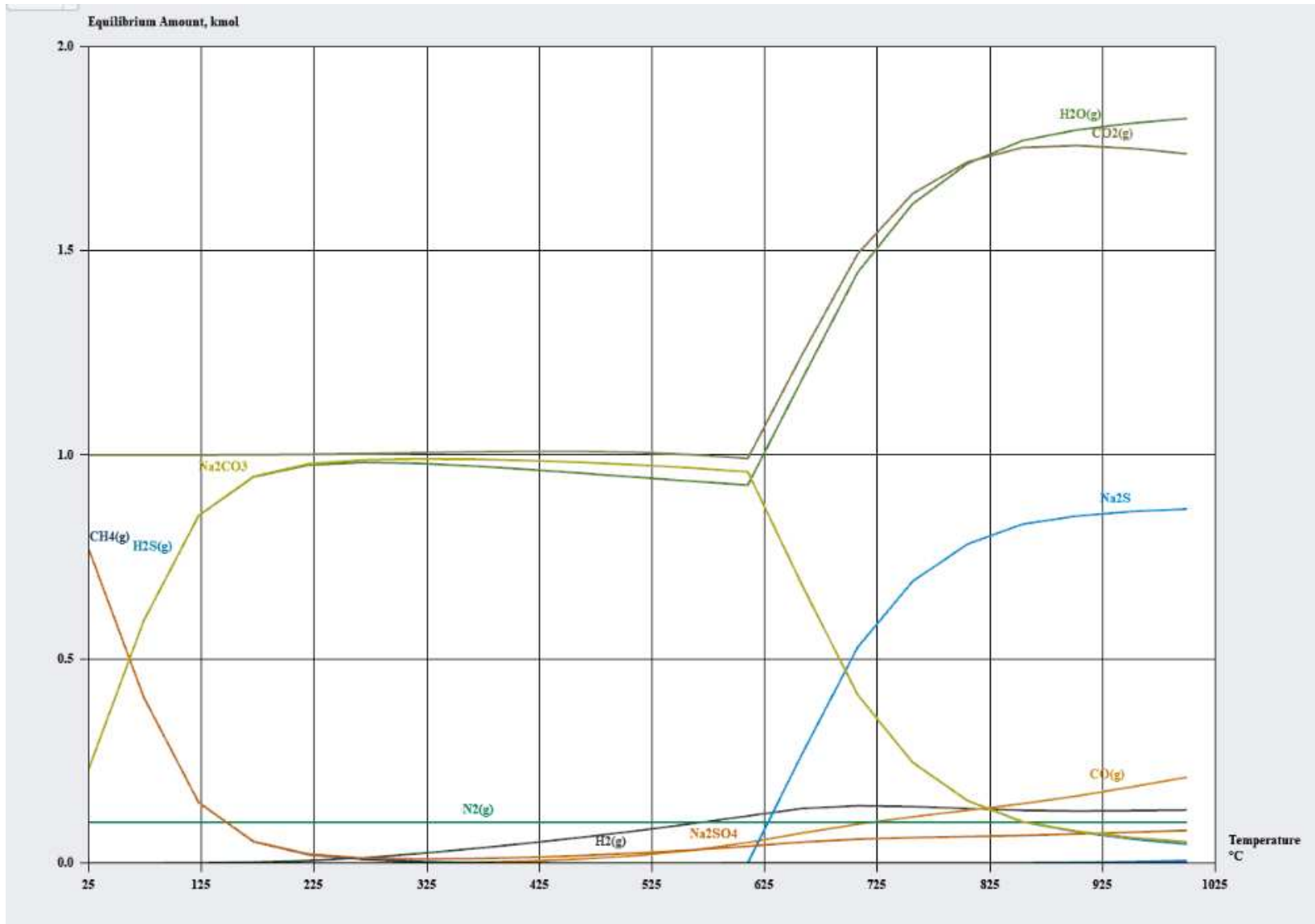


Table A.3: Equilibrium chart for feed gas ratio of 1CO:1H₂:0.25O₂

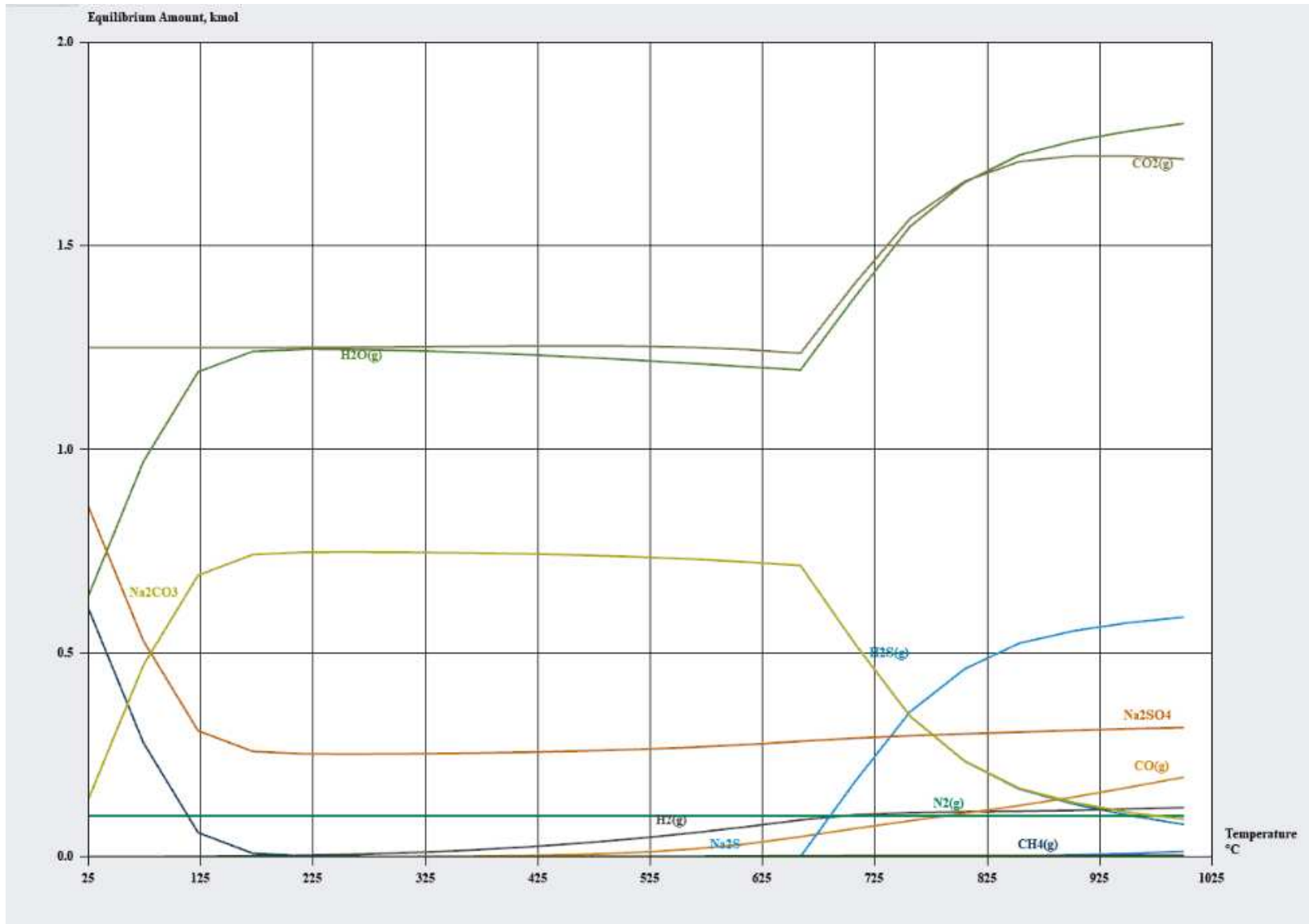
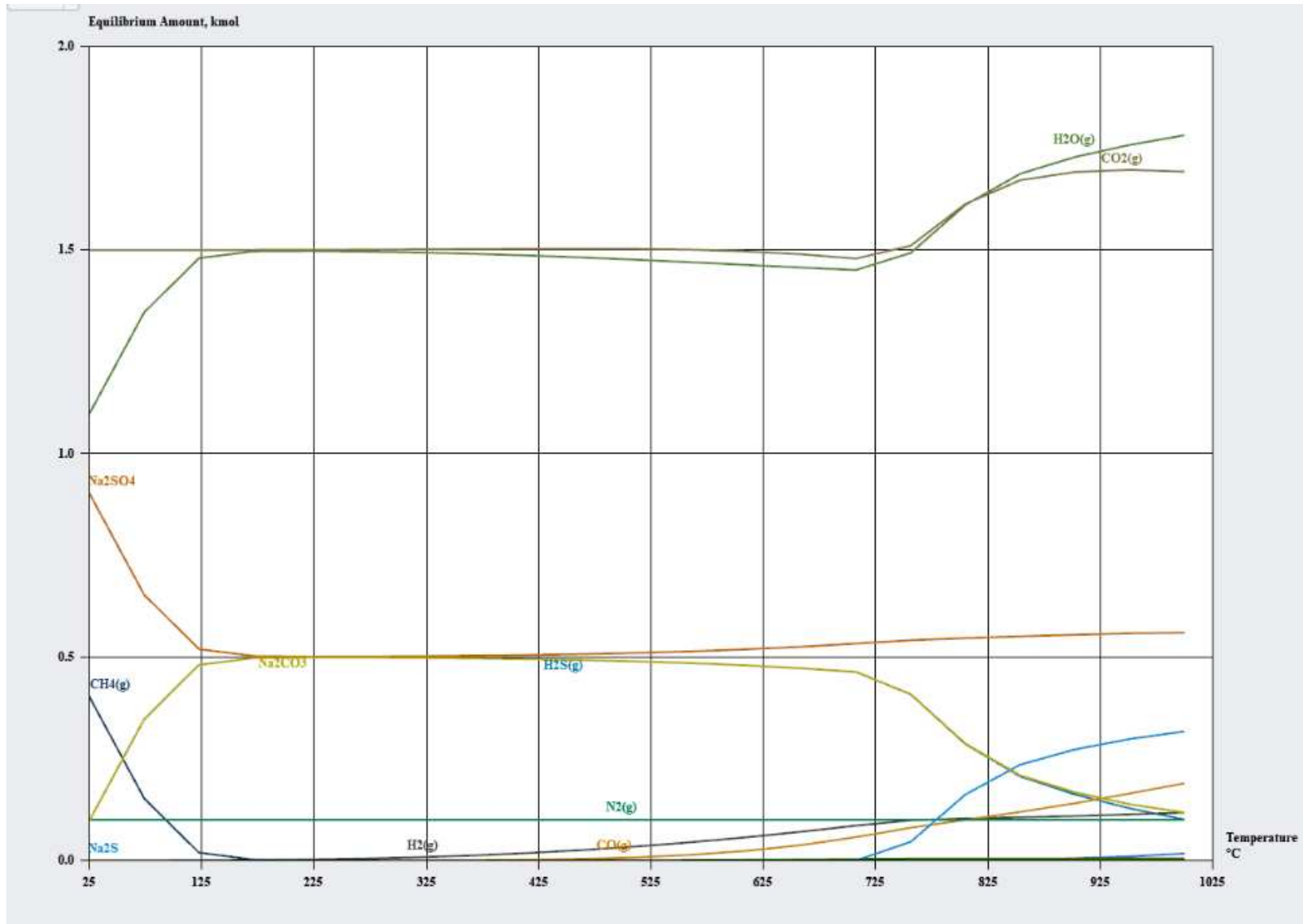


Table A.4: Equilibrium chart for feed gas ratio of 1CO:1H₂:0.5O₂



APPENDIX B

Table B.1: Summary chart of parameters effects on zinc recovery

SUMMARY OUTPUT								
<i>Regression Statistics</i>								
Multiple R	0.97532112							
R Square	0.951251288							
Adjusted R Square	0.30500515							
Standard Error	0.014626352							
Observations	9							
ANOVA								
	<i>df</i>	<i>SS</i>	<i>MS</i>	<i>F</i>	<i>Significance F</i>			
Regression	7	0.008348994	0.001192713	6.504454107	0.293350026			
Residual	2	0.00042786	0.00021393					
Total	9	0.008776855						
	<i>Coefficients</i>	<i>Standard Error</i>	<i>t Stat</i>	<i>P-value</i>	<i>Lower 95%</i>	<i>Upper 95%</i>	<i>Lower 95.0%</i>	<i>Upper 95.0%</i>
Intercept	0.051639933	0.004875451	10.59182743	0.008796266	0.030662562	0.072617305	0.030662562	0.072617305
A	0.033543299	0.005971183	5.617529571	0.03025814	0.007851371	0.059235227	0.007851371	0.059235227
B	-0.000540936	0.005971183	-0.090591158	0.936073401	-0.026232865	0.025150992	-0.026232865	0.025150992
C	-0.004033831	0.005971183	-0.675549698	0.56896688	-0.029725759	0.021658097	-0.029725759	0.021658097
AB	0.007509201	0.008956775	0.838382266	0.490049158	-0.031028691	0.046047094	-0.031028691	0.046047094
AC	0.011423856	0.008956775	1.275443031	0.330266596	-0.027114036	0.049961749	-0.027114036	0.049961749
BC	-0.023308897	0.008956775	-2.602376048	0.121358316	-0.061846789	0.015228996	-0.061846789	0.015228996
ABC	0	0	65535	#NUM!	0	0	0	0

Table B.2: Summary of leaching parameters effects on gallium recovery

SUMMARY OUTPUT								
<i>Regression Statistics</i>								
Multiple R	0.99158977							
R Square	0.983250272							
Adjusted R Square	0.43300109							
Standard Error	0.042045877							
Observations	9							
ANOVA								
	<i>df</i>	<i>SS</i>	<i>MS</i>	<i>F</i>	<i>Significance F</i>			
Regression	7	0.207554979	0.029650711	19.56748785	0.172389789			
Residual	2	0.003535712	0.001767856					
Total	9	0.211090691						
	<i>Coefficients</i>	<i>Standard Error</i>	<i>t Stat</i>	<i>P-value</i>	<i>Lower 95%</i>	<i>Upper 95%</i>	<i>Lower 95.0%</i>	<i>Upper 95.0%</i>
Intercept	0.231459755	0.014015292	16.5148003	0.003646471	0.171156819	0.291762691	0.171156819	0.291762691
Acid Con	0.177172804	0.017165157	10.32165331	0.009256328	0.103317093	0.251028516	0.103317093	0.251028516
Time	0.007446463	0.017165157	0.433812668	0.706735581	-0.066409249	0.081302174	-0.066409249	0.081302174
Slurry Density	-0.033644133	0.017165157	-1.960024749	0.189053804	-0.107499845	0.040211578	-0.107499845	0.040211578
AB	0.028896991	0.025747736	1.122311902	0.378369264	-0.081886577	0.139680558	-0.081886577	0.139680558
AC	0.015677485	0.025747736	0.608887893	0.604546917	-0.095106083	0.126461052	-0.095106083	0.126461052
BC	-0.066843314	0.025747736	-2.596085082	0.121843928	-0.177626881	0.043940254	-0.177626881	0.043940254
ABC	0	0	65535	#NUM!	0	0	0	0

Table B.3: Summary chart of parameters' effects on iron recovery

SUMMARY OUTPUT								
<i>Regression Statistics</i>								
Multiple R	0.988039023							
R Square	0.976221111							
Adjusted R Square	0.404884444							
Standard Error	0.033821107							
Observations	9							
ANOVA								
	<i>df</i>	<i>SS</i>	<i>MS</i>	<i>F</i>	<i>Significance F</i>			
Regression	7	0.093920904	0.013417272	13.68470318	0.205291321			
Residual	2	0.002287735	0.001143867					
Total	9	0.096208639						
	<i>Coefficients</i>	<i>Standard Error</i>	<i>t Stat</i>	<i>P-value</i>	<i>Lower 95%</i>	<i>Upper 95%</i>	<i>Lower 95.0%</i>	<i>Upper 95.0%</i>
Intercept	0.16196995	0.011273702	14.36705939	0.004809746	0.113463124	0.210476776	0.113463124	0.210476776
A	0.119179623	0.013807409	8.631570345	0.013157774	0.059771136	0.178588109	0.059771136	0.178588109
B	0.004829774	0.013807409	0.349795831	0.759892681	-0.054578712	0.06423826	-0.054578712	0.06423826
C	-0.021105641	0.013807409	-1.528573593	0.265968305	-0.080514127	0.038302845	-0.080514127	0.038302845
AB	0.023425018	0.020711114	1.131036132	0.375417665	-0.065687712	0.112537747	-0.065687712	0.112537747
AC	0.007198448	0.020711114	0.347564491	0.761336815	-0.081914282	0.096311177	-0.081914282	0.096311177
BC	-0.045916741	0.020711114	-2.217009758	0.156922772	-0.13502947	0.043195988	-0.13502947	0.043195988
ABC	0	0	65535	#NUM!	0	0	0	0